Aus der Klinik für Kardiologie, Pneumologie und Angiologie
der Heinrich-Heine-Universität Düsseldorf
Direktor Prof. Dr. med. Malte Kelm

Nitric oxide-dependent red cell sGC activity and sGC/cGMP pathway in coronary artery disease patients and healthy controls

Dissertation

zur Erlangung des Grades eines Doktors der Medizin
der Medizinischen Fakultät der Heinrich-Heine-Universität Düsseldorf

vorgelegt von
Thirumakal Manokaran
aus Jaffna, Sri Lanka

Düsseldorf, Juni 2019

Als Inauguraldissertation gedruckt mit der Genehmigung der Medizinischen Fakultät der Heinrich-Heine-Universität Düsseldorf

gez.:
Dekan: Prof. Dr. Nikolaj Klöcker
Erstgutachterin: Prof. Dr. rer. nat. Dr. Miriam Cortese-Krott
Zweitgutacherin: Prof. Dr. rer. nat. Inge Bauer

Tag der mündlichen Prüfung: 12.06.2019

Dedicated in gratitude to my deceased grandfather and dearest friend,
Mr. Thiyagarajah Nagamuthu.

Zusammenfassung

Atherosklerose und kardiovaskuläre Erkrankungen stehen im Zusammenhang mit verringerter Bioverfügbarkeit von Stickstoffmonoxid (*NO*). Die *NO* aktiviert die lösliche Guanylatzyklase (*sGC*), einen intrazellulären Rezeptor, der einen *second messenger*, die zyklische Guanosinmonophosphat (*cGMP*), produziert. Der Rezeptor spielt eine entscheidende Rolle bei der Regulierung des Gefäßtonus und kardiovaskulärer Ereignisse. Es ist bewiesen, dass menschliche Erythrozyten (*RBCs*) über eine Isoform der endothelialen *NO*-Synthase (*eNOS*) kontinuierlich *NO* zur Verfügung stellen. Viele Faktoren weisen darauf hin, dass RBCs ihren eigenen *NO/sGC/cGMP*-Signalweg enthalten und möglicherweise an der Regulierung der Bioverfügbarkeit von *NO* beteiligt sind. Jedoch wurden in den menschlichen *RBCs* bislang keine aktive *sGC* oder der zugehörige Signalweg nachgewiesen. Darüber hinaus wird vermutet, dass *RBCs* zusätzlich sogenannte "nicht-kanonische" Funktionen wie den *NO* Metabolismus und die Regulation des Redoxstatus besitzen.

Die vorliegende Arbeit basiert auf der Hypothese, dass menschliche *RBCs* sowohl einen aktiven *sGC/cGMP* Signalweg besitzen als auch am *NO*-Stoffwechsel beteiligt sind. Diese Zellfunktionen stehen im engen Zusammenhang mit koronaren Herzkrankheiten (*CAD*) und könnten Einflussfaktoren für letztgenannte darstellen. Folglich war Ziel der Arbeit, herauszufinden, ob (1) *NO*, (2) die *eNOS* und (3) die *sGC* eine Wirkung auf den *cGMP* Spiegel in humanen *RBCs* haben. Außerdem wurden Veränderungen der (4) *sGC* Aktivität und des *NO/sGC* Signalwegs in menschlichen *RBCs* mit stabiler und instabiler *CAD* untersucht. In diesem Bezug wurden sowohl (5) die *NO*-Metaboliten und der Redoxstatus in *RBCs* mit stabiler und instabiler *CAD* als auch bei (6) einer Anämie beurteilt.

Mittels einer *RIA*-Analyse wurden der *cGMP* Spiegel in den *RBCs* bestimmt. *FACS*-Analysen wurden durchgeführt, um die oben genannten *RBCs*-Funktionen zu evaluieren. Zusätzlich wurden zwei unabhängige klinische Studien von Patienten mit (A) stabiler und instabiler *CAD* im Vergleich zu einer Kontrollgruppe sowie (B) instabiler *CAD* mit und ohne begleitender Anämie durchgeführt. Darüber hinaus erfolgte eine *Longitudinal*-Studie mit Patienten mit instabiler *CAD* im Vergleich zur Kontrollgruppe, um die Rolle der *PCI* auf nicht-kanonische *RBC*-Merkmale zu bewerten.

Der Einfluss von *NO* durch die Applikation des *NO*-Donors *Diethylamin NONOate* (*DEA/NO)* führte zu einem Phosphodiesterase (*PDE*)-abhängigen Anstieg des cGMP Spiegels. Im Gegensatz dazu war der *cGMP*-Spiegel unverändert nach Manipulation der Arginase Aktivität, *eNOS* Aktivität, Kalziumeinstrom und Stimulation der *AC*. Die *sGC*-Stimulation mit *DEA/NO* und BAY 41-2272, einem *sGC*-Stimulator, erzielte einen signifikanten Anstieg des *cGMP* Spiegels in den *RBCs*. Die Wirkung von *NO* auf die *sGC* erlosch nach der Anwendung von *1H-[1,2,4]-oxadiazolo-[4,3-a]-quinoxalin-1-one (ODQ)*, einem *sGC*-Inhibitor. Hieraus lässt sich eine aktive *sGC* in menschlichen *RBCs* ableiten. Die stabile oder instabile *CAD* hat keinen Einfluss auf die *sGC*-Aktivität sowie die Reaktion von *sGC* auf *NO* und weitere Stimulatoren in den menschlichen *RBCs*. Gemäß dieser Erkenntnis waren auch der Redoxstatus und der *NO*-Metabolismus unbeeinflusst von einer *CAD* oder Anämie. Nach der *PCI* zeigten die Erythrozyten eine Tendenz zur Verbesserung des Redoxstatus 90 Tage nach dem Eingriff. Folglich kann angenommen werden, dass die *PCI* auch für die nicht-kanonischen Charakteristiken der *RBCs* eine Rolle spielt.

Zusammenfassend veranschaulichen die vorliegenden Daten, dass die menschlichen *RBCs* eine aktive *sGC* und einen funktionsfähigen *sGC/cGMP* Signalweg enthalten. Trotz einer *CAD* bleiben in den RBCs der Signalweg und die Reaktion von der *sGC* auf *NO* vollständig erhalten. Zusätzlich bleiben auch der *NO* Metabolismus und der Redoxzustand in *CAD* und zusammenhängenden anämischen Zuständen bestehen. Folglich bieten *RBCs* und deren Signalweg einen neuen therapeutischen Ansatz zur Behandlung von kardiovaskulären Erkrankungen.

Summary

Lack of nitric oxide (NO) bioavailability is correlated with endothelial dysfunction and cardiovascular disease (CVD). NO activates the intracellular receptor soluble guanylate cyclyse (sGC), which produces the second messenger cyclic guanosine monophosphate (cGMP). This receptor plays a crucial role in regulation of vascular tone of blood vessels and cardiac function. Human red blood cells (RBCs) were considered to synthetize NO via an isoform of the endothelial NO-synthase (eNOS). Consequently, they are proposed to contain its own NO/sGC/cGMP signaling pathway and might be involved in the regulation of NO bioavailability. However, an active sGC and associated pathway are not proven in RBCs so far. Besides, RBCs are supposed to obtain non-canonical features, such as NO metabolism and redox state.

The present work is based on the hypothesis that human RBCs contain an active sGC/cGMP pathway and own non-canonical functions, which may be influenced by or influence coronary artery disease (CAD). Therefore, this work aimed at finding out, whether (1) NO, (2) eNOS and (3) sGC have an effect on cGMP levels in human RBCs. Secondly, changes in (4) sGC activity and NO/sGC signaling were investigated in human RBCs from patients with stable and unstable CAD as compared to age-matched controls. Along with this, (5) NO metabolism and redox state in human RBCs with stable and unstable CAD and (6) correlated anemia were investigated.

Using radioimmunoassay (RIA), cGMP levels in human RBCs were determined. Fluorescence-activated cell sorting (FACS) was executed to evaluate human RBC features. Two independent controlled clinical studies of patients with (A) stable and unstable CAD patients compared to healthy controls and (B) unstable CAD with and without anemia were performed. In a follow-up study, the role of percutaneous coronary intervention (PCI) on non-canonical functions of RBCs from patients with unstable CAD as compared to healthy subjects was evaluated additionally.

The cGMP levels increased by NO application with NO-donor diethylamin NONOate (DEA/NO) in a phosphodiesterase (PDE)-dependent manner in healthy human RBCs. In contrast, cGMP levels were independent of arginase activity, eNOS activity, calcium (Ca^{2+}) influx and adenylate cyclase (AC) stimulation. Significant cGMP level increase was observed via sGC stimulation using DEA/NO and sGC stimulator BAY 41-2272 in human RBCs. The effect of NO was diminished by the use of sGC inhibitor 1H-[1,2,4]-oxadiazolo-[4,3-a]-quinoxalin-1-one (ODQ). These results show that human RBCs contain an active sGC. Moreover, sGC activity, sGC responsiveness to NO and further stimulators were preserved in human RBCs with stable or unstable CAD. In accordance, redox regulation and NO metabolism were preserved in RBCs with CAD or unstable CAD with anemia as well. After PCI, the RBCs showed a tendency towards an anti-oxidative change in redox state after 90 days. These results indicate clinical relevance of PCI also for non-canonical features of RBCs.

Overall, present data show that there exists an active sGC and a functional sGC/cGMP signaling in human RBCs. Furthermore, this pathway and response of sGC to NO are fully preserved in CAD despite low NO levels. In addition, NO metabolism and redox state are also preserved in human RBCs with CAD. Hence, RBCs and its signaling provide a new therapeutical approach in pathological conditions such as CVD.

Abbreviations

-	without $CaCl_2$ + $MgCl_2$
+	with $CaCl_2$ + $MgCl_2$
$^{\cdot}O_2^-$	superoxide anion
AB	antibody
AC	adenylyl cyclase
ATP	adenosine triphosphate
BAY 41	BAY 41-2272
BAY 60	BAY 60-2770
BD	Becton, Dickinson biosciences
BH_4	tetrahydrobiopterin
BMI	Body Mass Index
BSA	bovine serum albumin
°C	celsius
Ca-I	calcium-ionophore
Ca^{2+}	calcium
$CaCl_2$	calcium chloride
CAD	coronary artery disease
cAMP	cyclic adenosine monophosphate
cGMP	cyclic guanosine monophosphate
CLD	chemiluminescence detector
CO	carbon monoxide
CO_2	carbon dioxide
CRP	C-reactive protein
CTRL	control
CVD	cardiovascular disease
DAF-FM-DA	4-amino-5-methylamino-2',7'-difluorescein-diacetate
DCF-DA	2',7'-dichloridhydrofluorescein-diacetate
DE	germany
DEA/NO	diethylamine nonoate diethylammonium salt
DMSO	dimethylsulfoxid
ELISA	enzyme linked immunobsorband assay
eNOS	endothelial nitric oxide synthase
FACS	fluorescence-activated cell sorting
FI	fluorescence intensity
FMD	flow-mediated dilatation
FSC	forward scatter
g	gravitational force
GC	guanylate cyclase
GCP	good clinical practice
GFR	glomerular filtration rate
GSH	free glutathione (reduced)
GSSG	glutathione disulfide
GTP	guanosine triphosphate
H_2O_2	hydrogen peroxide
Hb	hemoglobin
HbA1c	glycated hemoglobin
HBSS	Hanks'Balanced Salt solution
HCl	hydrochloride acid

Hct	hematocrit
HDL	high densitiy lipoprotein
HR	heart rate
IBMX	3-isobutyl-1-methylxanthin
IU	International unit
L-Arg	L-arginine
LDL	low density lipoprotein
L-NAME	N^G-nitro-l-arginine-methylester (hydrochloride)
Lorca	Laser-assisted Optical Rotational Cell Analyzer
M	molar
MCH	Mean Corpuscular Hemoglobin
MCHC	Mean Corpuscular Hemoglobin Concentration
MCV	Mean Corpuscular Volume
MDRD	Modification of Diet in *Renal* Disease
NaCl	sodium chloride
NaOH	sodium hydroxide
NCDs	Non-communicable diseases
NO	nitric oxide
NO_2^-	nitrite
NO_3^-	nitrate
NSB	non-specified binding
NSTEMI	non ST-elevation myocardial infarction
O_2	oxygen
ODQ	1H-[1,2,4] oxadiazolo[4,3-a] quinoxalin-1-one
$ONOO^-$	peroxynitrite
PBS	phosphate buffer saline
PDE	phosphodiesterase
PDE5	phosphodiesterase 5
PKA	protein kinase A
PKG	protein kinase G
PS	phosphatidylserine
RBC	red blood cell
RBCs	red blood cells
RIA	radioimmunoassay
ROS	reactive oxygen species
RRdiastolic	diastolic blood pressure
RRsystolic	systolic blood pressure
RT	room temperature
SD	sample diluent
SDS	sodium dodecyl sulphate
SEM	standard error of the mean
sGC	soluble guanylate cyclase
STEMI	ST-segment elevation myocardial infarction
TCA	trichloroacetic acid
tGSH	total glutathione
TT	Thiol Tracker
VSMC	vascular smooth muscle cells
WHO	world health organization

Table of content

Figure index

Table index

1 Introduction

1.1 Atherosclerosis and CVD

Atherosclerosis and consequences, such as heart attack and stroke represent major causes of morbidity and mortality in western industrial nations [1]. Furthermore, atherosclerosis is the main cause of CVD for instance CAD, cerebrovascular disease and peripheral arterial disease [2, 3].

CVD represents one of the "four main types of non-communicable diseases (NCDs) [4], beside cancer, chronic respiratory diseases and diabetes" [4]. Moreover, CVD causes most NCDs associated deaths each year, about 44.25 % or 17.7 million people [4]. Annual CVD mortality is estimated to increase to 22.2 million people in 2030 [5].

Several risk factors were identified to promote CVD through atherosclerosis by Framingham in 1961 [6]. Hypertension [6], hypercholesterolemia [7], modified low density lipoproteins (LDL) [8], cigarette smoking [9], diabetes mellitus [10] and physical inactivity are longer known causes of CVD [11]. Turbulent blood flow [12], increased level of lipoprotein A [13] as well as a low fibrinogen concentration [14] are confirmed as further risk factors. Elevated plasma homocysteine concentration is also defined as a marker for CVD [15].

A key role in the pathogenesis of atherosclerosis is attributed to the endothelial dysfunction [2, 16, 17] and the interruption of endothelial homeostasis, which causes reduced bioavailability [18, 19, 20, 21] and activity [21] of NO, a short living radical gas [22, 23]. Endothelial dysfunction can be characterized as a dysregulation in vascular tone [24], thrombosis and endothelial remodeling of vessels [2]. Furthermore, in hypertension patients Perticone et al. regarded endothelial dysfunction as a "marker for cardiovascular events" [25].

The pathology of atherosclerosis can be described as an "inflammatory disease" with infiltration of lymphocytes and macrophages into the vascular intima [2] and manifests as follows.

At first, permeability for inflammatory agents as well as the adherence of platelets and leukocytes to the endothelium in the vascular wall increase (Figure 1 A) [2]. Immigration of macrophages and lymphocytes into the arterial wall leads to a release of pro-coagulative hydrolytic enzymes and other signaling proteins, which can cause subsequent illness (Figure 1 A) [2]. In inflammatory conditions oxidative stress is increased by the formation of reactive oxygen species (ROS) like superoxide ($^{\cdot}O_2^-$) [26].

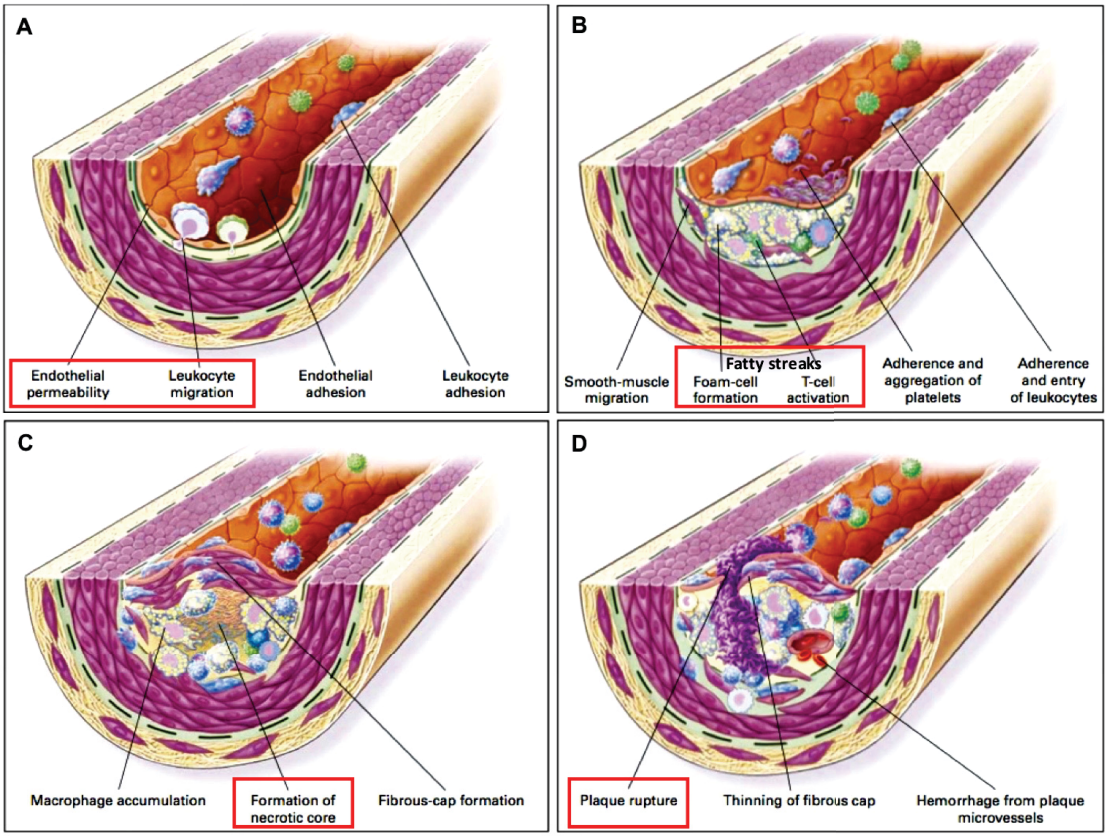

Figure 1 | Pathophysiology of atherosclerosis

Image modified from Ross, R., 1999 [2]. Formation of atherosclerosis induced by endothelial-cell injury and dysfunction. (A) Earliest signs of atherosclerosis are increased endothelial permeability and leukocyte migration. (B) Fatty-streaks progress by foam-cell formation, adherence of platelets and T-cell activation. (C) Platelet-derived growth factors and smooth muscle cell migration lead to a fibrous-cap formation with necrotic core. (D) Thrombus and occlusion of the artery cause instability and rupture of the fibrous plaques [2].

Oxidative stress causes release of foam cells (monocytes and macrophages loaded with lipids) and inflammatory mediators (Figure 1 B) [2, 27]. Growth factors stimulate the proliferation of smooth muscle cells [28], which causes arterial walls to become thicker (Figure 1 B) [2]. Adherence of platelets and T-cell activation increase (Figure 1 B) [2]. Subsequently, so called "fatty streaks", initially consisting of foam cells and T lymphocytes, form (Figure 1 B) [2].

The repetition of these cycles of cell migration and proliferation causes an advanced lesion in vasculature [2]. Below the fibrotic cover, a mixture of leukocytes, lipids and cell detritus form a necrotic core (Figure 1 C) [2]. Growth of the plaque, activation as well as diapedesis of macrophages and the release of proteolytic enzymes thin the fibrous cap (Figure 1 D) [2]. This process causes bleeding in the plaque and leads to rupture or ulceration of the lesion (Figure 1 D) [2]. This can result in a thrombosis and hemodynamically hindering occlusion of the vascular lumen (Figure 1 D) [2].

Acute ischemic events like coronary heart disease, cerebrovascular disease or peripheral arterial occlusive disease [29, 30] can take place at this final stage of atherosclerosis.

1.2 Human RBCs and their features

Human whole blood consists of cellular components and plasma [31]. The main cellular components are RBCs, leukocytes and thrombocytes [31]. Four to six million RBCs per milliliter blood circulate in the human body for 110 to 130 days until they get removed by the mononuclear phagocyte system [32].

Erythrocytes have a diameter of 7.5 µm and a thickness of about 1.5 µm at their thinnest point [32]. Their form can be described as biconcave. Since the capillaries only have a lumen of circa 3 to 5 µm the scale of deformability of the RBCs is vital for blood circulation [33, 34]. Besides the lipid bilayer [33] structure of the erythrocyte membrane, the degree of deformability of the RBCs is given by additional membrane skeleton [32]. Main components of the membrane skeleton in RBCs are spectrin [33], actin, protein 4.1 [35], protein 4.2 [36], ankyrin and band 4.9 protein [37].

One third of the RBCs' mass consists of hemoglobin, a protein with crucial role [32]. Hemoglobin has a quaternary structure consisting of four subunits [32]. Each subunit contains a globin chain and a heme group with a centrally located iron (Fe^{2+}) [32]. O_2 is transported coupled on Fe^{2+} of each heme group [32]. The globin chain protects the Fe^{2+} from oxidation to Fe^{3+} in presence of O_2. Additionally, Hemoglobin is considered to modulate blood flow through reduction of nitrite [38].

1.2.1 Canonical and non-canonical functions of human RBCs

In 1674 Lee Van Hock began to elucidate the RBCs [39]. Since then RBCs have been content of research and are not fully characterized till date. One of the main functions of human RBCs is the transport of oxygen (O_2) and carbon dioxide (CO_2) between lungs and human tissue bound on hemoglobin [31]. Secondly, they maintain the acid-base balance in human blood via hemoglobin [31].

Moreover, RBCs were considered as "intravascular NO storage" and transporter [40] under hypoxic [41] and normoxic conditions [40, 42, 43]. Recently, RBCs are also supposed to have non-canonical functions, such as NO metabolism [44, 45] or maintenance of redox state [46, 47]. RBCs do not only transport a high amount of the so called "NO-scavenger" hemoglobin, but are also rich in antioxidants [48]. In 2000 Tsuda et al. showed that there is a positive correlation between NO bioavailability and

membrane fluidity of RBCs [44, 49]. Loss of deformability leads to microvascular diseases [50]. It still needs to be further examined whether non-canonical features of human RBCs are affected in CVDs like CAD.

1.2.2 Anemia

Hemoglobin concentrations below 120 g/l blood in women and below 140 g/l blood in men are defined as anemia [32].

Several factors can lead to anemia. The important causes are: impaired production (etiopathology disorders), increased destruction of RBCs (hemolysis), blood loss and interference in cell distribution [51]. Etiopathology disorders include amongst others erythropoiesis malfunction, stem cell disorders and hemoglobin production [51]. Hemolysis can be caused by changes in RBCs (morphology, membrane components, hemoglobin deficiency, autoantibody etc.), for instance by sickle cell disease (SCD) [51].

Retrospective analysis of Valsartan Heart Failure Trial indicated a positive correlation between anemia and increased mortality and morbidity of heart failure patients [52]. Recent observations show that anemia worsens the recovery after heart failure or myocardial infarction [44, 53]. Others have considered anemia as a predictor for acute coronary syndrome [54].

However, it is not clear whether anemia is correlated with non-canonical functions in RBCs in CVD.

1.3 NO and NO-metabolism in human RBCs

Furchgott and Zawadzki showed that the so called endothelium-derived relaxing factor [55], later identified as NO [56], has a vasorelaxant effect [57].

NO is produced by type III nitric oxide synthase (NOS) in the vascular endothelium [58] and in RBCs [43]. It is an essential, non-durable signaling molecule for vascular homeostasis [59] and resistance [60]. External [61] as well as internal NO release [55] leads to vasorelaxation in smooth muscle cells [61]. Moreover, it acts anti-inflammatory [62] and plays a central role in the development and progression of CVD [27].

In 1995 Moncada et al. already described the therapeutic importance of NO for endothelial dysfunction [64]. Decreased NO signaling in endothelium can be observed a long time before pathological adaptions [20], such as hyperplasia of vascular intima [2], appear. In pathological conditions with elevated oxidative stress, such as atherosclerosis NO bioavailability is reduced [65]. Diminished NO metabolism can

provoke myocardial ischemia in patients with CAD [28]. Hence, an inverse correlation between endothelial dysfunction and NO signaling is assumed [22, 66].

Due to a free electron, the radical gas can diffuse across cell membranes into the vascular lumen. In smooth muscle cells, it conveys vasodilatory functions via further signaling cascade [67, 68] (Figure 3). Therefore, it is involved in various physiological and pathological processes [69].

NO is produced in myocardium, platelets and macrophages [69] and RBCs [45, 46]. In the endothelium, NO is produced continuously by eNOS [59, 70, 71] using cofactors, such as L-arginine and O_2 [72]. Primary products of the NO oxidation are nitrite and nitrate (Figure 2) [73, 74]. NO reacts with O_2 to form nitrite (NO_2^-) [41, 74, 75 76] (Figure 2), which acts as an intravascular storage for NO [24]. Consequently, nitrite can be reduced to NO [42].

Recent findings showed that human RBCs are also involved in NO metabolism [45, 46]. They do not only store, but also generate NO [46, 77]. In RBCs, NO reacts also with oxyhemoglobin (HbO_2) to form nitrate (NO_3^-) and methemoglobin (MetHb) (Figure 2) [41, 78]. In addition, it was observed, that RBCs cause vasorelaxation under hypoxic conditions by reducing NO_2^- to NO [42, 79].

By interacting with ROS, such as $^{\cdot}O_2^-$, NO gets inactivated [18]. Consequently, an increase in $^{\cdot}O_2^-$ is inversely linked to NO bioavailability. Furthermore, NO_2^- was supposed to be a marker for NO bioavailability [42]. Thus, human RBCs might play a key role in NO metabolism in pathological conditions, such as CAD as well.

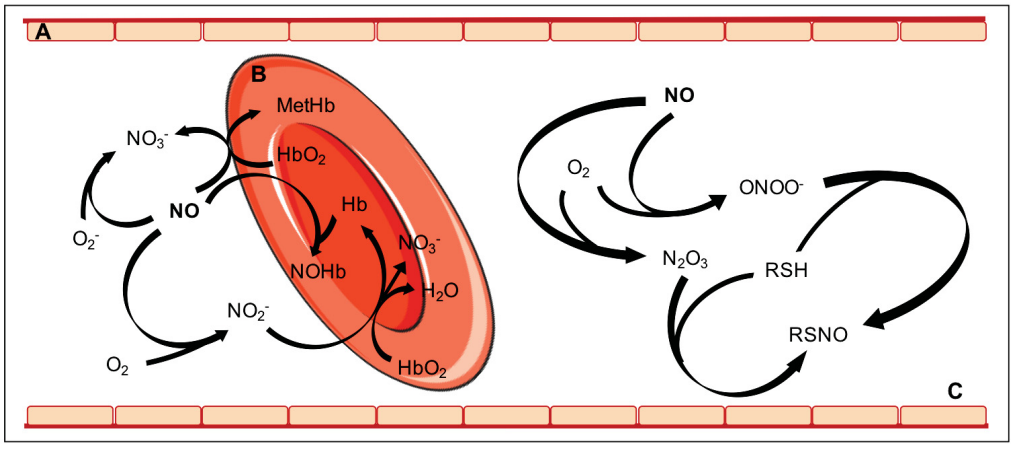

Figure 2 | NO metabolism in RBCs and plasma

Image modified from Dejam, A., et al., 2005 [41]. A: Vascular wall. B: RBC. C: Plasma. The NO of the erythrocyte reacts with HbO_2 to form NO_3^- and MetHb. In plasma NO reacts with thiol (RSH) groups to form S-nitrosothiols (RSNO). Nitrosylated species like dinitrogen trioxide (N_2O_3), NO_2^-, NO_3^- or peroxynitrite ($ONOO^-$) are other possible intermediates of the NO metabolism [41].

1.4 Redox status of human RBCs

Mismatch between the production of free radicals and antioxidant capacity towards pro-oxidative state results in oxidative stress [80]. In an inflammatory condition, cells produce high amounts of ROS [27], such as $^{\cdot}O_2^-$, $ONOO^-$ and hydrogen peroxide (H_2O_2) [81]. Accumulation of ROS inactivates NO [27, 82, 83] and decreases the NO bioavailability in smooth muscle cells [84]. Thus, it dysregulates vascular tone [27].

Hence, increased oxidative stress is supposed to be associated with high risk for atherosclerosis [85, 86]. Besides that, it is correlated to CVD [81, 87, 88], such as stable and unstable CAD, heart failure [89] and SCD [90].

Human RBCs own a wide-ranging antioxidant capacity using "enzymatic and non-enzymatic" mechanisms [91]. On the one hand, they contain antioxidant molecules, such as thiols and vitamins [91, 92, 93]. On the other hand, RBCs contain antioxidant enzymes, such as superoxide dismutase, catalase, glutathione (GSH) peroxidase or GSH reductase [91, 92, 93]. The main antioxidant source of the RBCs is GSH [94]. A huge number of intracellular free thiols exists in form of reduced GSH in RBCs [95]. Thiols form S-nitrosothiols (RSNO) with other nitrogen species and function as NO supplier [96].

GSH itself is a co-substrate of the glutathione peroxidase [97], which reduces ROS [98, 99] and acts against the oxidative stress [100]. It catalyzes the reduction of H_2O_2 to H_2O [98]. GSH gets oxidized and forms the disulfide molecule GSSG [98]:

$ROOH + 2\ GSH \xrightarrow{\text{GSH peroxidase}} ROH + GSSG$ [99]

Superoxide dismutase and catalase also catalyze this reaction [101]. Then glutathione reductase reduces GSSG by oxidation of nicotinamide-adenine-dinucleotide phosphate (NADPH) [90].

In 2003 Blankenberg et al. confirmed a positive correlation between low activity of glutathione peroxidase and cardiovascular events [102]. Diminished catalase- and superoxide dismutase activity was observed in RBCs suffering from CAD [103]. However, possible effects of CAD and anemia on redox regulating function in human RBCs need to be evaluated further.

1.5 Characteristics of eNOS and its presence in human RBCs

In human cells, there are three types of NOS [104]. The eNOS is located in endothelial cells, cardiac muscle cells [59] and corpus cavernosum cells [105]. The inducible NOS (iNOS) exists in monocytes [106]. The neuronal NOS (nNOS) is found in neurons and skeletal muscle cells [107].

Recently, an active eNOS (type 3 NOS) was detected in RBCs (Figure 4) [44, 46, 104], which consistently produces NO [108]. The eNOS is regulated in a Ca^{2+}/calmodulin-dependent [44] and independent manner [109, 110, 111]. Shear stress also activates the eNOS [112]. Furthermore, it is supposed that protein kinase A (PKA) is able to activate the eNOS in a Ca^{2+}-dependent or independent way [113]. PKA is activated by the second messenger cyclic adenosine monophosphate (cAMP) [33]. cAMP is converted from ATP by membrane bound adenylate cyclase (AC) [33] and deactivated by phosphodiesterase (PDE) [33].

The eNOS forms L-citrulline and NO by oxidizing L-arginine with molecular oxygen (O_2) (Figure 3) [45, 114] in endothelial cells (Figure 3) [114] and in RBCs (Figure 4) [44, 45]. Tetrahydrobiopterin (BH_4) [115], Ca^{2+} [115] and NADPH [116] are cofactors of this reaction (Figures 3 and 4).

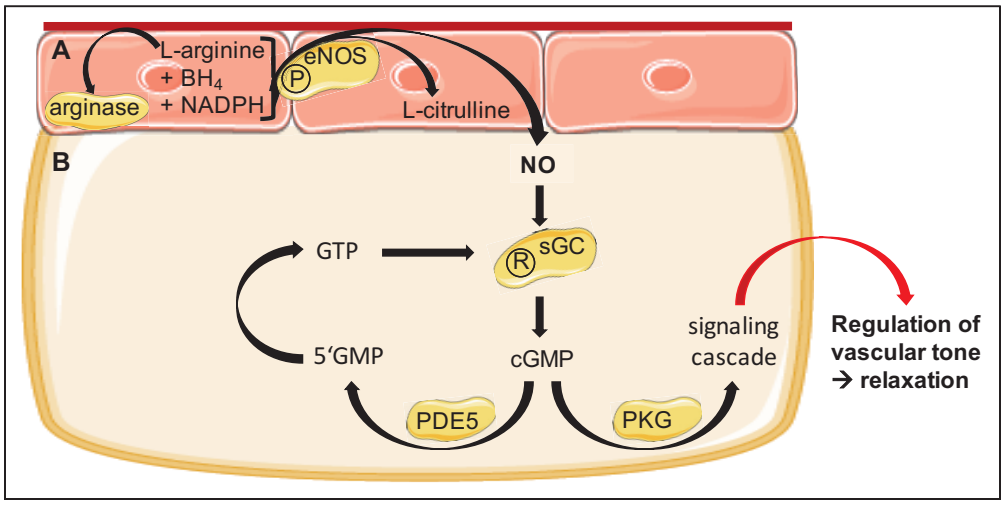

Figure 3 | The NO/sGC/cGMP pathway in endothelial cells

Image leaned on Heinzel, B., et al.,1992, Ignarro, L.J., 1989 and Denninger, J. W. et al., 1999 [67, 115, 117]. A: Endothelial cell. B: Smooth muscle cell. In endothelial cells, the eNOS oxidizes L-arginine. This reaction forms NO and L-citrulline with the co-substrates NADPH and BH_4 [115]. Arginase is sharing L-arginine with eNOS [118]. NO diffuses into the smooth muscle cell and activates reduced sGC (R sGC), which converts guanosine-5'-triphosphate (GTP) to second messenger cyclic guanosine-3',5'-monophosphate (cGMP) [119, 120]. Thus, cGMP activates the protein kinase G (PKG), a cGMP-dependent protein kinase, or gets reduced to guanosin-5'-monophosphat (5'GMP) by PDE type 5 (PDE5) [105, 121, 122]. Then it forms again GTP [67, 122]. Finally, following signaling cascade regulates the tone in vasculature [67].

L-arginin is a common substrate of eNOS [64, 123] and arginase [118, 123]. Thus, arginase and eNOS compete for L-arginine concentration [118] (Figures 3/4). Already in 1995 it was questioned, whether increase of L-arginine concentration in plasma can cause improved physiological NO levels [64]. Low L-arginine levels are considered to be a reason for $\cdot O_2^-$ production by the eNOS [116]. Recent data also demonstrate that

inhibition of arginase improves endothelial function in patients with CAD and diabetes [118, 124].

In RBCs, the eNOS regulates blood pressure [126], vascular homeostasis and microcirculation (Figure 4) [126, 127]. Inhibition of eNOS resulted in elevated mean arterial blood pressure [128]. In addition, red cell eNOS improves the deformability of erythrocytes through NO [129]. A decrease in red cell eNOS expression [44] was observed in patients with CAD [21].

Moreover, studies determined an increased plasma concentration of asymmetrical dimethylarginine (ADMA), a competitive inhibitor of eNOS, in patients with cardiovascular risk factors [130]. Low NO bioavailability is correlated with reduced eNOS function in the endothelium [19, 131] and RBCs [44]. However, the eNOS including pathway in human RBCs needs to be investigated further.

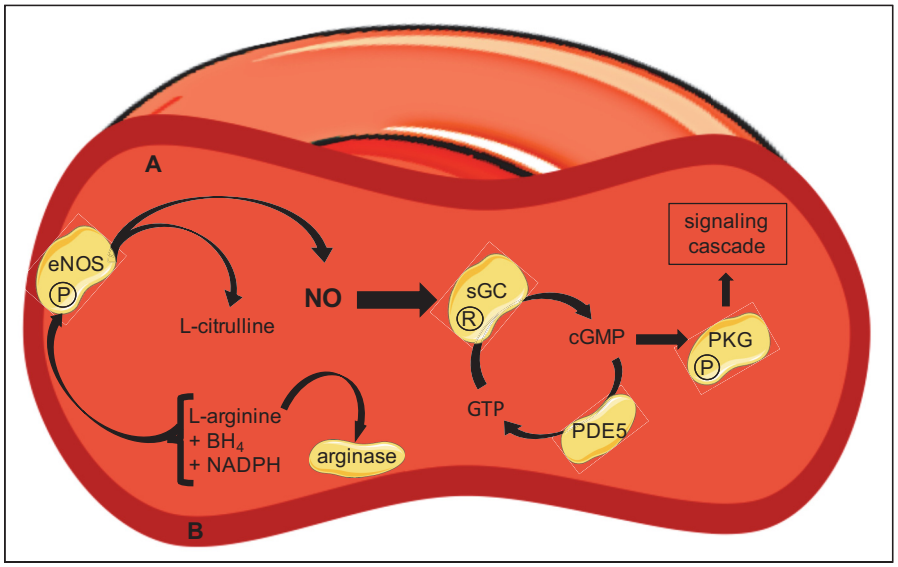

Figure 4 | Hypothesis of NO/sGC/cGMP signaling in human RBCs

Image modified from Heinzel, B., et al.,1992, Ignarro, L.J., 1989 and Denninger, J. W. et al., 1999 [67, 115, 117]. A: RBC. B: RBC membrane. The eNOS is localized in the RBC membrane [45]. In RBCs, eNOS is producing NO with L-arginine and L-citrulline as a by-product [45]. The NO/sGC/cGMP pathway and further vascular regulation in RBCs [125] are supposed to be similar to endothelial cells (Figure 3).

1.6 Characteristics of sGC and existence in human RBCs

The sGC is a cGMP producing enzyme, which is activated by NO [117, 120], NO releasing drugs [132] and by carbon monoxide (CO) [66, 133]. Moreover, it is a part of the endothelial sGC/cGMP pathway [117, 134, 135]. Impairment of this pathway is a

reason for endothelial dysfunction [136]. In addition, sGC modulates RBC-deformability [137], platelet activation and hemostasis [138].

Furthermore, existence of the sGC was described in erythroid cells [125, 139, 140]. The existence of an active sGC in mature human RBCs is content of research since Petrov in 1996.

As mentioned in chapter 1.5, sGC catalyzes the conversion of GTP to cGMP [117, 135, 141] (Figure 3). A cGMP-dependent protein kinase (PKG) signaling cascade causes vasodilatation (Figure 4) [105, 121, 122, 125]. The cGMP is also regulated by PDE, which decompose cGMP and other second messengers [33]. Some PDEs are specific for cGMP, such as PDE5 [142].

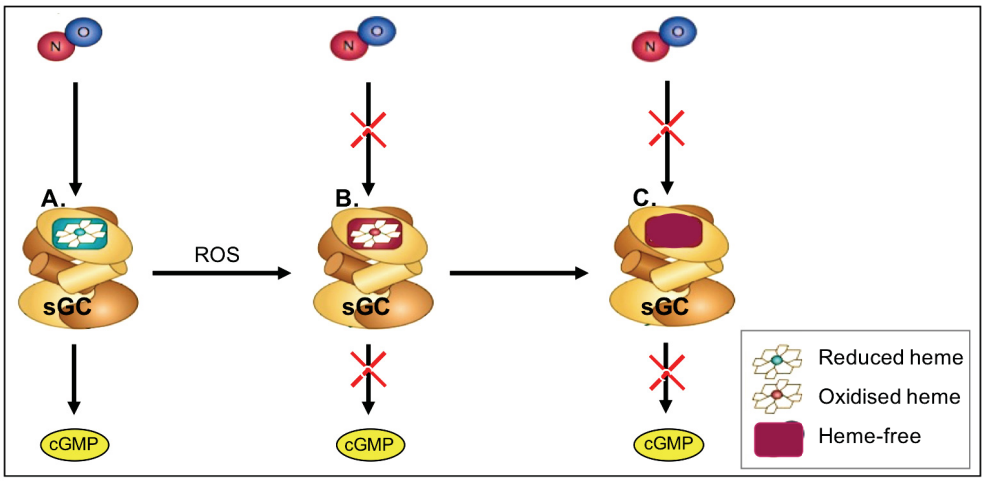

Figure 5 | Redox states of sGC

Modified from Evgenov, O.V., et al., 2006 [66]. (A) Physiologically, NO binds to sGC with reduced heme. Hence, GTP is transformed to cGMP by the activated sGC. (B) ROS oxidize the heme. Thus, NO is not able to bind and activate sGC. The cGMP concentration decreases. (C) Oxidation of sGC induces loss of heme from the sGC, which again prohibits the cGMP formation [66].

The sGC enzyme forms a heterodimer of the homologous alpha and beta subunits. Both exist in three different isoforms $\alpha1/\alpha2/\alpha3$ and $\beta1/\beta2/\beta3$ [132], which are encoded by GUCY1A3 and GUCY1B3 genes [143]. Only the heterodimer formation of both subunits forms a catalytic active sGC (Figure 5) [144]. The smaller β-subunit carries a prosthetic ferrous heme (Figure 5) [65], which contains a central Fe^{2+} atom [66]. NO targets mainly the reduced Fe^{2+} of the heme group [66, 145, 146]. The NO binding causes a nitrosyl-heme-complex and a conformation change of sGC [66]. Subsequently, activity of the enzyme increases [141] in a heme-dependent manner. This effect is potentiated by sGC stimulators, such as BAY 41-2272 [66]. Loss or

oxidation of heme [86] leads to inactivation of sGC (Figure 5) [141, 147, 148]. In this state, the sGC is unresponsive to NO [149] and NO-releasing drugs [150].

Increased ROS levels are able to oxidize the heme group of sGC [66]. Atherosclerosis causes an imbalance in the redox status of sGC [66, 151, 150]. This imbalance in the redox state of sGC abolishes the effect of NO [149] and dysregulates the signaling pathway [66, 150].

Thus, the sGC is considered as an essential receptor in the sGC/cGMP pathway and important for CVD and regulation of vascular tone [134, 150]. However, correlation between reduced CVD and sGC activity needs to be investigated further in RBCs.

2 Aim of the dissertation

Low NO bioavailability is correlated with CAD and the progression of CVD. The intracellular receptor sGC plays a crucial role in regulation of vascular tone and cardiac function. Although RBCs' primary function is to store intravascular NO, human mature RBCs are also supposed to be involved in the sGC/cGMP pathway and own non-canonical functions. The exact mechanisms, and whether RBCs contain a functional sGC and a sGC/cGMP pathway in human RBCs were not figured out yet.

Thus, the present work is based on the hypothesis that human RBCs contain an active NO/sGC pathway and own non-canonical functions, which may be influenced by CAD or effect its outcome (Figure 6).

In consequence, the main aim of this study was to find out whether (1) NO, (2) eNOS and (3) sGC have an effect on cGMP levels in human RBCs. Secondly changes in (4) sGC activity and sGC/cGMP signaling were investigated in human RBCs from patients with stable and unstable CAD as compared to age-matched controls. Along with previous aims, (5) NO metabolism and redox state in human RBCs from patients with CAD and (6) anemia were investigated (Figure 6).

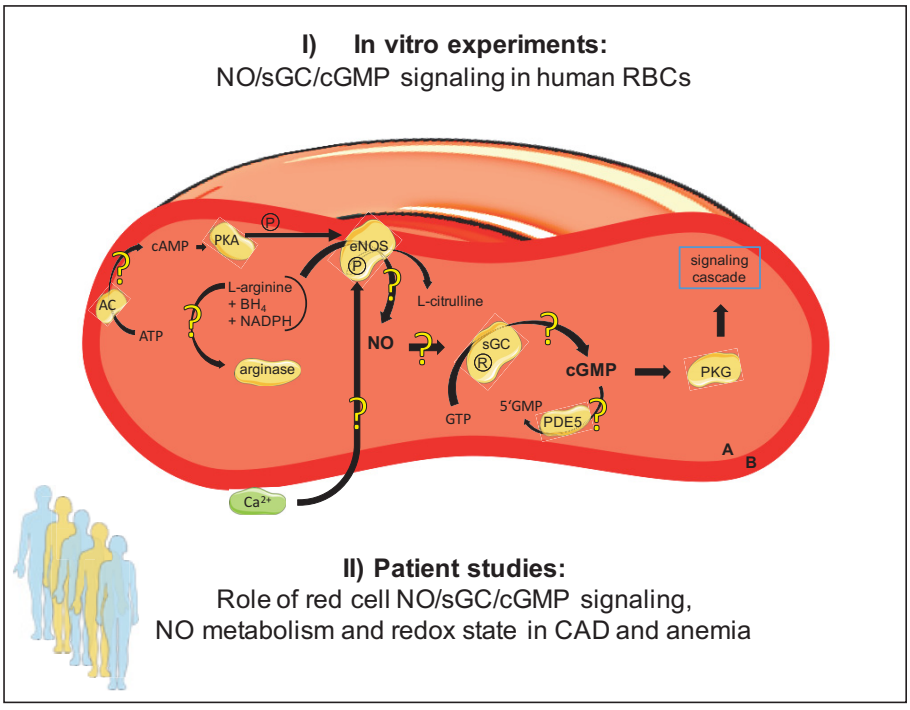

Figure 6 | Primary aims of this work

Present work will analyse the I) NO/sGC/cGMP signaling in human RBCs in correlation to II) possible changes in red cell signaling, NO metabolism and redox state in CAD and anemia.

In detail:

(1) Earlier studies showed that cGMP levels increase by the use of NO donors in human RBCs. In addition, PDE inhibition is supposed to elevate cGMP levels in a NO-independent manner in human RBCs. Based on these facts, the study investigates whether NO has an influence on cGMP levels and whether this effect is dependent on PDE activity in human RBCs.

(2) Human RBCs contain an active eNOS, which produces NO. This seems to be regulated in a Ca^{2+}/calmodulin-dependent manner. To verify the relevance of eNOS and eNOS regulating mechanisms in sGC/cGMP signaling in human RBCs, the present study analyzes whether cGMP levels are effected by eNOS activity, arginase activity, Ca^{2+} influx and AC stimulation in mature human RBCs.

(3) There is evidence for the existence of an active sGC in mature RBCs. Hence, this work analyzes whether mature human RBCs contain an active sGC, which responds to NO, and whether chemical compounds influence sGC activity. In this context, present study examines the dependency of cGMP levels on sGC activity in healthy human RBCs.

(4) Previous data indicate that eNOS activity is degraded in RBCs of stable CAD patients. Based on these findings, the CAD-study investigates whether sGC activity as well as sGCs' response to NO and further stimulation are changed in RBCs from patients with (stable or unstable) CAD as compared to age-matched controls. In this context, the sGC/cGMP pathway is examined as well.

(5) Reduced NO bioavailability and augmented oxidative stress were described in CVD. The CAD-study examines whether non-canonical functions of human RBCs, such as NO metabolism and redox state are preserved or changed in stable and unstable CAD compared to age-matched controls. In a follow-up study, RBC functions are investigated after PCI in unstable CAD as well.

(6) Anemia is presumed as one of the main risk factors for CVD. The anemia-study investigates whether levels of NO and redox state in mature RBCs of patients with unstable CAD with anemia differ from those with normal hemoglobin levels.

3 Materials and Methods

3.1 Materials

3.1.1 Equipment and resources

Table 1 | Appliances

Name	Company	Main office
Autoclave DX-65	Systec	Linden, DE
Bench DGN1500(DG03)	Wesemann	Wangen, DE
Centrifuge Micro 200R	Hettich	Tuttlingen, DE
Centrifuge Micro R	Hettich	Tuttlingen, DE
Centrifuge Micro Star 17R	VWR International	PA, USA
Centrifuge Rotina 38R	Hettich	Tuttlingen, DE
CP225D-OCE	Sartorius	Göttingen, DE
Flowcytometer FACS Verse	BD Bioscience	SanJose, USA
FluoStar Omega	BMG Labtech	Ortenberg, DE
Heating cabinet TH15	Edmund Bühler	Tübingen, DE
ImageQuant LAS400	GE Healthcare	Buc.hamshire, UK
Micro pipettes	Eppendorf	Hamburg, DE
Milli-Q Millipore	EMD Milipore Co.	California, USA
Minishaker MS1	IKA Labortechnik	Staufen, DE
pH Meter Lab870	Schott Instruments	Mainz, DE
Pipet boy comfort	Integra Bioscience	Zizers, SW
RCT Basic	IKA Labortechnik	Staufen, DE
Refrigerator	Bosch	Gerlingen, DE
Rotator	NeoLab	Heidelberg, DE
Sonyfiyer sonorexsuper RK255H	Bandelin	Berlin, DE
Concentrator 5301	Eppendorf	Hamburg, DE
Test tube heater	Stuart Scientific	Staffordshire, UK
TH 15 Incubator	Edmund Bühler	Hechingen, DE
Water bath GFL 1083	GFL	Burgwedel, DE

Table 2 | Expendable Material

Name	Company	Main office
96-well-micro-plates clear flat bottom	Greiner Bio One	Frickenhaus, DE
96-well-micro-plates white flat bottom	Greiner Bio One	Frickenhaus, DE
Beaker 5 ml	Schott Instruments	Mainz, DE
Beaker 10 ml	Schott Instruments	Mainz, DE
Beaker 500 ml	Schott Instruments	Mainz, DE
Beaker 800 ml	Schott Instruments	Mainz, DE
Combi-Stopper	B. Braun Melsungen AG	Melsungen, DE
Dewar Transportable	KGW Isotherm	Karlsruhe, DE
FACS-tubes 5 ml, 75x12 mm, PS	Sarstedt	Nümbrecht, DE,
Flacons 15 ml	Greiner Bio One	Frickenhaus., DE
Flacons 50 ml	Greiner Bio One	Frickenhaus., DE
Gloves, nitril powder free	Ansell	Tamworth, UK
Magnetic part. concentrator	Invitrogen	Darmstadt, DE
Magnetic stirrer	Sigma Aldrich	St. Louis, USA
Multistepper	Eppendorf	Hamburg, DE
Octanisept spray 250 ml	Schülke	Norderstedt, DE
Parafilm "M"	Pechiney Plastic	Ohio, USA
Pipette filter tip	Star Lab	Milton Keynes, UK
Pipette tip TipOne 10 µl	Star Lab	Milton Keynes, UK
Pipette tip TipOne 100 µl	Star Lab	Milton Keynes, UK
Pipette tip TipOne 200 µl	Star Lab	Milton Keynes, UK
Pipette tip TipOne 1000 µl	Star Lab	Milton Keynes, UK
Plaster Universal	Hansaplast	Hamburg, DE
Roller mixer	Stuart Scientific	Staffordshire, UK
Safe-Lock tubes clear, 1.5 ml	Eppendorf	Hamburg, DE
Safe-Lock tubes clear, 2.0 ml	Eppendorf	Hamburg, DE
Safe-Lock tubes dark, 1.5 ml	Eppendorf	Hamburg, DE
Safe-Lock tubes dark, 2.0 ml	Eppendorf	Hamburg, DE
Shaker KL-2	Edmund Bühler	Hechingen, DE
Single-use Syringes 10 ml	B. Braun Melsungen AG	Melsungen, DE
Single-use Syringes 20 ml	B. Braun Melsungen AG	Melsungen, DE
Stripetten Costar® 5 ml	Corning	NY, USA
Stripetten Costar® 10 ml	Corning	NY, USA
Stripetten Costar® 25 ml	Corning	NY, USA
Swab	L&R	Regensdorf, DE
Tube rotator	Eppendorf	Hamburg, DE
Volumetric flask	VWRInternational	PA, USA

Table 3 | Experimental assays

Name	Company	Main office
DC Protein Assay	BioRad	Munich, DE
Direct Cyclic GMP, Immunoassay Kit, DetectX	Arbor Assays	Michigan, USA

Table 4 | Chemicals

Name (article no.)	Company	Main office
Acetic acid (3738.4)	Carl Roth	Karlsruhe, DE
Aqua bidest	Millipore	Darmstadt, DE
Bay 41-2272	Bayer	Wuppertal, DE
Bay 60-2770	Bayer	Wuppertal, DE
BSA	Sigma Aldrich	St. Louis, USA
$CaCl_2$ (C7902)	Sigma Aldrich	St. Louis, USA
Ca-I (C7522)	Sigma Aldrich	St. Louis, USA
DAF-FM-DA (D23844)	Invitrogen	Darmstadt, DE
DCF-DA (D-399)	Invitrogen	Darmstadt, DE
DC protein assay (Lowry assay)	Biorad	California, USA
DEA/NO (D5431)	Sigma Aldrich	St. Louis, USA
Diethyl ether	Sigma Aldrich	St. Louis, USA
DMSO (5179.1)	Sigma Aldrich	St. Louis, USA
Ethanol 99 %	Merck	New York, USA
FACS clean (340345)	BD	SanJose, USA
FACS flow (342003)	BD	SanJose, USA
Forskolin	Sigma Aldrich	St. Louis, USA
GTN	B. Braun Melsungen	Melsungen, DE
$HBSS^+$ (14025-100)	Sigma Aldrich	St. Louis, USA
$HBSS^-$ (14175095)	Sigma Aldrich	St. Louis, USA
Heparin 25000 I. E. (PZN3029843)	Ratiopharm	Ulm, Germany
HCl 25 % (1.09911.0001)	VWR	Pennsylvania, USA
H_2O_2 30 % (216763)	Sigma Aldrich	St. Louis, USA
IBMX	Sigma Aldrich	St. Louis, USA
L-NAME	Enzo Life Sciences	Lörrach, DE
NaCl 0.9 % (s7653)	Sigma Aldrich	St. Louis, USA
NaOH (s8045)	Sigma Aldrich	St. Louis, USA
norNOHA	Cayman Chemicals	Tallinn, Estland
ODQ (ACRO328800100)	VWR	Pennsylvania, USA
PBS^+ (D8537)	Sigma Aldrich	St. Louis, USA
PBS^-(D8662)	Sigma Aldrich	St. Louis, USA
Reagent A (500-0113)	Biorad	California, USA
Reagent B (500-0114)	Biorad	California, USA
Reagent S (500-0115)	Biorad	California, USA
Sample Diluent	Arbor Assays	Michigan, USA
SDS 10 %-solution (A06760599)	Life technologies	California, USA
TCA	Sigma Aldrich	St. Louis, USA
TT (T10095)	Invitrogen	Darmstadt, DE

Table 5 | Software

Name	Company	Main office
Endnote	Thomson Reuters	New York, USA
FACS Suite V1.0.53841, 2013	BD	SanJose, USA
FlowJo V10	Tree Star	Ashland, USA
FluoStar Omega	BMG Labtech	Ortenberg, DE
Graph Pad Prism 6	AD Instuments	Dunedin, New Zealand
Microsoft Office 2011	Microsoft	Albuquerque, USA
OMEGA Control, Software 2007-2012	BMG Labtech	Ortenberg, DE
OMEGA DataAnalysis Software V2.41	BMG Labtech	Ortenberg, DE

3.1.2 Buffers

Table 6 | ELISA/Arbor Assay Kit

Name	Composition
Washing buffer	5 ml dilute wash buffer concentrate 95 ml Milli-Q water
cGMP conjugate buffer	125 µl conjugate concentrate 2.375 ml conjugate diluent
Acetylation reagent	400 µl acetic anhydride 800 µl triethylamine

Table 7 | Formulation of PBS

i) PBS$^+$	
Components	**Concentration (mM)**
Calcium chloride ($CaCl_2$)	0.90
Magnesium choride $(MgCl)_2$	0.50
Potassium chloride (KCl)	2.67
Potassium phosphate monobasic (KH_2PO_4)	1.47
Sodium chloride (NaCl)	138.0
Sodium phosphate dibasic (Na_2HPO_4)	8.10
ii) PBS$^-$	
Components	**Concentration (mM)**
Calcium chloride ($CaCl_2$)	0.00
Magnesium choride ($MgCl_2$)	0.00
Potassium chloride (KCl)	2.67
Potassium phosphate monobasic (KH_2PO_4)	1.47
Sodium chloride (NaCl)	136.9
Sodium phosphate dibasic (Na_2HPO_4)	8.10

Table 8 | Formulation of HBBS without phenol red

i) HBBS$^+$	
Components	**Concentration (mM)**
Calcium chloride ($CaCl_2$)	1.26
Magnesium chloride ($MgCl_2$)	0.49
Magnesium sulfate ($MgSO_4$)	0.41
Potassium chloride (KCl)	5.33
Potassium phosphate monobasic (KH_2PO_4)	0.44
Sodium carbonate (Na_2CO_3)	4.17
Sodium chloride (NaCl)	137.93
Sodium bicarbonate ($NaHCO_3$)	0.34
Glucose	5.56
Phenol red	0.00
ii) HBBS$^-$	
Components	**Concentration (mM)**
Calcium chloride ($CaCl_2$)	0.00
Magnesium chloride ($MgCl_2$)	0.00
Magnesium sulfate ($MgSO_4$)	0.00
Potassium chloride (KCl)	5.33
Potassium phosphate monobasic (KH_2PO_4)	0.44
Sodium carbonate (Na_2CO_3)	4.17
Sodium chloride (NaCl)	137.93
Sodium bicarbonate ($NaHCO_3$)	0.34
Glucose	5.56
Phenol red	0.00

3.1.3 Activators, stimulators and inhibitors

All used substances were prepared on the day of use and kept chilled on ice.

3.1.3.1 BAY 41-2272

BAY 41-2272 is a NO-independent, but heme-dependent sGC stimulator. Furthermore, it inhibits platelet aggregation and induces vasorelaxation without nitrate tolerance. 10 mM stock solution of BAY 41-2272 was prepared in 0.01 % dimethylsulfoxid (DMSO). It was provided by Dr. J-P. Stasch and Dr. L. Rössig (Bayer Healthcare Pharmaceuticals GmbH, Germany).

3.1.3.2 BAY 60-2770

BAY 60-2770 is an activator of oxidized sGC. 10 mM stock solution of BAY 60-2770 was diluted in 0.01 % DMSO. It was provided by Dr. J-P. Stasch and Dr. L. Rössig (Bayer Healthcare Pharmaceuticals GmbH, Germany).

3.1.3.3 Calcium-ionophore (Ca-I)

Ca-I is a substance, which is able to elevate the permeability of divalent ions into biological membranes. It is selective for Ca^{2+}. Thus, it stimulates indirectly the nitric oxide production through the calmodulin-dependent constitutive NOS by increasing intracellular Ca^{2+} levels. 9.5 mM stock solution of Ca-I were prepared in 0.01 % DMSO.

3.1.3.4 DMSO

DMSO is a highly polar, aprotic organic solvent with many applications, routinely used in polymerase chain reaction (PCR), amplification of cDNA libraries, DNA sequencing and more. 0.01 % DMSO was used to dissolve the above-mentioned substances.

3.1.3.5 Diethylamin NONOate (DEA/NO)

DEA/NO is a nitric oxide (NO)-donor. It spontaneously dissociates in a pH-dependent first-order process. 50 mM stock solution of DEA/NO was diluted in 0.01 M NaOH.

3.1.3.6 Forskolin

Forskolin is a cell-permeable diterpenoid that possesses anti-hypertensive, positive inotropic and adenylyl cyclase activating properties. It was diluted in PBS^- to a 12.18 mM stock solution.

3.1.3.7 Glyceroltrinitrate (GTN)

GTN is a NO-donor, which spontaneously dissociates pH-dependently. 4 mM solution of GTN was used.

3.1.3.8 3-Isobutyl-1-methylxanthine (IBMX)

IBMX is a non-specific PDE inhibitor. 300 mM stock solution of IBMX was prepared in 0.01 % DMSO.

3.1.3.9 N^G-Nitro-L-arginine-methylester (L-NAME)

L-NAME is a NOS inhibitor. It suppresses the release of NO by endothelial cells. 300 mM stock solution of L-NAME was resolved in double distilled water.

3.1.3.10 Nω-hydroxy-L-arginine (norNOHA)

The substance norNOHA is formed as an intermediate while eNOS catalyzes the oxidation of L-arginine to L-citrulline and NO. It is a potent, reversible inhibitor of arginase. L-arginine serves as a common substrate for both, eNOS and arginase in the cell. 57 mM stock solution of norNOHA was diluted in PBS^-.

3.1.3.11 1H-[1,2,4]-oxadiazolo-[4,3-a]-quinoxalin-1-one (ODQ)

ODQ is a competitive, irreversible and selective inhibitor of sGC by oxidizing the heme group of the beta subunit. 50 mM stock solution of ODQ was prepared in 0.01 % DMSO.

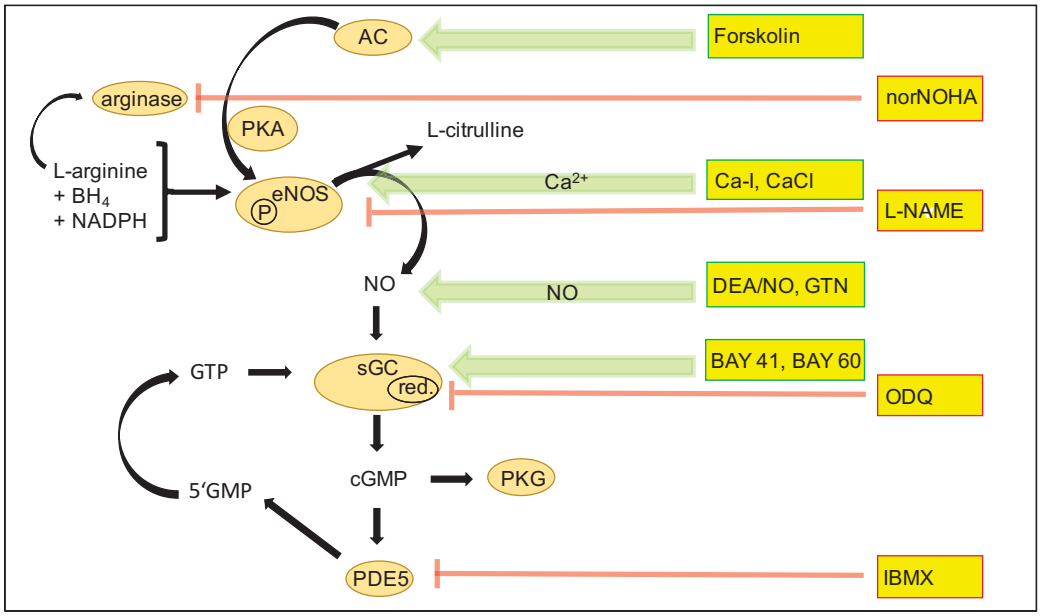

Figure 7 | Overview of the activators, stimulators and inhibitors

Summary of the functional mechanisms of the used substances in the NO/sGC/cGMP pathway. Forskolin activates AC. AC induces eNOS phosphorylation via PKA. NorNOHA inhibits arginase, which competes with eNOS for L-arginine. The eNOS produces NO and L-citrulline with L-arginine, BH_4 and NADPH. Ca-I increases the permeability for Ca^{2+} through the biological membrane. Together with $CaCl_2$, CA-I increases the intracellular Ca^{2+} concentration and activates the eNOS. L-NAME inhibits eNOS. DEA/NO and GTN are NO-donors. NO binds to sGC and activates the cGMP production. BAY 41-2272 stimulates and BAY 60-2770 activates the sGC, which is inhibited by ODQ. cGMP activates PKG. The non-specific PDE inhibitor IBMX inhibits amongst others PDE5, which reduces cGMP to 5'GMP.

Figure 7 demonstrates the mechanisms of the used substances in this work: As described before, NO is produced by phosphorylated eNOS using L-arginine [59], BH_4 and NADPH [115], which is inhibited by L-NAME (Figure 7). Arginase competes with eNOS for L-arginine [118], which can be inhibited by norNOHA (Figure 7).

Stimulated by Forskolin [67], adenylyl cyclase (AC) activates via cAMP PKA. This activates eNOS by phosphorylation (Figure 7). $CaCl_2$ causes Ca^{2+}-influx. Ca-I elevates intracellular Ca^{2+} via increasing the membrane permeability for Ca^{2+}. Thus, $CaCl_2$ and Ca-I support NO production by eNOS in a Ca^{2+}/calmodulin-dependent manner. DEA/NO and GTN are NO donors, which increase NO levels (Figure 7).

NO activates sGC, which converts GTN to cGMP. ODQ inhibits sGC [152], while BAY 41-2272 stimulates [66] and BAY 60-2270 activates sGC [152] (Figure 7). cGMP stimulates PKG, followed by vasodilatation (Figure 7) [105, 121, 122, 153]. PDE5 converts cGMP to 5'GMP [122], which is inhibited by IBMX, a non-specific PDE inhibitor (Figure 7). After oxidation cGMP forms GTP (Figure 7).

3.1.4 Fluorescent dyes

All used dyes and stock solutions were prepared just before use.

3.1.4.1 4-Amino-5-methylamino-2,7-difluorescein-diacetate (DAF-FM-DA)

DAF-FM-DA is a reagent for the quantitative detection of low concentrations of NO. Until it reacts with NO to form a fluorescent benzotriazole, DAF-FM-DA itself is non-fluorescent. The excitation maximum is 495 nm and emission maximum is 515 nm.

The detection of NO, a very unstable substance, in RBCs was performed with DAF-FM-DA via FACS analysis. Due to two acetate groups, DAF-FM-DA is able to permeate through cell membranes. Once inside, cell esterases cause the loss of these groups and DAF-FM-DA is trapped inside the cell. The use of DAF-FM-DA for the detection of NO in RBCs was validated before [43].

3.1.4.2 2,7-Dichlorodihydrofluorescein-diacetate (DCF-DA)

DCF-DA is the chemically reduced form of fluorescein, used as an indicator for ROS in cells. The excitation maximum is 492 to 495 nm and the emission maximum is 517 to 527 nm.

3.1.4.3 Thiol Tracker (TT)

TT is an intracellular thiol indicator for reproducible GSH detection. Because of its reaction with reduced thiols in intact cells, it can be used to estimate the cellular level of

reduced glutathione. The excitation maximum is 405 nm and the emission maximum is 525 nm.

3.2 Methods

3.2.1 RBC purification

Human blood was taken from subjects heparinized and centrifuged at 800 g for 10 minutes at 4 °C. Supernatant, plasma and buffy coat were aspirated carefully and the RBC pellets were filled into a new flacon. For FACS analysis, heparinized whole blood was used.

3.2.2 Preparation of stock solutions

i) 0.1 % Sodium dodecyl sulfate solution (SDS)

Sodium dodecyl sulfate (SDS) is a protein denaturant, which can be used to disrupt cell membranes for protein determination. 1 M sodium hydroxide (NaOH) was added to ultra-pure 10 % SDS-solution and then filled up to a 0.1 % stock solution with Milli-Q water.

ii) Trichloroacetic acid solution (TCA)

5 % TCA stock solution (1.75 g TCA with 35 ml Milli-Q water) was used to determine cGMP concentration. TCA was diluted in distilled water to a 0.5 % solution.

3.2.3 Protein determination

Protein determination was performed with the DC protein assay kit from BioRad (Munich, Germany). 10 % bovine serum albumin (BSA) stock solution was prepared with a concentration of 2 mg/ml by Aqua bidest and the same puffer solution was used for lysis of the RBCs. Working solution A' was prepared by mixing 20 µl of solution S and 1 ml of solution A. Standard dilutions ranging from 0.2 mg/ml up to 2.0 mg/ml (Table 9) were arranged for the standard curve and various protein lysate dilutions.

Then, 25 µl of provided reagent and 200 µl of reagent A’ were added to 5 µl of protein lysate. After 15 minutes of incubation at room temperature in the dark, the optical density was determined at 740 nm absorption with Omega analysis. Protein concentration was determined using Omega Mars software.

Table 9 | Standard dilutions

Standards	BSA concentration in puffer solution (mg/ml)
A	0.0
B	0.2
C	0.4
D	0.8
E	1.0
F	1.2
G	1.4
H	1.5
I	2.0

3.2.4 Extraction of cGMP

3.2.4.1 Sample treatment

In case of the CAD-study and the anemia-study, 15 ml heparinized blood and 30 ml of 0.9 % NaCl were added to a flacon and centrifuged at 800 g for 10 minutes at 4 °C (Figure 8). Supernatant, plasma and buffy coat were aspirated carefully and the RBC pellets were filled into a new flacon. These steps were repeated twice (Figure 8).

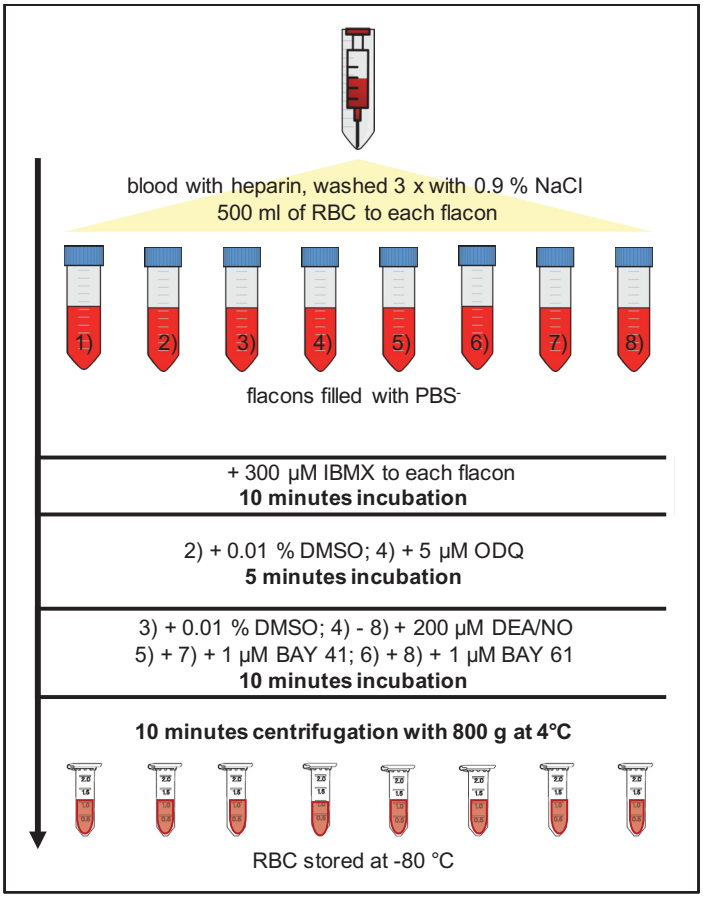

Figure 8 | Overview of sample-treatment in the CAD-study

Flacons were filled with 30 ml PBS$^-$ and treated with 300 µM IBMX. Then flacons were incubated with following additions (cf. Figure 8):

1) Control (CTRL)

2) 0.01 % DMSO

3) 200 µM DEA/NO + 0.01 % DMSO

4) 200 µM DEA/NO + 5 µM ODQ

5) 200 µM DEA/NO + 1 µM BAY 4-2272

6) 200 µM DEA/NO + 1 µM BAY 60-2770

7) 1 µM BAY 60-2770

8) 1 µM BAY 41-2272.

All incubations were conducted in a heating cabinet on a roller mixer at 37 °C. These samples were centrifuged with 800 g for 10 minutes at 4 °C (Figure 8). At last, the supernatant was pipetted with vacuum and the RBC pellets were decanted to 2 ml safe lock tubes each. All samples were frozen at -80 °C (Figure 8).

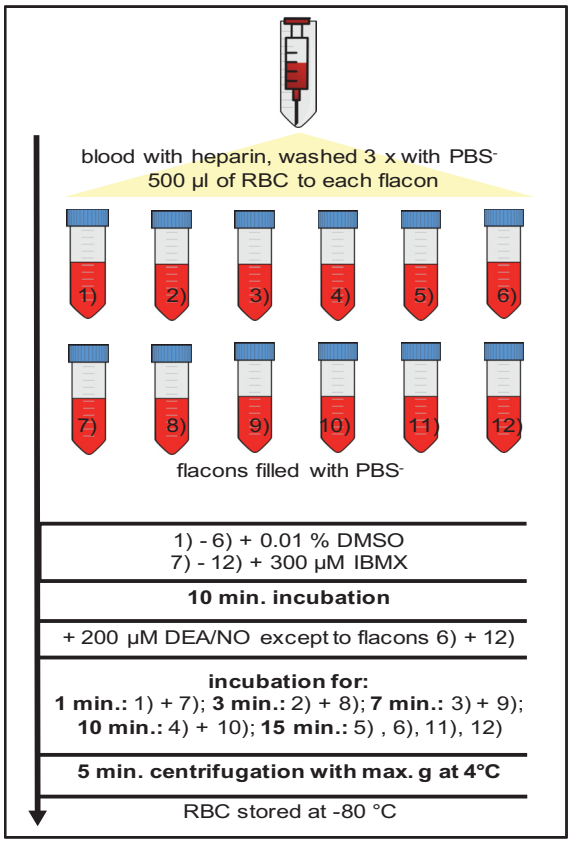

Figure 9 | Overview of the sample process for the DEA/NO Kinetic

In case of the DEA/NO Kinetic, blood was treated the same way as in the CAD-study (Figure 8), but the samples were washed 3 times with PBS$^-$ (instead of 0.9 % NaCl as

conducted in the CAD-study, cf. Figure 8). 500 µl of pellets were pipetted into 12 flacons, which were filled up with PBS^- and heated in a water bath at 37 °C (Figure 9).
Flacons for the DEA/NO Kinetic were incubated with 0.01 % DMSO or 300 µM IBMX as demonstrated in Figure 9 for 10 minutes:
1) - 5) 0.01 % DMSO + 200 µM DEA/NO
6) CTRL 1, incubated just with 0.01 % DMSO
7) - 11) 300 µM IBMX + 200 µM DEA/NO
12) CTRL 2, incubated only with 300 µM IBMX.
Flacons 6) and 12) were treated as negative controls. 200 µM DEA/NO were added to flacons 1) to 5) and 7) to 11). After a certain incubation time (Figure 9), the flacons were centrifuged with maximum g (1780 g) for 5 minutes at 4 °C. The supernatant was removed and frozen at -80 °C (Figure 9).
The kinetic series was repeated with 4 mM GTN, another NO-donor, instead of DEA/NO without any change in the protocol (Figure 9). One part of this experiment was done together with Jonathan Schmidt.
Sample treatment for the following experiments: 15 ml heparinized blood and 30 ml of PBS^- were added to a flacon and centrifuged at 800 g for 10 minutes at 4 °C. Supernatant, plasma and buffy coat were aspirated carefully and the RBC pellets were filled into a new flacon. These steps were repeated twice. 500 µl of pellets were pipetted into 12 flacons, which were filled up with PBS^- and heated in a water bath at 37 °C. Flacons were incubated with 300 µM IBMX for 10 minutes in a heating cabinet on a roller mixer at 37 °C. Then the substances were added to the flacons in the order as described below and were incubated again for 10 minutes in a heating cabinet on a roller mixer at 37 °C. Then, samples of each experiment were centrifuged with 1780 g (maximum g of used centrifuge) at 4 °C. After this procedure supernatant was removed and snap frozen in liquid nitrogen. All flacons were frozen at -80 °C for further steps. Afterwards, cGMP concentrations were measured by ELISA or RIA.
Concentration series with norNOHA and L-NAME (added substances and their final concentration):
1) CTRL
2) 100 µM norNOHA
3) 100 µM norNOHA with 3 mM L-NAME
4) 500 µM norNOHA
5) 500 µM norNOHA with 3 mM L-NAME
6) 1 mM norNOHA
7) 1 mM norNOHA with 3 mM L-NAME
57 mM norNOHA and 300 mM L-NAME were prepared.

Investigation with Ca-I and $CaCl_2$ (added substances and their final concentration):

1) CTRL
2) 1 mM $CaCl_2$
3) 10 µM Ca-I
4) 10 µM Ca-I with 1 mM $CaCl_2$
5) 10 µM Ca-I with 2.5 mM $CaCl_2$
6) 10 µM Ca-I with 5 mM $CaCl_2$
7) 200 µM DEA/NO with 10 µM $CaCl_2$
8) 200 µM DEA/NO.

Treatments with Forskolin and L-NAME (added substances and their final concentration):

1) CTRL
2) 5 µM Forskolin
3) 5 µM Forskolin with 3 mM L-NAME
4) 10 µM Forskolin
5) 10 µM Forskolin with 3 mM L-NAME
6) 50 µM Forskolin
7) 50 µM Forskolin with 3 mM L-NAME.

All treatments with Forskolin were also repeated with $HBSS^+$ instead of PBS^-.

3.2.4.2 Cell lysis for cGMP level determination

i) For ELISA:

RBC pellets were thawed from -80 °C on ice. 5 % TCA was prepared newly as described in chapter 3.2.2 ii). Thereafter, the defrosted samples were sonicated for 1 minute. 7 µl of that sonicated clear lysate was pipetted into a safe-lock tube and frozen at -20 °C. 250 µl of each sample was decanted into flacons and mixed up with 5 ml of the 5 % TCA solution and incubated on ice for 15 minutes.

Then, the samples were centrifuged at 2000 g for 10 minutes at 4 °C. Carefully the supernatant of each flacon was decanted into 3 test tubes. Every aliquot was filled with 3 ml saturated diethyl ether. Afterwards it was first vortexed to then remove the upper layer. This step was repeated 3 times.

After that, the rest of each supernatant was aliquoted and further processed in the speedvac for vacuum centrifugation at 60 °C for 3 to 4 hours until the RBC pellets were dry. Those pellets were re-suspended at room temperature in 50 µl of Sample Diluent (SD). Then, all samples were centrifuged at 14000 RPM for 30 seconds at 4 °C. Finally, the probes were frozen at -80 °C.

ii) For RIA:

RBC pellets were weighed and thawed. 500 µl Milli-Q water was added to the samples, which were vortexed. Each sample was aliquoted evenly about 250 µl into 2 separate safe lock tubes. Both tube series were filled up with 1.5 ml of 99 % ethanol and mixed up well, followed by centrifugation at 13000 g for 10 minutes at 4 °C.

In the next step, the supernatant of each sample was decanted into a safe lock tube. Those tubes were processed with an open lock in the speedvac at 60 °C for 2 to 3 hours. The dry supernatant was re-suspended in 75 µl of SD, prepared as 10 ml SD concentrate with 30 ml Milli-Q water. All samples were centrifuged at 13000 g for 10 minutes at 4 °C. The two aliquots of one origin were pooled together in a safe lock tube and frozen at -80 °C. Those samples were further processed by Dr. rer. nat. Evanthia Mergia the laboratory of the Ruhr-University of Bochum.

An aliquot of the pellet from the first centrifugation was treated further for protein determination. For that purpose, all pellets were incubated on a horizontal shaker for 15 minutes at 60 °C until the RBCs were free of supernatant with open lock. 1.5 ml of 0.1 % SDS-solution, prepared as described in chapter 3.2.2 i), was added to the tubes. Again, all samples were incubated on a horizontal shaker at 60 °C until the RBCs were fully diluted. 100 µl of diluted pellets from each tube of the same sample were pooled together and frozen at -20 °C.

3.2.4.3 Trial for the method of cGMP extraction

Before the studies were arranged, blood samples of independent subjects were treated with the same activators and inhibitors as described in chapter 3.1.3, but only with treatments 1-7 (same concentrations as in Figure 8).

At first PBS^- was used instead of 0.9 % NaCl. cGMP was determined using ELISA. In addition, the experiment was repeated with 8 treatments for each subject, completely similar to 3.2.4.1. This time, cGMP was determined by RIA (see chapter 3.2.6).

3.2.5 Enzyme linked immunosorbent assay (ELISA)

cGMP was measured using an enzyme immunoassay kit (Arbor Assays, Michigan, USA) according to manufacturer's descriptions (Assay protocol, insert, 2010). The simplified ELISA model is demonstrated in Figure 10, in which the ELISA technique can be described as a sandwich model. Here, two antibodies bind specifically the antigen or used sample (Figure 10). It is important that both antibodies bind to different

sites of the antigen to avoid interference of the antibodies with each other (Figure 10 B III).

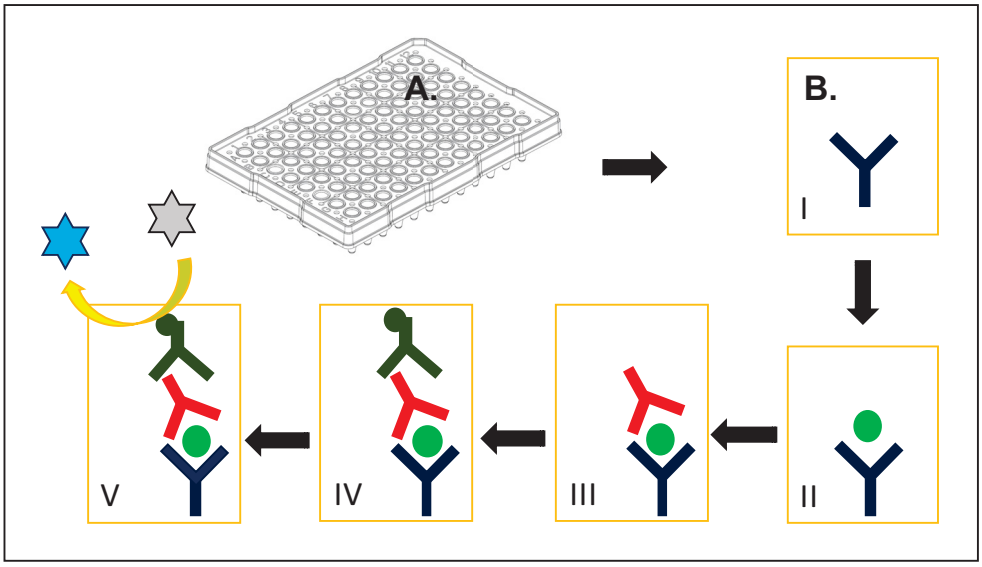

Figure 10 | ELISA

Image modified from Löffler and Petrides, Biochemie & Pathobiochemie, Heidelberg: Springer 7th edition [33]. Simplified ELISA technique. (A) Antibody coated micro plate [154]. (B) Micro plate well. I) The coat antibody is added to the 96 wells of the micro plate. II) Sample, *here:* RBC lysates that potentially carry cGMP, were added and incubated. After the incubation, the plate was washed, unbound sample components get removed, and the on coat antibody bound antigen remains. III) Detection antibody was added. This second antibody binds the antigen and forms an antibody-antigen-antibody complex. IV) Excess detection antibody was washed out. A suitable substrate, a reagent, which can be converted by the enzyme of the formed complex, was added. V) The reagent gets converted and thus enables its detection by color change, fluorescence or chemiluminescence. This was measured in a photometer at dual wavelengths of 450 and 540 nm. The amount of fluorescence correlates to the cGMP amount.

All samples were diluted to specific concentration and prepared as duplicates. The concentration of cGMP in the standard row was prepared with sample diluent (SD) and cGMP stock solution from 1.0 up to 0.0313 pmol/ml as described in Table 10.

Table 10 | Standard Preparation

Non-Acetylated	**Stock 2**	**Standard:**					
		1	**2**	**3**	**4**	**5**	**6**
SD (µl)	150	585	300	300	300	300	300
Addition	**cGMP Std**	**Stock 2**	**Std 1**	**Std 2**	**Std 3**	**Std 4**	**Std 5**
V (µl)	10	15	300	300	300	300	300
C (pmol/ml)	40	1	0.5	0.25	0.125	0.0625	0.03125

300 µl of SD were pipetted into a glass tube to act as the non-specified binding (NSB) standard tube. 15 µl of acetylation reagent was added to this tube and vortexed immediately. 200 µl content of standard and sample tubes was decanted separately to another fresh tube. 10 µl of acetylation solution was added and vortexed immediately. Acetylated samples and SD turned from orange to yellow. Within 30 minutes the next steps of the experiment were conducted.

The next steps were the following. At first, 50 µl of Plate Primer were added to all wells (Figure 10 B I). 75 µl acetylated SD were added to the NSB wells. 50 µl of acetylated SD was pipetted into new wells (B0 or 0 pmol/ml). 50 µl of acetylated samples or standards were pipetted into the other wells in the plate (Figure 10 B II). 25 µl of the diluted DetectX cGMP CLIA Conjugate were added to each well. Then DetectX cGMP CLIA Antibody was added to each well, except for the NSB wells (Figure 10 B III). The plate was incubated on a horizontal shaker for 15 minutes at room temperature and stored in a refrigerator at 4 °C for 16 hours.

The next morning each well was washed 4 times with 300 µl of wash buffer. The plate was put on clean absorbent towels in order to dry (Figure 10 B IV). 100 µl of the mixed chemiluminescent substrate was pipetted to each well (Figure 10 B IV). After 5 minutes of incubation time the luminescence was generated by the chemiluminescent plate reader. The absorbance was measured at dual wavelengths of 450 nm and 540 nm (Figure 10 B V).

For quantitative determinations a series of known antigen concentrations, the standard series, was carried out to obtain a calibration curve for the measured signal. Concentrations of samples were calculated by the standard curve.

Finally, it was decided to use RIA for the studies and further examinations. Following chapter 3.2.4.2, steps were conducted in the laboratory of the Ruhr-University of Bochum.

3.2.6 Radioimmunoassay (RIA)

RIA for the quantitative determination of cGMP was executed in the laboratory of the Ruhr-University of Bochum, Germany. Besides ELISA, RIA is a valid method to determine the cGMP-level correctly and with high accuracy.

Briefly explained, this method seeks to determine low cGMP levels with the immunological precipitation of radiolabeled cGMP analogue 125I-Sc-cGMP-TME (tracer) and a specific antiserum. Balance of bound and free form of the tracer can be shifted by non-labelled cGMP towards the free tracer. Hence, the precipitable bound fraction decreases. After protein precipitation and decanting of the supernatant, amount

of the bound tracer can be determined by measuring the radioactivity. The distribution of the tracer is determined at various concentrations of unlabeled cGMP.

At presence of an increased concentration of unlabeled cGMP, the bound fraction of the tracer and the measured radioactivity decrease. A standard curve was used for calculation.

Conditions for carrying out the RIA, treatment of the sample and antibody incubation were performed as described in Steiner, A. L., R. E. Wehmann, C. W. Parker and D. M. Kipnis "Radioimmunoassay for the measurement of cyclic nucleotides" [155].

Steps for RIA (following chapter 3.2.4.2) were performed by Dr. rer. nat. Evanthia Mergia in the laboratory of the Ruhr-University of Bochum.

3.2.7 Fluorescence-activated cell sorting (FACS)

FACS is a flow cytometry, which permits sorting of a heterogeneous mixture of biological cells based on the specific light scattering and fluorescent characteristics of each cell. This allows an objective and quantitative measurement of fluorescent signals from individual cells. It also enables a physical separation of cells of particular interest.

FACS analysis was carried out on the basis of previously standardized experimental protocols [43] with only minor modifications.

3.2.7.1 Preparation of the RBCs

RBCs obtain auto-fluorescent abilities, so that all experiments were performed with a control sample without the incubation of any dyes and additions.

Collected blood was anticoagulated immediately with 1 µl heparin (5000 IE/ml blood sample). Anticoagulated blood was diluted 1:500 in cooled PBS^{+} buffer.

FACS tubes were ordered in three rows with three FACS tubes, each containing:

1) Control
2) L-NAME (3 mM)
3) H_2O_2 (3 mM)

Additionally, there was one unlabeled tube, only filled with 500 µl of diluted blood as a negative control.

The tubes of the first row were filled with 500 µl of diluted blood. The tubes in the other two rows were filled with 495 µl diluted blood.

The NOS inhibitor L-NAME was added to all tubes of the second row and incubated for 30 minutes at 37 °C in water.

Then, all blood suspensions were loaded with the following dyes (final concentration): DAF-FM-DA (10 µM), DCF-DA (6.67 µM) and TT (6.67 µM).

Those samples were vortexed and then incubated again for 30 minutes at room temperature in the dark. After that, all samples were centrifuged for 10 minutes at 300 g and at 4 °C. Afterwards, the supernatant was removed and the RBCs were re-suspended in 500 µl PBS^+.

Diluted samples of RBCs in the third row were treated with H_2O_2 (3 mM) a radical. Afterwards, the sample were vortexed and incubated a second time at room temperature in the dark for 15 minutes. Then it was measured by the flow cytometer.

Finally, 500 µl of PBS^+ was added to all tubes and analyzed via FACS verse (FACS Suite software) and FlowJo.

3.2.7.2 Flow cytometry measuring

In order to be able to compare the results, the settings of the flow cytometer were kept the same in each experiment. To verify these settings SpheroTM Rainbow Calibration Particles were measured in PBS^+ buffer each day. The fluorescence level was determined in all decisive fluorescence channels (Figure 11) and adjusted if necessary before the measurement of samples started. The samples were measured directly after the end of the incubation period.

All measurements were performed at the same flow cytometer (FACS VERSE) using the software FACS Suite. The data was then analyzed by the FlowJo software V 9 (TreeStar, Ashland, OR, USA). The red blood cells were identified by their size (forward light scatter, FSC) and granularity (side light scatter, SSC). An unstained sample with RBCs was used as a control of the auto fluorescence.

The fluorescent dyes DAF-FM-DA and DCF-DA were excited by an argon laser with 488 nm. The emitted fluorescent signal was measured in the FITC channel for DAF-FM-DA DA and DCF-DA or V 500 channel for TT.

Basal fluorescent signals were subtracted from gained data in the flow cytometer and demonstrated as mean fluorescence intensity (MFI).

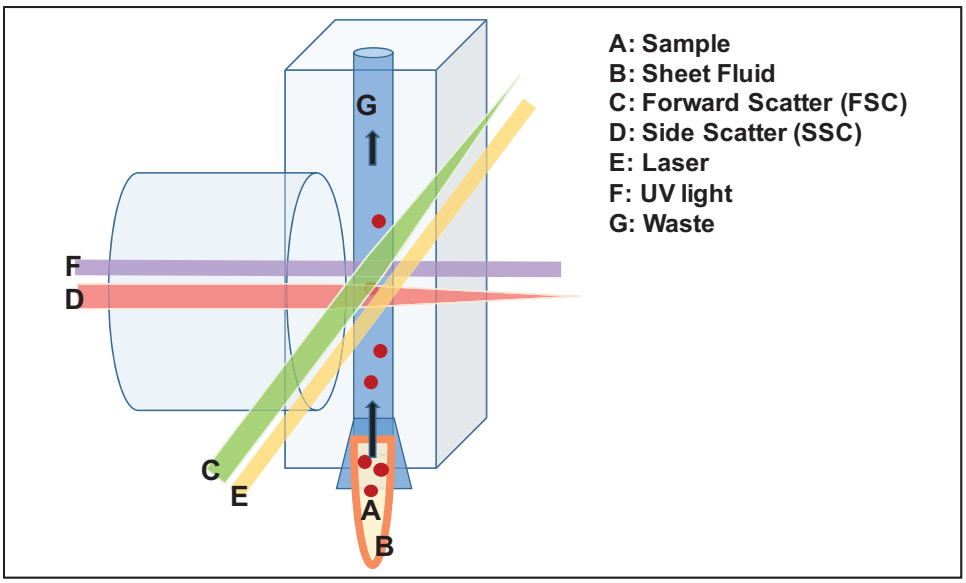

Figure 11 | FACS

Image modified from Alice Longobardi Givan, Flow Cytometry, Weinheim: Wiley-Liss, 2. edition [156]. The simplified mechanism of FACS. The principle is based on the emission of optical signals on the part of the cell as it passes through a thin laser beam. The sample gets into a microchannel, a highly precise cell of glass or quartz. This reaction is caused by sheath flow. Each cell passes through the measuring range of the laser beam. Here, a detector measures the scattered light or fluorescence signal. The forward scattered light determines the diffraction of light at a flat angle and is depended on the volume of the cell. The side scattered light counts the refraction of the light at right angles. This is influenced by the granularity of the cell, the size and structure of its nucleus, and the amount of vesicles in a cell. The amount of scattered light correlates with the size of the cell and with their complexity, so that different cell types can be counted separately by the used computer.

3.2.7.1 Loading the RBCs with DAF-FM-DA

To detect intracellular NO, diluted RBCs were incubated with DAF-FM-DA for 30 minutes at room temperature in dark. 0.01 % DMSO was pipetted into the vial of DAF-FM-DA.

3.2.7.2 Loading the RBCs with DCF-DA

To quantify free radicals like H_2O_2 and $^{\cdot}O_2$, DCF-DA was used. A 40 mM stock solution of DCF-DA diluted in 0.01 % DMSO was prepared in the time of the first incubation.

3.2.7.3 Loading the RBCs with TT

Differences in GSH levels in response to oxidative stress in subpopulations of cells were reported indirectly via the fluorescent dye Thiol Tracker (TT), which stains

reduced thiols. TT was dissolved in 30 ml 0.01 % DMSO and diluted 1:500 with chilled PBS^+ buffer.

3.2.8 Subjects and blood sampling

For the investigations human RBCs from healthy volunteers' blood (23-33 years) were gained from the antecubital vein and anticoagulated with heparin [5000 IU/ml].

All investigations were performed according to the Declaration of Helsinki as well as the GCP and were approved by the local ethics committee (no. 3857). The ethic vote for the use of human blood is approved by ENOS2010. All investigations were started after the subjects had agreed to it by written informed consent according to the legal data protection requirements. Afterwards, the blood was processed for further examination.

Blood sampling for CAD and anemia-study were described in 3.2.9.

3.2.9 Clinical study protocol

The present work includes two patient studies. The studies were led by Prof. Dr. med. Malte Kelm, head of the cardiology department, and coordinated by Prof. Dr. rer. nat. Dr. Miriam M. Cortese-Krott.

The department of cardiology, pneumology and angiology at the University Hospital of Düsseldorf recruited the subjects for both studies, performed mainly by Dr. med. G. Wolff, doctor of the cardiology department.

The cardiovascular risk factors were determined by medical history and physical examination of the subjects. In addition, routine clinical parameters were determined in the central laboratory of the University Hospital of Düsseldorf (cf. Figure 13).

The studies were approved by the local ethic committee (CAD-study: no. 4460 and anemia-study: no. 3875) and performed in accordance to the guidelines of good clinical practice (GCP) as well as to the Declaration of Helsinki. The ethic vote for the use of human blood was approved by ENOS2010.

Subjects were informed about the methods and investigations of this work. They signed a written informed consent before indexing according to the legal data protection requirements.

Studies were carried out on an empty stomach on the examination day. Blood was taken by cubital venial puncture with BD safety lock system from the volunteers avoiding hemolysis. Then it was anticoagulated with heparin [5000 IU/ml].

Analysis was performed on pseudonymized data. This pseudonymized data will be archived for 10 years at the University Hospital of Düsseldorf.

3.2.9.1 CAD-study

The CAD-study is a monocentric, prospective and controlled cross-sectional 3 armed study including patients with stable and unstable CAD and age-matched healthy subjects. This study was sponsored by BAYER Healthcare Pharmaceuticals GmbH, Leverkusen, Germany. The main aim of the CAD-study was to investigate eNOS expression and activity as well as the levels of NO-metabolites in plasma and RBCs. Other objectives of this study (clinical parameters, nitrate/nitrite levels, cGMP levels etc.) are mentioned in Figure 13.

The aim of this particular work was to find out, whether the sGC activity, the sGC/cGMP pathway, NO-metabolism and redox state are affected in RBCs with stable and unstable CAD.

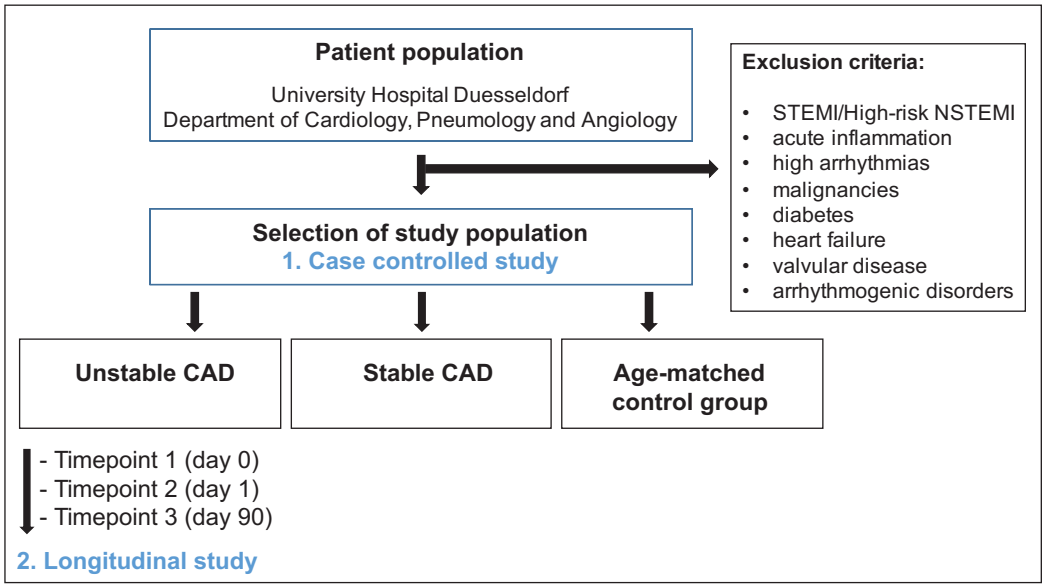

Figure 12 | Main structure of the CAD-study

The department of Cardiology, Pneumology and Angiology of the University Hospital of Düsseldorf recruited subjects for all three cohorts (stable and unstable CAD patients and age-matched healthy humans) of the case-controlled study. Main selection criteria were PCI and flow mediated-dilatation (FMD). An additional longitudinal study was performed in the unstable CAD group before, 1 day and 90 days after ischemia treatment.

The structure of the CAD-study was demonstrated in Figure 12. Blood samples were collected additionally in the unstable CAD group at different points in time for a controlled, longitudinal study (Figure 12). The unstable CAD group analysis was assessed before, after the first day as well as after 90 days after the ischemia treatment via PCI (Figure 12).

Male patients (between 50-70 years) were selected via PCI and FMD as well as routine clinical parameters.

The sample groups feature the following criteria:

1) **Stable CAD (n=8):**
   - Angiographically diagnosed CAD
   - Abstinence of acute coronary syndrome (ACS) for at least 3 months
2) **Unstable CAD (n=20):**
   - Angiographically diagnosed CAD
   - Acute coronary syndrome
   - Unstable angina pectoris with significant coronary stenosis (troponin -, no significant ST increase) and low-risk Non-STEMI (troponin +, no significant ST-elevation)
3) **Age-matched healthy humans (n=26):**
   - Angiographically or clinically no atherosclerosis

Acute inflammation (C-reactive protein (CRP) > 1.0 mg/dl, blood leukocytes > 11000/µl), malignancies, high arrhythmias, diabetes, heart failure, valvular disease or treatments with sGC/cGMP affecting medicines as well as patients with STEMI or high-risk NSTEMI were exclusionary criteria.

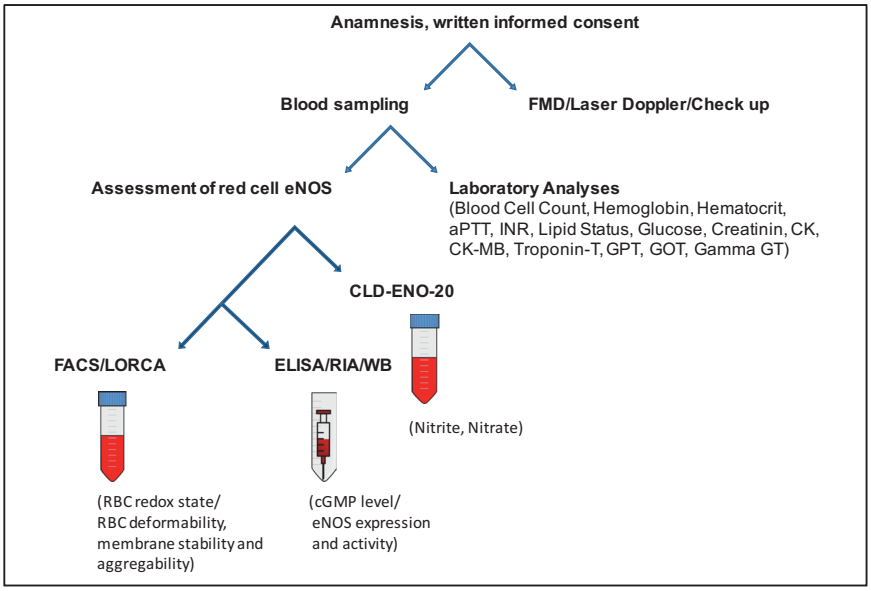

Figure 13 | Overview of the study protocol of the CAD-study

Cardiovascular measurements, hemodynamic investigations, blood sampling and analysis were done following a defined protocol.

The study includes biochemical, cell biological analysis as well as hemodynamic and cardiovascular investigations. Figure 13 summarizes all included investigations of the CAD-study.

Vital signs like non-invasive blood pressure and heart rate were measured in the clinic. Moreover, comorbidities and cardiovascular risk factors were determined as well (Table 11).

The endothelial function was determined by ultrasound using established, standardized protocols. Flow-mediated dilation (FMD), microvascular function and pulse wave were measured (Table 11).

The above-mentioned parameters were measured by Dr. Georg Wolff and Dr. med. Ralf Erkens from the department of Cardiology, Pneumology and Angiology, University Hospital of Düsseldorf. The study was performed together with Cand. med. Claudio Parco, Cand. med. Jonathan Schmidt and PhD student Dr. rer. nat. Christina Panknin.

In this particular work, cGMP level in RBCs was pointed out by cGMP assays or RIA. Redox state in RBCs of CAD patients and age-matched healthy subjects was measured using FACS analysis.

3.2.9.2 Anemia-study

The anemia-study is a cross-sectional study with three groups of healthy humans of different age groups as well as a group of patients with atherosclerosis (coronary heart disease, cerebral vascular disease, degenerative valvular heart disease) and anemia or normal hemoglobin levels.

The study includes biochemical analysis and hemodynamic studies (Table 12). Overall, the main aim of this study was to find out whether RBCs show age related changes in endothelial function via FMD. Moreover, the study was analyzing circulating NO-pool in plasma and RBCs, further parameters of RBCs (redox state, NO-signaling, RBC function and aging, cell-to-cell-interaction and quantity) as well as inflammatory and cardiovascular features (hemodynamics and microcirculation values).

Especially, presented study intended to investigate whether NO levels and redox state differ in RBCs of patients with atherosclerosis (group 4: unstable CAD) and anemia compared to atherosclerosis patients with healthy hemoglobin levels by FACS analysis. Additionally, parameters such as iron, transferrin saturation, free transferrin receptor, ferritin, ferritin-index, RPI, reticulocytes, erythropoietin, haptoglobin, LDH and free hemoglobin were measured in all groups.

The mentioned parameters were measured by Dr. Georg Wolff and Dr. med. Ralf Erkens from the department of Cardiology, Pneumology and Angiology, University Hospital of Düsseldorf.

The laboratory experiments were performed together with Cand. med. Claudio Parco and PhD student Dr. rer. nat. Christina Panknin.

The sample group feature the following criteria (male and female subjects):

- **Group 1:** Healthy humans aged 18-25 years
- **Group 2:** Healthy humans aged 35-45 years
- **Group 3:** Healthy humans aged > 70 years
- **Group 4:** Patients with atherosclerosis (coronary heart disease, cerebral vascular disease, degenerative valvular heart disease, profound valvular aortic stenosis) with anemia or normal hemoglobin levels (heamoglobin concentrations below 12 g/dl blood in women and below 14 g/dl blood in men).

Malignancies, high arrhythmias, arterial hypertension (blood pressure ≥140/90 mmHg) and hypotension (≤100/60 mmHg), diabetes (fasting plasma glucose ≥128 mg/dl), hypercholesterolemia (low-density lipoprotein (LDL) ≥250 mg/dl, high-density lipoprotein (HDL) ≤45 mg/dl), acute inflammation (CRP >0.5 mg/dl), high arrhythmias, heart failure (NYHA III-IV), intolerance to GTN as well as terminal renal insufficiency were exclusionary criteria.

3.2.10 Statistical analyses

If not stated otherwise, the data was referred as mean +/- standard error of the mean (SEM). The means of separate groups were determined by one-way ANOVA followed by an appropriate *post hoc* test (*Bonferroni/Tukey*) for multiple comparisons between groups as described in the legends in chapter 3. Paired or unpaired Student's *t*-test was used to compare two groups. Values were considered as statistically significant, if $p \leq 0.05$ tested by GraphPad Prism 6.0.

The data was expressed as box & whiskers plots or column mean, error bars & mean plots in accord with Tukey for outlier analysis.

The statistical data processing was accomplished with Microsoft Office 2011 and GraphPad Prism 6.0.

4 Results

4.1 Analysis of NO/sGC/cGMP signaling in human RBCs

4.1.1 NO increases cGMP levels in a PDE activity-dependent manner

The objective of this investigation was to evaluate whether cGMP levels in RBCs are dependent on NO application. For that purpose, blood samples were incubated with two NO-donors, DEA/NO (200 µM) and GTN (4mM), in PBS$^-$.

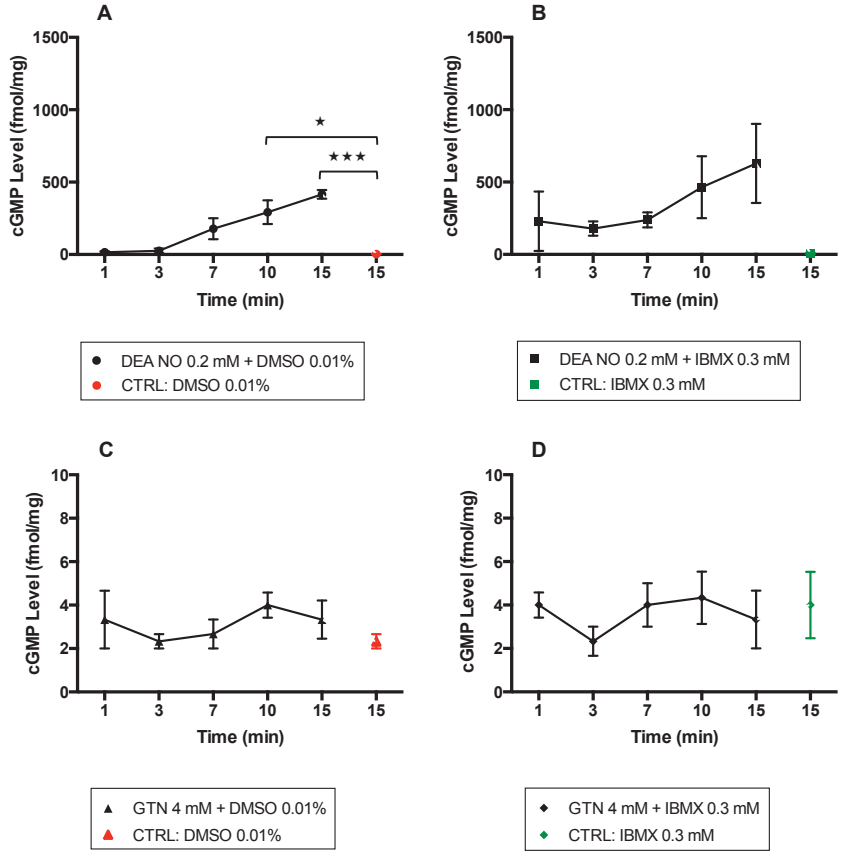

Figure 14 | NO influx by DEA/NO raises cGMP levels in human RBCs

(A/B) Time-dependent increase of cGMP levels after NO application by NO-donor DEA/NO (0.2 mM) in absence (A) and presence of non-specific PDE inhibitor IBMX (0.3 mM) (B) in human RBCs. (C/D) GTN, another NO-donor, does not show any effect on cGMP levels in absence (C) and presence of IBMX (D) in human RBCs. (A-D) Blood samples were incubated with NO-donors for 1-15 minutes at 37 °C in PBS$^-$ and were compared to CTRL. RBCs were lysed and protein content was determined by RIA. Unpaired one-way ANOVA against each data: post-hoc test Tukey, n=6, ★ $p \leq 0.05$, ★★★ $p \leq 0.0005$. Outlier analysis was performed graphically by column mean, error bars & mean connected plot according to mean with SEM. One part of the GTN kinetic measurement was performed together with Cand. med. Jonathan Schmidt. RIA measurement was performed by Dr. rer. nat. Evanthia Mergia, Ruhr-University of Bochum.

The cGMP levels were determined in absence or presence of non-specific PDE inhibitor IBMX (300 µM). DEA/NO and GTN were solved in 0.01 % DMSO, an organic solvent. cGMP levels were analyzed by RIA.

Figure 14 A shows that DEA/NO caused time-dependent cGMP level increase in human RBCs. Compared to the control sample, significant (up to 700-fold) growth in this sample is observed after 10 and 15 minutes (Figure 14 A).

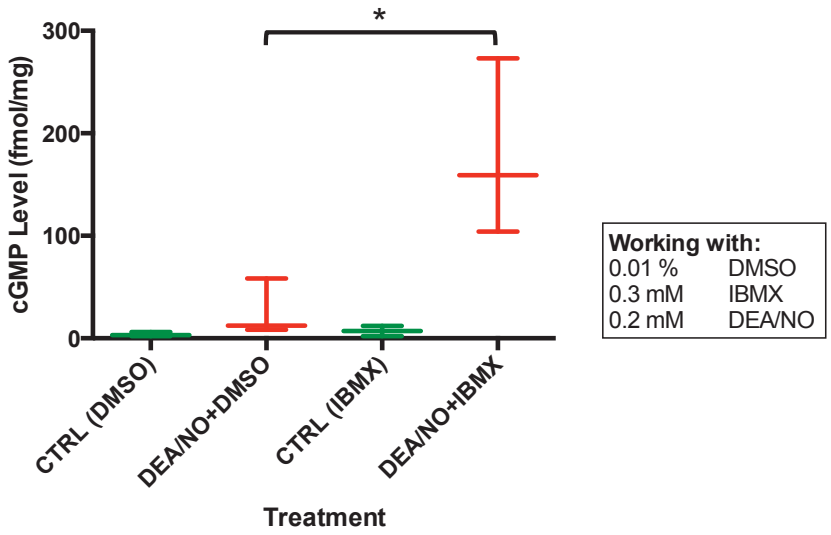

Figure 15 | Significant effect of PDE inhibition on cGMP levels in presence of NO

NO induced increase in cGMP levels is heightened by PDE inhibition with 0.3 mM IBMX in presence of 0.2 mM DEA/NO in human RBCs. Blood samples were incubated for 3 minutes at 37 °C in PBS^{-}. Protein content of lysed RBCs was determined by RIA. Data are expressed as box and whiskers plot according to Tukey, unpaired *t*-test, n=6, * $p \leq 0.05$. RIA measurement was performed by Dr. rer. nat. Evanthia Mergia, Ruhr-University of Bochum.

PDE inhibition with non-specific IBMX (0.3 mM) further indicates increase of cGMP levels compared to those samples incubated without IBMX (Figure 14 B) only in presence of NO. After 3 minutes of incubation cGMP levels raise significantly by PDE inhibition in presence of NO (Figure 15).

Samples incubated with GTN (4 mM) and IBMX do not cause any differences in the cGMP levels (Figure 14 C/D).

In conclusion, NO application by DEA/NO induces cGMP level increase in human RBCs, which is further boosted by PDE activity.

4.1.2 Role of eNOS and regulating mechanisms in human RBCs

To analyze the impact of red cell eNOS and eNOS/NO pathway associated enzymes or mechanisms on cGMP levels in human RBCs, RIA was used. In detail, influence of arginase inhibition, Ca^{2+} influx and AC activation on cGMP levels in human RBCs was investigated in this context. The experiment was performed jointly with Dr. rer. nat. Evanthia Mergia, Ruhr-University of Bochum, who performed the RIA measurement (steps following 3.2.4.2 ii).

4.1.2.1 Inhibition of arginase and eNOS do not effect cGMP levels

Both enzymes, eNOS and arginase, compete for L-arginine for different purposes. To identify whether activity of arginase and red cell eNOS influences cGMP levels in human RBCs arginase inhibitor norNOHA (0.1/0.5/1 mM) and eNOS inhibitor L-NAME (3 mM) were used in this experiment.

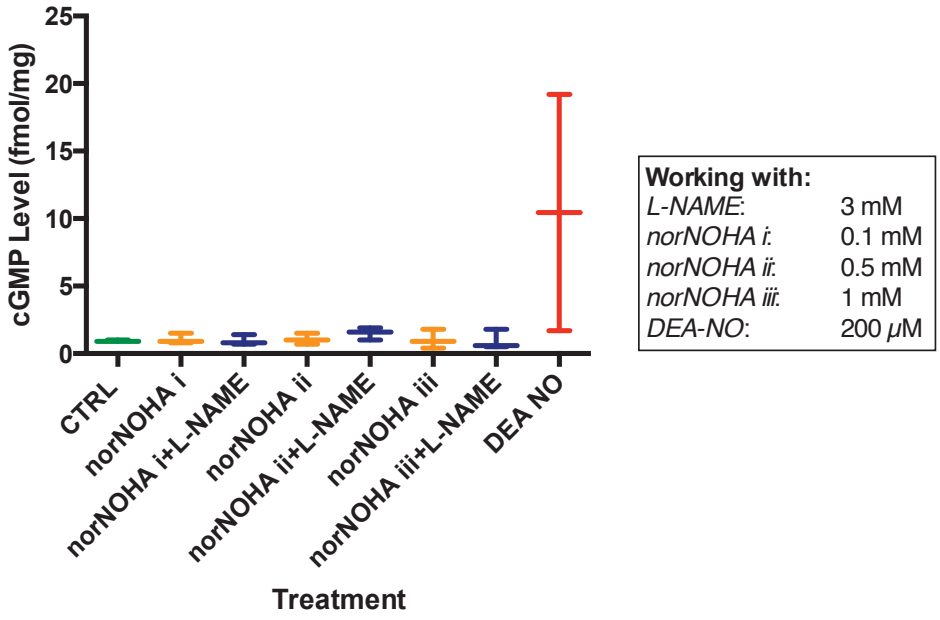

Figure 16 | cGMP levels are independent of arginase and eNOS activity

Arginase inhibition by norNOHA (0.1/0.5/1 mM) and eNOS inhibition by L-NAME (3 mM) do not change cGMP levels in human RBCs. Apparent cGMP increase is caused by NO influx via NO-donor DEA/NO (200 µM) only. RBCs were incubated with norNOHA, L-NAME and DEA/NO in PBS^{-} at 37 °C for 10 minutes. Protein content of lysed RBCs was analyzed via RIA. Data are expressed as median in a Tukey distribution, box and whiskers plot, unpaired one-way ANOVA against each data: post-hoc test Tukey, n=3. RIA measurement was performed by Dr. rer. nat. Evanthia Mergia, Ruhr-University of Bochum.

Figure 16 does not demonstrate any change in cGMP levels after incubation with 3 mM L-NAME or norNOHA in neither of the 3 concentrations (0.1/0.5/1 mM).

Notable increase in cGMP levels is observed only after NO influx by 200 µM DEA/NO (Figure 16). However, this result is not significant.

In summary, it can be supposed that, cGMP levels are dependent on NO, but not on the activity of arginase or eNOS.

4.1.2.2 Ca^{2+} influx does not influence cGMP levels

In order to investigate, whether Ca^{2+} influx changes cGMP levels in RBCs, 10 µM Ca-I, a substance, which increases permeability of the biological membrane for Ca^{2+}, and hence, elevates the intracellular Ca^{2+} level, was used. $CaCl_2$ was added in different concentrations (1/2.5/5 mM) to increase extracellular Ca^{2+} level and assure its availability.

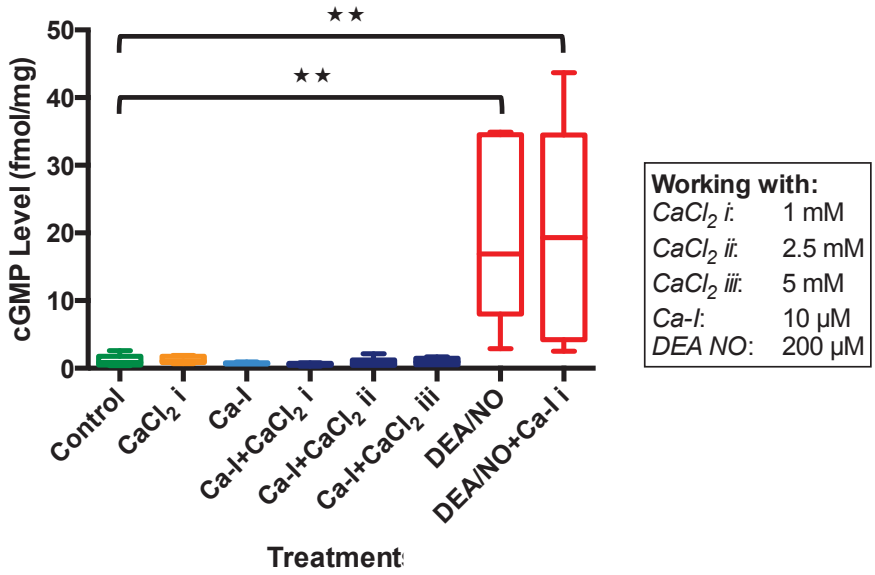

Figure 17 | Ca^{2+} influx has no effect on cGMP levels

Ca^{2+} influx by $CaCl_2$ (1/2.5/5 mM) and using Ca-I (10 µM) via increasing permeability of the biological membrane for Ca^{2+} do not change cGMP levels in human RBCs. Significant positive influence on cGMP levels is only indicated by NO-donor DEA/NO (200 µM). RBCs were incubated with Ca-I and $CaCl_2$ in PBS^- at 37 °C for 10 minutes. The cGMP levels were measured by RIA. Unpaired one-way ANOVA against each data: post-hoc test Tukey, ★★ $p \leq 0.005$. Outlier analysis was performed graphically by box and whiskers plot according to Tukey, n=6. RIA measurement was performed by Dr. rer. nat. Evanthia Mergia, Ruhr-University of Bochum.

Figure 17 demonstrates that there is no change in cGMP levels in human RBCs by Ca-I and $CaCl_2$. On the contrary, incubation with NO-donor DEA/NO (200 µM) results in a significant increase in cGMP levels (Figure 17). Treatment of the samples together with DEA/NO (200 µM) and Ca-I (10 µM) does not differ from the result by the treatment only with DEA/NO. The cGMP levels only changes when DEA/NO is used.

Overall, the investigation shows that Ca^{2+} influx does not influence cGMP levels in human RBCs. As already mentioned in 4.1.1 and 4.1.2.1, cGMP levels are dependent on NO.

4.1.2.3 cGMP levels are independent of AC activation

Forskolin activates adenylyl cyclase (AC). AC stimulates via cAMP the protein kinase A (PKA). PKA phosphorylates eNOS [33]. Thus, it stimulates the sGC/cGMP signaling through NO production.

To analyze whether this kind of stimulation of eNOS has an effect on the cGMP level in human RBCs, blood samples were treated with (5/10/50 µM) Forskolin and 3 mM L-NAME in PBS^- (Figure 18 A) and $HBSS^+$, a buffer containing Ca^{2+}among other substances, (Figure 18 B) for 30 minutes.

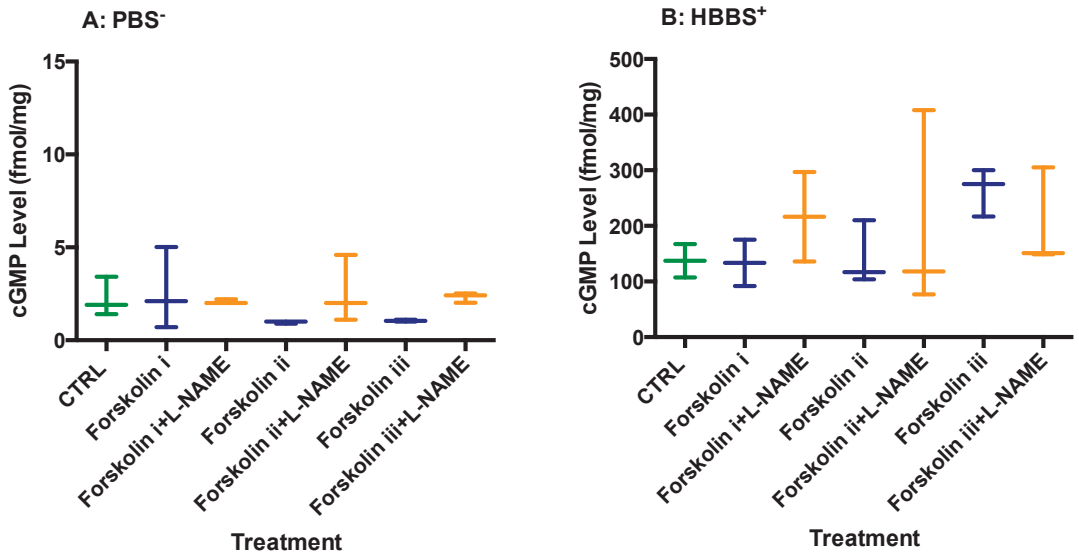

Working with:
Forskolin i: 5 µM, *Forskolin ii*: 10 µM, *Forskolin iii*: 50 µM, *L-NAME*: 3 mM

Figure 18 | cGMP levels are independent of AC activation by Forskolin

(A/B) AC activation by Forskolin (5/10/50 µM) does not have an impact on cGMP levels in human RBCs. AC stimulation is not dependent on eNOS inhibition by L-NAME (3 mM). (A/B) Blood samples were incubated with Forskolin and L-NAME at 37 °C for 10 minutes in (A) PBS^-, a buffer without Ca^{2+}, and (B) $HBSS^+$, a buffer containing Ca^{2+}. Data were analyzed via RIA, expressed as box and whiskers plot according to Tukey. Unpaired one-way ANOVA against each data: post-hoc test Tukey, n=3. RIA measurement was performed by Dr. rer. nat. Evanthia Mergia, Ruhr-University of Bochum.

Compared to the control sample, the results show that neither in PBS^- (Figure 18 A) nor in $HBSS^+$ (Figure 18 B) there is a significant change in cGMP levels by AC

stimulation via Forskolin. However, changes in cGMP levels by Forskolin are also not dependent on eNOS inhibition by L-NAME. Besides that, it can be observed that cGMP levels are higher in $HBSS^+$ (Figure 18 B) than in PBS^- (Figure 18 A) in general.

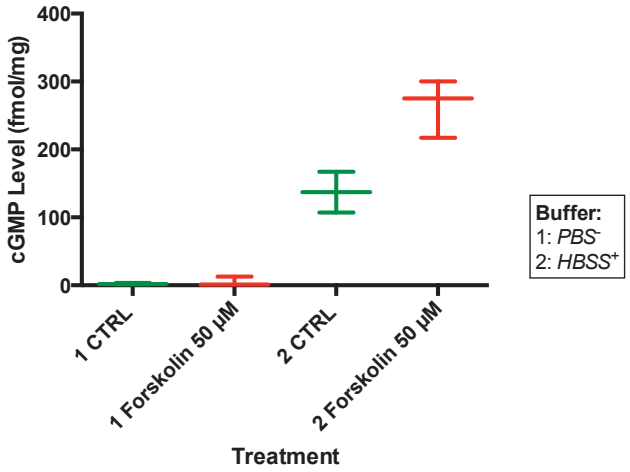

Figure 19 | Significant increase of cGMP levels in $HBSS^+$, a Ca^{2+} containing buffer

The cGMP levels increase significantly in $HBSS^+$, a buffer containing Ca^{2+} amongst others, compared to those levels in PBS^-, a buffer without Ca^{2+} in presence and absence of Forskolin (50 µM). Blood samples were incubated with Forskolin at 37 °C for 10 minutes and values were determined by RIA. Unpaired *t*-test, ★★ $p \leq 0.01$, ★★★ $p \leq 0.0005$, expressed as box and whiskers plot according to Tukey, n=3. RIA measurement was performed by Dr. rer. nat. Evanthia Mergia, Ruhr-University of Bochum.

Figure 19 shows significantly higher levels of cGMP in the control sample and by AC activation using 50 µM Forskolin in $HBSS^+$ compared to PBS^-. Here, Ca^{2+} is one of the main differences between the buffers indicating influence of Ca^{2+} on cGMP levels in human RBCs.

In summary, AC activation by Forskolin has no effect on the cGMP levels in human RBCs. This mechanism is independent from red cell eNOS activity. The results indicate that changes in cGMP levels might be influenced by Ca^{2+} in human RBCs.

4.1.3 Functional sGC stimulation in mature human RBCs

To verify, whether a functional sGC exists in human RBCs and whether sGC activation, stimulation or inhibition results in cGMP level changes, blood samples were treated with sGC stimulator BAY 41-2272 (1 µM), sGC activator BAY 60-2770 (1 µM) and sGC inhibitor ODQ (5 µM) in presence of the NO-donor DEA/NO (200 µM). The cGMP level outcome was assessed by ELISA (Figure 20 A) and RIA (Figure 20 B).

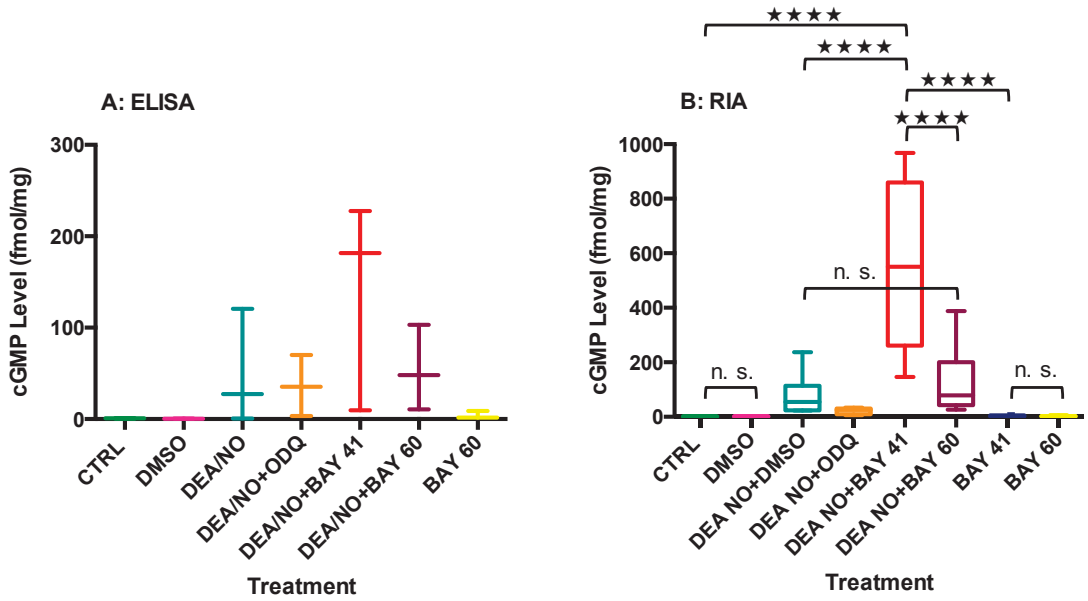

Working with:
Bay 41: 1 µM, *Bay 60*: 1 µM, *DEA-NO*: 200 µM, *DMSO*: 0.01 %, *ODQ: 5* µM

Figure 20 | sGC stimulation increases cGMP levels in a NO-dependent manner

(A) ELISA. (B) RIA. (A/B) cGMP levels increase after sGC stimulation by BAY 41-2272 in presence of NO by DEA/NO in human RBCs. sGC activation with BAY 60-2770 or sGC stimulation in absence of the NO-donor do not effect cGMP levels. (A/B) RBCs were incubated with BAY 41-2272 (1 µM), BAY 60-2770 (1 µM), sGC inhibitor ODQ (5 µM), DEA/NO (200 µM) and 0.01 % DMSO in the presence of IBMX (300 µM) at 37 °C for 10 minutes in PBS^-. Lysed RBCs were analyzed by (A) ELISA and (B) RIA. Unpaired one-way ANOVA against each data: Bonferroni post-hoc test, ★★★★ $p \leq 0.0001$, n.s. not significant. Outlier analysis was performed graphically by box & whiskers plot according to Tukey, n=6. RIA measurement was performed by Dr. rer. nat. Evanthia Mergia, Ruhr-University of Bochum.

As already explained above (see chapter 4.1.1), again NO influx by DEA/NO significantly increases cGMP levels in human RBCs. Furthermore, samples were treated with ODQ, an inhibitor of sGC, and DEA/NO together. Addition of ODQ indicates a tendency to decline NO-dependent increase of cGMP levels (Figure 20 B).
The sGC stimulator BAY 41-2272 stabilizes the nitrosyl-heme formation of sGC and keeps it as a target for NO [65, 66, 180]. In contrast, BAY 60-2770 addresses inactive, oxidized sGC [66]. In both experiments, sGC stimulation by BAY 41-2272 and sGC activation by BAY 60-2770 increase cGMP levels in human RBCs only in presence of NO (Figure 20 A/B). The sGC stimulation and sGC activation without NO do not influence the cGMP levels. However, the effect on cGMP level increase by sGC stimulation is potentiated by treatment with DEA/NO (Figure 20 A/B).

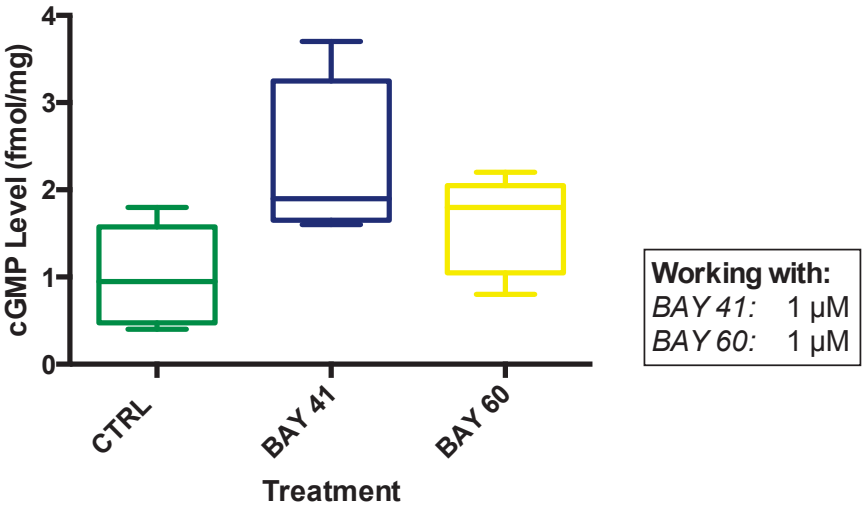

Figure 21 | sGC stimulation and activation do not effect cGMP levels without NO

The sGC stimulation and activation do not effect cGMP levels in absence of NO. RBCs were incubated with BAY 41-2272 (1 µM) and BAY 60-2770 (1 µM) at 37 °C for 10 minutes in PBS^{-}. Lysed RBCs were analyzed via RIA. Data are expressed as box and whiskers plot according to Tukey, unpaired *t*-test, n=6. RIA measurement was performed by Dr. rer. nat. Evanthia Mergia, Ruhr-University of Bochum.

Moreover, NO-dependent cGMP level increase by sGC stimulation with BAY 41-2272 was significantly higher than by sGC activation with BAY 60-2770 (Figure 20 A/B). Even in absence of NO, stimulation with BAY 41-2272 shows a tendency to cause higher cGMP levels compared with BAY 60-2770 (Figure 21).

Collectively, these results show that human RBCs contain an active sGC, which is responsive to stimulation via chemical compounds. The cGMP levels increase by sGC stimulation with BAY 41-2272 only in presence of NO in human RBCs. Moreover, this data demonstrate lower levels in cGMP by BAY 60-2770 compared to BAY 41-2272 in RBCs of healthy young subjects (23-33 years).

4.2 Patient studies

To investigate, whether sGC/cGMP signaling, NO levels and redox state in human RBCs are influenced by morbidity- and mortality-determining disease like CAD, two independent studies, such as CAD study (3.2.1) and anemia study (3.2.2) were performed.

4.2.1 Role of sGC signaling, NO metabolism and redox state in CAD

Present work aimed to encounter whether there are any consequences in sGC/cGMP signaling in RBCs caused by stable and unstable CAD. Furthermore, redox state of RBCs was investigated in this context.

As explained in detail in 3.2.9.1, the department of cardiology, pneumology and angiology at the University Hospital of Düsseldorf recruited subjects with stable and unstable CAD as well as age-matched healthy humans. A short overview of the study design is given in Figure 12.

Cardiovascular risk factors, routine clinical parameters and biochemical parameters were determined. Figure 13 demonstrates the used methods and ascertained parameters.

This work includes laboratory parameters, results of the cGMP analysis by ELISA and RIA as well as FACS analysis of redox state in human RBCs.

Clinical and demographical characteristic of all three cohorts of the study were listed in Table 11. On average, cohorts were 55 years old and had an average BMI of 27 kg/m^2. Most of the presented data were approximately equal, but all CAD patients had a higher amount of risk factors.

Table 11 | Clinical and demographic characteristics of the CAD study population

Parameters	Unit	Control	STABLE CAD	UNSTABLE CAD	P
n		26	20	8	
Age	y	54.04 ± 6.34	58.85 ± 10.31	51.38 ± 9.67	n. s.
Gender	m/f	26/0	20/0	8/0	n. s.
Weight	kg	88.46 ± 8.75	82.15 ± 11.91	99.13 ± 20.30	★★[1]
Height	cm	179.60 ± 6.74	175.30 ± 6.47	180.50 ± 5.13	n. s.
BMI	kg/m²	27.52 ± 3.26	26.77 ± 4.06	30.32 ± 5.38	n. s.
RRsystolic	mmHg	128.70 ± 11.53	132.10 ± 10.98	139.60 ± 12.35	n. s.
RRdiastolic	mmHg	76.50 ± 9.13	77.53 ± 11.12	80.63 ± 7.69	n. s.
HR	1*/sec	67.73 ± 7.36	63.15 ± 8.72	64.38 ± 10.27	n. s.
Hb	g/dl	14.9 ± 1.1	14.6 ± 0.8	14.6 ± 0.6	n. s.
HbA1c	%	5.35 ± 0.32	5.54 ± 0.42	5.46 ± 0.24	n. s.
Cholesterol	mg/dl	208.80 ± 43.08	164 ± 32.44	188.50 ± 28.18	★★★[2]
LDL	mg/dl	147.00 ± 39.84	96.82 ± 22.71	128.30 ± 26.18	★★★★[2]
HDL	mg/dl	56.77 ± 14.47	52.53 ± 13.40	47.13 ± 14.22	n. s.
GFR (MDRD)	ml/min	0.26 ± 0.20	0.24 ± 0.17	0.27 ± 0.12	n. s.
CRP	mg/dl	0.27 ± 0.20	0.24 ± 0.17	0.28 ± 0.13	n. s.
FMDmax	%	7.58 ± 3.34	4.74 ± 2.96	6.05 ± 3.03	★[1]
Pack-years		11.92 ± 14.43	32.00 ± 28.95	17.50 ± 16.69	★★[2]
Risk-factors		1.23 ± 0.86	3.25 ± 0.85	2.75 ± 1.04	★★★★[2]/ ★★★[1]

*P value was gathered by one-way ANOVA against each group and Bonferroni post hoc test, ★★★★ $p < 0.0001$, ★★★ $p < 0.001$, ★★ $p < 0.01$, ★ $p < 0.05$, n. s. not significant, [1] stable CAD vs. unstable CAD; [2] control vs. stable CAD. Blood was collected by Dr. med. Georg Wolff and Dr. med. Ralf Erkens from the department of Cardiology, Pneumology and Angiology, Düsseldorf, Germany. Above mentioned parameters were determined in the central laboratory of the University Hospital of Düsseldorf, Germany.

4.2.1.1 Role of sGC/cGMP signaling in CAD patients

In order to analyze, whether sGC activity is maintained in human RBCs in pathological conditions, cGMP levels in RBCs of stable and unstable CAD patients were investigated by RIA.

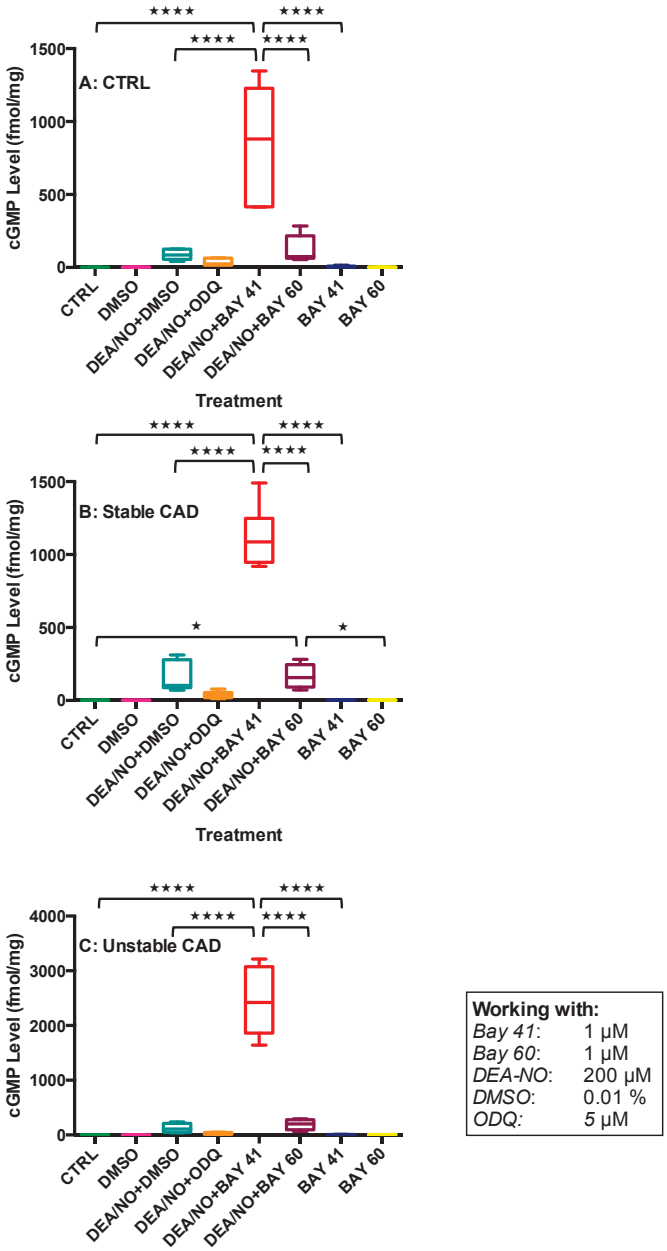

Figure 22 | No impact of CAD on sGC/cGMP signaling in RBCs

(A) CTRL. (B) Stable CAD. (C) Unstable CAD. (A-C) sGC stimulation in presence of NO increases cGMP levels significantly in human RBCs independent of (B) stable or (C) unstable CAD. The cGMP levels increase to a greater extent in the RBCs of unstable and stable CAD patients. (A-C) sGC stimulator BAY 41-2272 (1 µM), sGC activator BAY 60-2770 (1 µM), NO-donor DEA/NO (200 µM), sGC inhibitor ODQ (5 µM) and DMSO (0.01 %) were used in presence of PDE inhibitor IBMX (300 µM). Samples were incubated at 37 °C for 10 minutes in PBS^{-}. Lysed RBCs were analyzed via RIA. Data are expressed as box & whiskers plot according to Tukey, unpaired one-way ANOVA against each data: post-hoc test Tukey, CTRL: n=6, stable CAD: n=6, unstable CAD (before ischemia treatment): n=6, ★ $p \leq 0.05$, ★★★★ $p \leq 0.0001$. RIA measurement was performed by Dr. rer. nat. Evanthia Mergia, Ruhr-University of Bochum.

Therefore, blood samples of stable and unstable CAD (before ischemia treatment) patients and age-matched healthy subjects were approached with sGC stimulator BAY 41-2272 (1µM), sGC activator BAY 60-2770 (1 µM), sGC inhibitor ODQ (5 µM) and NO-donor DEA/NO (200 µM) in 0.9 % NaCl at 37 °C for 10 minutes. RIA measurement was performed by Dr. rer. nat. Evanthia Mergia in the laboratory of the Ruhr-University of Bochum.

The results in Figure 22 show that the NO-dependent increase in cGMP levels by sGC stimulation in human RBCs with 1 µM BAY 41-2272 is not effected by stable or unstable CAD compared to age-matched controls. The cGMP baseline values are almost similar in all three groups (Figure 22/23 D). Moreover, the cGMP levels increase after incubation with BAY 41-2272 together with NO to a greater extent in both CAD groups compared to the control group.

Overall, the distribution of the cGMP levels by several incubations is approximately the same in all study populations. NO increases and sGC inhibition by ODQ decreases the cGMP level in human RBCs independent of stable or unstable CAD (Figure 22/23 B).

The sGC stimulation by BAY 41-2272 combined with 200 µM DEA/NO significantly elevates the cGMP levels compared to the treatment with DEA/NO and DMSO in RBCs of all cohorts (Figure 22/23 A). Highest cGMP levels are pointed out in RBCs of patients with unstable CAD followed by RBCs of stable CAD compared to age-matched controls (Figure 23 A).

Outcome in cGMP levels distinguishes between sGC stimulation by BAY 41-2272 and sGC activation by BAY 60-2770 in presence of NO (Figure 21 A-C, 22 C). In comparison, Figure 22 C and D present a difference between BAY 41-2272 and BAY 60-2770. The outcome of cGMP levels after sGC stimulation is higher than caused by sGC activation independently of NO or CAD.

To sum up, NO induced sGC-dependent increase in cGMP levels is preserved in RBCs with stable and unstable CAD. Here, the effect by DEA/NO and BAY 41-2272 seem to be present to a greater extent in RBCs of both CAD groups compared to age-matched controls (Figure 22/23 B). BAY 41-2272 elevates cGMP levels to a higher extent than BAY 60-2770 in all groups.

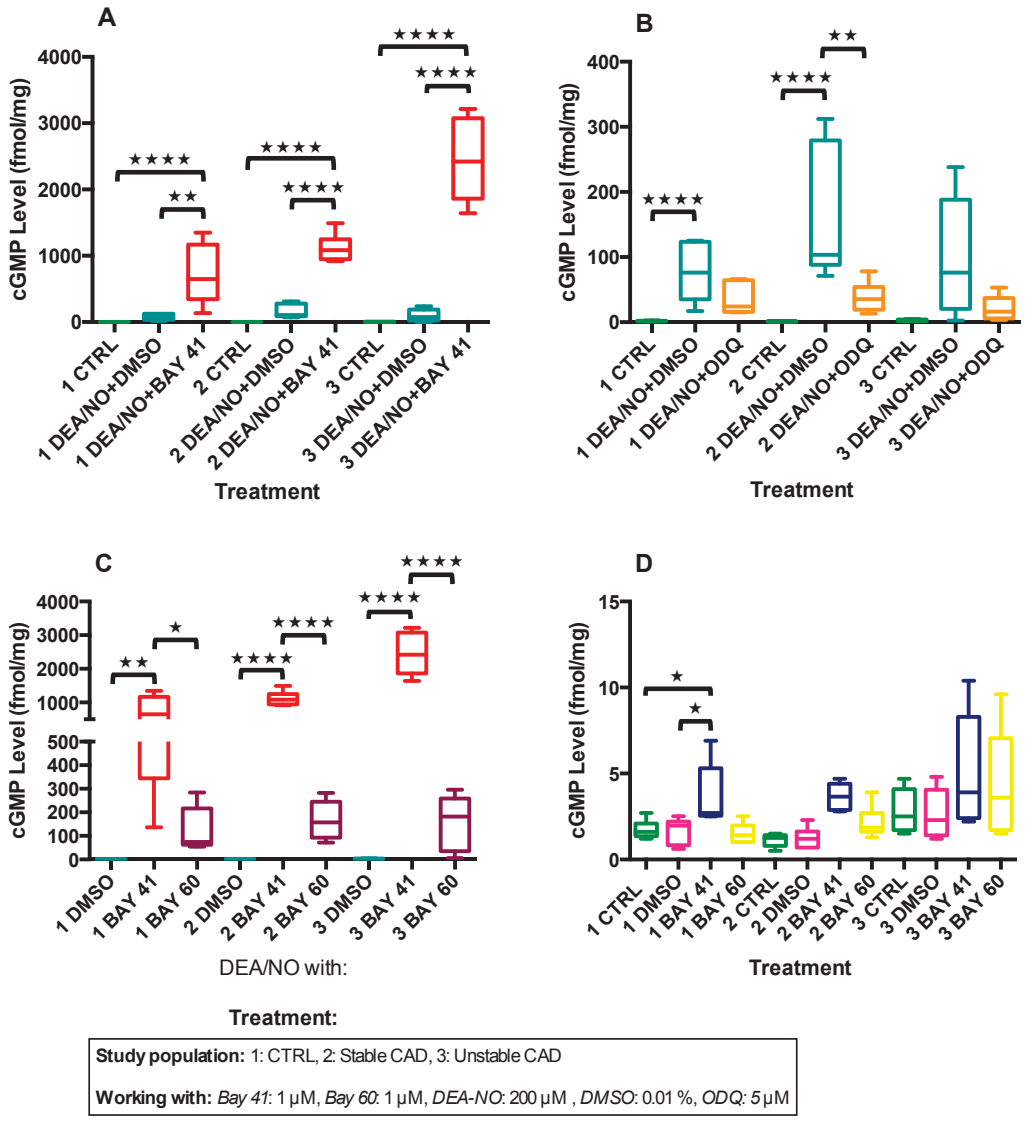

Figure 23 | NO induced sGC stimulation is preserved in RBCs with CAD

(A) NO-dependent cGMP level increase by sGC stimulation with BAY 41-2272 (1 µM) is independent of CAD. (B) cGMP levels decrease by sGC inhibition with ODQ (5 µM) in all three groups. (C) Outcome in cGMP levels is significantly higher with sGC stimulation with BAY 41-2272 than sGC activation with BAY 60-2770 (1 µM) in presence of NO independent of CAD. (D) sGC stimulation and activation without NO influx do not change the cGMP levels in all groups. Additionally, DMSO (0.01 %) was used in presence of PDE inhibitor IBMX (300 µM) and samples were incubated at 37 °C for 10 minutes in PBS^{-}. RBC pellets were lysed and analyzed by RIA (A-C). Data are expressed as box & whiskers plot according to Tukey, unpaired one-way ANOVA against each data: post-hoc test Tukey, CTRL: n=6, stable CAD: n=6, unstable CAD (before ischemia treatment): n=6, ★ $p \leq 0.05$, ★★★★ $p \leq 0.0001$. RIA measurement was performed by Dr. rer. nat. Evanthia Mergia, Ruhr-University of Bochum.

4.2.1.2 Levels of NO and redox state do not differ in CAD

Aiming to investigate whether NO levels and redox state in RBCs are influenced by stable and unstable CAD, FACS analysis was used. Levels in NO, ROS and reduced thiols were analyzed and compared to levels in RBCs of age-matched healthy subjects.

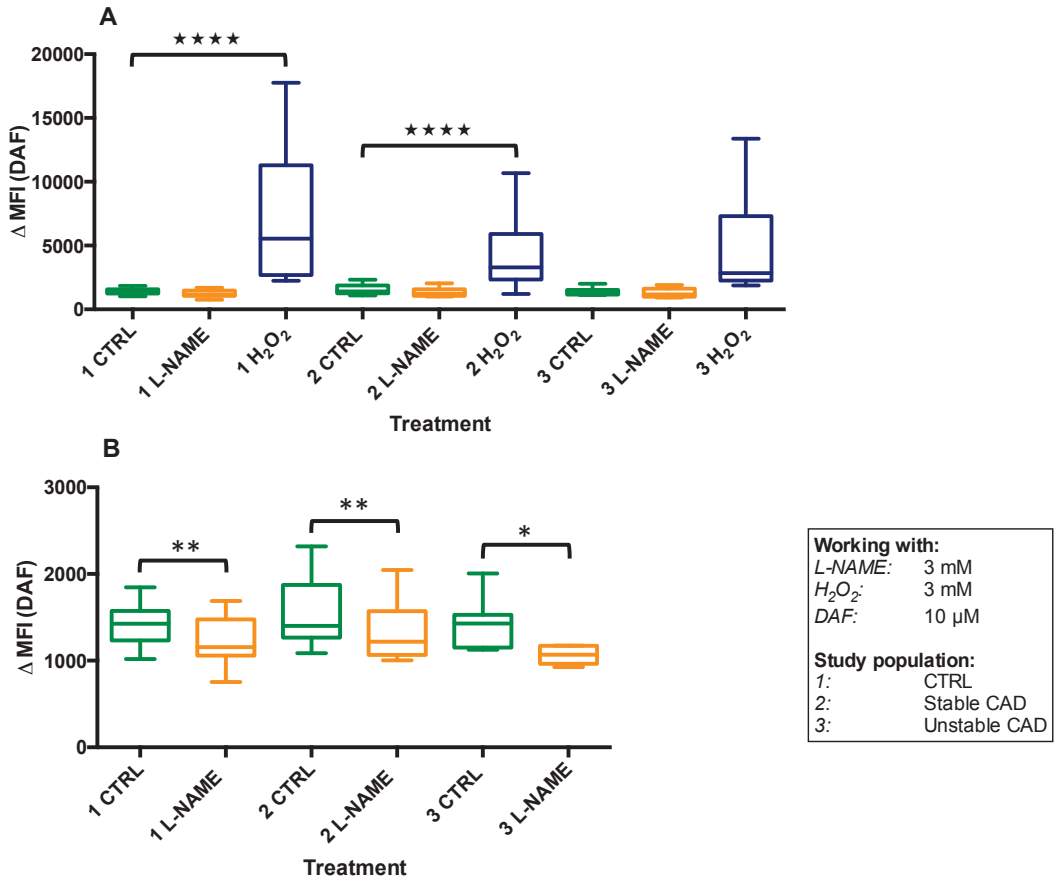

Figure 24 | NO levels are unchanged in stable and unstable CAD

(A) Basal NO levels in whole blood of patients with CAD do not differ from NO levels of age-matched healthy humans. 3 mM of radical H_2O_2 increases NO levels in all groups. (B) After incubation with NOS inhibitor L-NAME (3 mM) NO levels decrease in whole blood independent of CAD. (A/B) Blood samples were loaded with 10 µM DAF-FM-DA in PBS^+ for 30 minutes and measured with FACS analysis. Unpaired one-way ANOVA against each data: post hoc test Tukey, CTRL: n=19, stable CAD: n=17, unstable CAD (before ischemia treatment): n=7, ★★★★ $p \leq 0.0001$, paired *t*-test, CTRL against L-NAME: * $p \leq 0.05$, ** $p \leq 0.005$. For outlier analysis box & whiskers plot according to Tukey was used graphically. Part of the experiment was performed together with Dr. rer. nat. Christina Panknin from the department of Cardiology, Pneumology and Angiology, Düsseldorf, Germany.

Experiments were carried out as described in detail in chapter 3.2.7. Fluorescent dye DAF-FM-DA (10 µM), a reagent for quantitative detection, was used to evaluate NO levels (Figure 24). NO levels were analyzed additionally in presence of 3 mM of NOS inhibitor L-NAME and 3 mM of the radical H_2O_2 (Figure 23 A).

Results show no differences in basal NO levels in all three study groups (Figure 24 A/B). Additionally, Figure 24 B underlines that NO levels decrease by the use of NOS inhibitor L-NAME (3 mM) in all cohort groups. Furthermore, Figure 24 A shows that NO levels increase almost in all groups by using H_2O_2.
In conclusion, NO levels in RBCs are not influenced by stable or unstable CAD, but are dependent on eNOS activity and presence of radicals.

To verify whether ROS state in RBCs is changed in pathological condition like CAD, whole blood of patients with stable and unstable CAD (without ischemia treatment) as well as age-matched healthy subjects was incubated with 6.67 µM DCF-DA and 6.67 µM TT. DCF-DA determines ROS levels and TT measures free thiol levels. FACS analysis was performed (Figure 25).

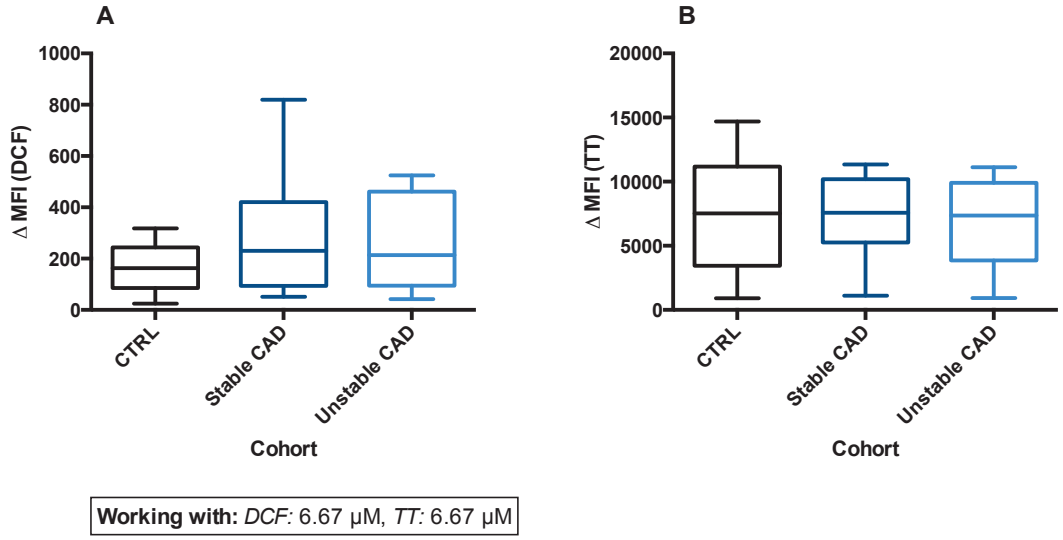

Figure 25 | Unchanged ROS and thiol levels in stable and unstable CAD

(A) No difference in ROS levels in stable and unstable patients compared to age-matched healthy subjects. Whole blood was incubated with 6.67 µM DCF-DA in PBS^+ for 30 minutes. (B) Free thiol levels are unchanged in stable and unstable CAD. Whole blood was loaded with 6.67 µM TT in PBS^+ for 30 minutes. (A/B) Data were analyzed via FACS and expressed as box & whiskers plot according to Tukey. Unpaired one-way ANOVA against each data, post hoc test Tukey, CTRL: n=19, stable CAD: n=17, unstable CAD (before ischemia treatment): n=7. Part of the experiment was performed together with Dr. rer. nat. Christina Panknin from the department of Cardiology, Pneumology and Angiology, Düsseldorf, Germany.

In Figure 25, it is depicted that there is no difference in ROS levels (Figure 25 A) and free thiol levels (Figure 25 B) between stable or unstable CAD patients compared to age-matched healthy subjects.

To sum up, stable and unstable CAD does not influence the NO levels and redox state in human RBCs.

4.2.1.3 Role of PCI on NO levels and redox state in unstable CAD

To verify whether NO levels differ in RBCs after treatment of ischemia via PCI, blood samples of unstable CAD patients were incubated with 10 µM DAF-FM-DA, 6.67 µM DCF-DA and 6.67 µM TT (Figure 26).

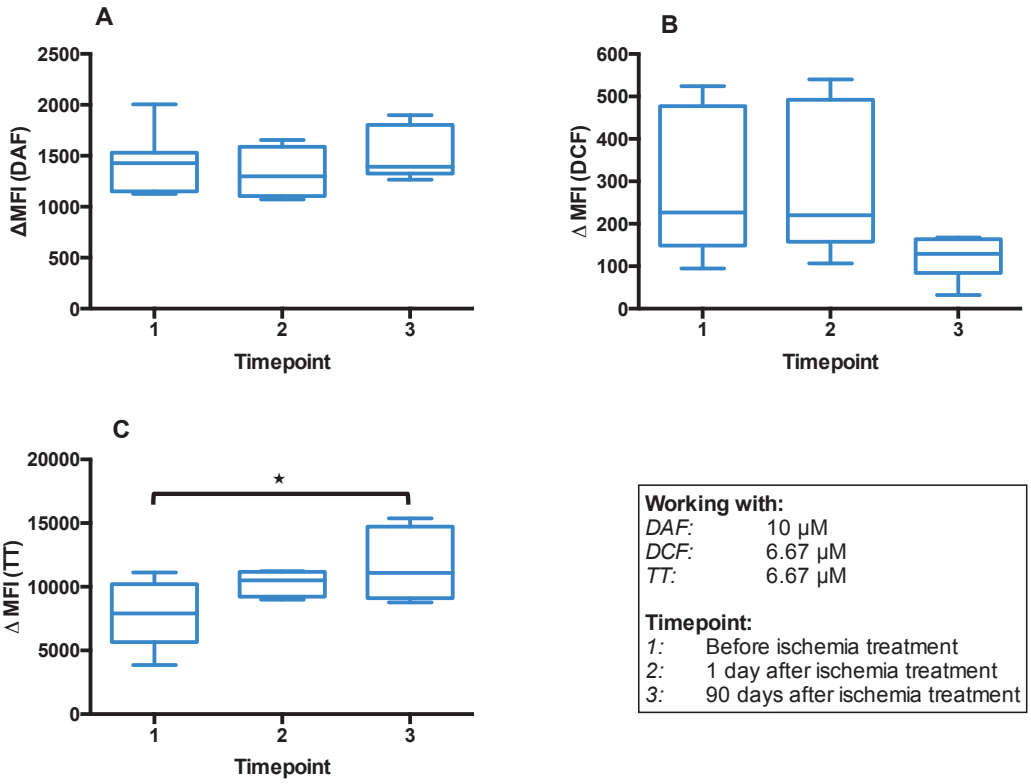

Figure 26 | Effect of PCI in RBCs from patients with unstable CAD

(A) Basal NO levels in RBCs of unstable CAD patients do not show any difference after PCI. (B) 90 days after the ischemia treatment ROS levels decrease significantly. (C) Free thiol levels increase 90 days after PCI. (A-C) Whole blood of patients with unstable CAD was analyzed via 10 µM DAF-FM-DA, 6.67 µM DCF-DA and 6.67 µM TT with flow cytometry analysis. Samples were incubated in PBS^{+} for 30 minutes. Unpaired one-way ANOVA against each data: post hoc test Tukey, timepoint 1: n=7, timepoint 2: n=6, timepoint 3: n=6, ★ $p \leq 0.05$. Data are expressed as box & whiskers plot according to Tukey.

NO levels do not change after ischemia treatment in whole blood of unstable CAD patients. ROS levels only indicate a tendency to decrease 90 days after the treatment (Figure 26 B).

Levels of free thiols elevate 90 days after the PCI compared to the status before treatment (Figure 26 C).

In conclusion, PCI has an influence upon free thiol levels in human RBCs 3 months after ischemia treatment. It may also effect the ROS levels in human RBCs after 90 days. However, NO levels are unchanged at any point of time.

4.2.2 Role of anemia in RBCs of patients with unstable CAD

The objective of the anemia study was to find out, whether NO levels and redox state differ in RBCs of patients with atherosclerosis such as unstable CAD (group 4, cf. 3.2.9.2) and anemia compared to patients with normal hemoglobin levels by FACS analysis.

A detailed description about the study is explained in 3.2.9.2. The study includes biochemical analysis and hemodynamic studies (Table 12). Clinical and analytical characteristics of the study population are resumed in Table 12.

Table 12 | Clinical and demographic characteristics of the anemia study population

Parameters	Unit	Control	Anemia	P
n		9	15	
Age	y	81.78 ± 4.94	79.47 ± 6.21	n. s.
Gender	m/f	5/4	8/7	n. s.
Weight	kg	81.78 ± 4.94	76.20 ± 11.78	n. s.
Height	cm	170.10 ± 10.18	167.20 ± 9.36	n. s.
BMI	kg/m²	28.59 ± 4.26	27.26 ± 3.77	n. s.
RRsystolic	mmHg	136.00 ± 20.04	135.60 ± 10.94	n. s.
RRdiastolic	mmHg	71.00 ± 14.68	67.92 ± 9.84	n. s.
HR	1*/sec	67.67 ± 12.93	75.92 ± 11.57	n. s.
Hb	g/dl	13.99 ± 0.97	11.24 ± 0.75	★★★★
MCV	pg	90.46 ± 6.13	91.16 ± 5.50	n. s.
MCH	fl	30.19 ± 1.82	29.59 ± 2.07	n. s.
MCHC	g/dl	33.40 ± 1.17	32.46 ± 1.21	n. s.
HbA1c	%	5.57 ± 0.42	6.08 ± 1.29	n. s.
Cholesterol	mg/dl	169.60 ± 44.38	159.60 ± 42.69	n. s.
LDL	mg/dl	106.40 ± 37.41	95.13 ± 37.48	n. s.
HDL	mg/dl	51.50 ± 10.04	49.80 ± 15.46	n. s.
Creatinine	g/cm^3	1.21 ± 0.73	1.34 ± 0.98	n. s.
CRP	mg/dl	0.92 ± 1.88	0.65 ± 0.67	n. s.
Packyears		8.75 ± 9.91	35.38 ± 42.35	n. s.
Risk factors		2.22 ± 0.44	2.79 ± 1.12	n. s.

*P value was gathered by unpaired *t*-test, ★★★★ $p < 0.0001$, n. s. not significant. Blood was collected by Dr. med. Georg Wolff and Dr. med. Ralf Erkens from the department of Cardiology, Pneumology and Angiology, Düsseldorf, Germany. Above mentioned parameters were determined in the central laboratory of the University Hospital of Düsseldorf, Germany.

4.2.2.1 NO levels are preserved in RBCs with anemia in unstable CAD

To analyze possible changes in NO levels and redox state in RBCs of patients with unstable CAD and anemia, blood samples were loaded with 10 µM DAF-FM-DA (NO detection), 6.67 µM DCF-DA (ROS detection) and 6.67 µM TT (free thiol detection).

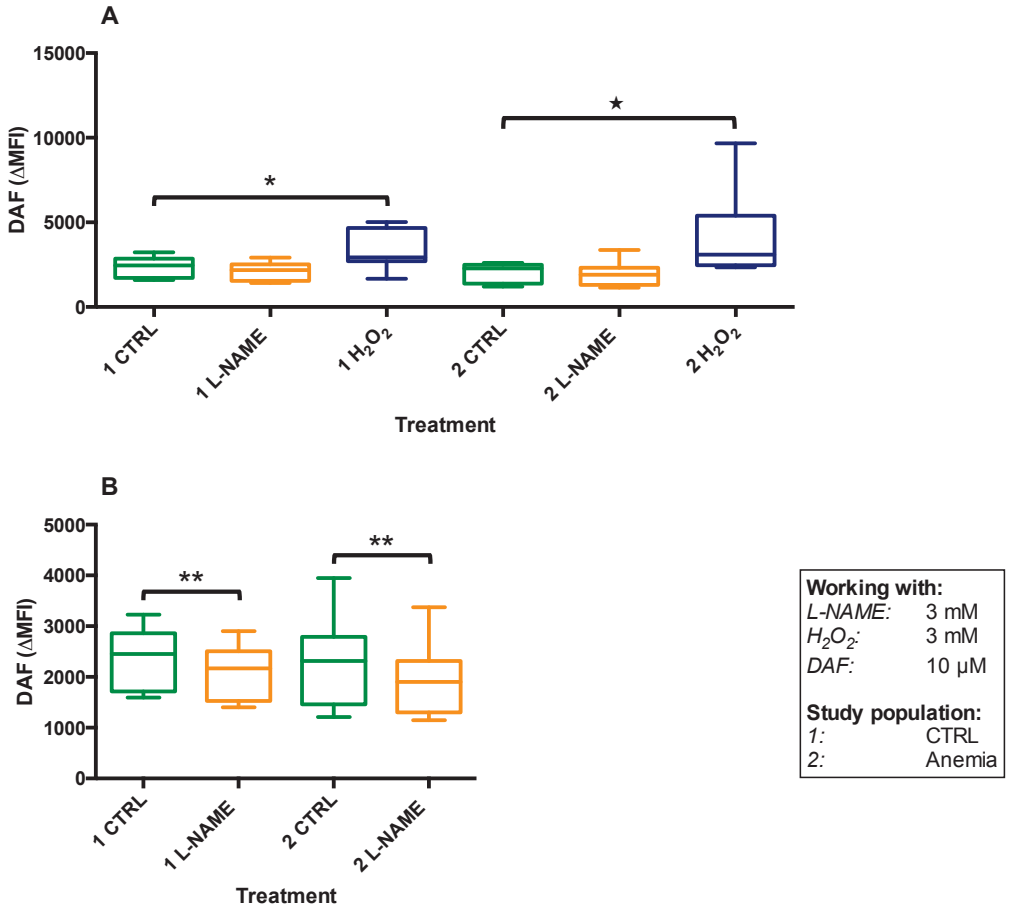

Figure 27 | NO levels are unchanged by DAF-FM-DA-dependent fluorescence

(A) Basal NO levels in RBCs of patients with unstable CAD are unchanged in presence of anemia compared to normal hemoglobin levels. The radical H_2O_2 (3 mM) increases the NO levels in both groups. (B) The eNOS inhibition by 3 mM L-NAME decreases NO levels in both groups. (A/B) Blood samples were incubated in PBS^+ for 30 minutes and analyzed via 10 µM DAF-FM-DA with flow cytometry analysis. Unpaired one-way ANOVA against each data: post hoc test Tukey, n=9, ★ $p \leq 0.05$, paired *t*-test, ** $p \leq 0.005$. Outlier analysis was performed graphically by box & whiskers plot according to Tukey.

Figure 27 depicts that basal NO levels are unchanged in RBCs of patients with unstable CAD and anemia compared to RBCs of unstable CAD patients with healthy hemoglobin levels. The results also demonstrate that NO levels increase by the use of 3 mM H_2O_2 (Figure 27 A). Levels of NO in RBCs of both study populations decreased by eNOS inhibition with 3 mM L-NAME (Figure 27 B).

To conclude, levels in NO in RBCs are independent of anemia in patients with atherosclerosis disease like unstable CAD. They are dependent on eNOS activity and the presence of radicals.

4.2.2.2 Redox state in RBCs is independent of anemia in unstable CAD

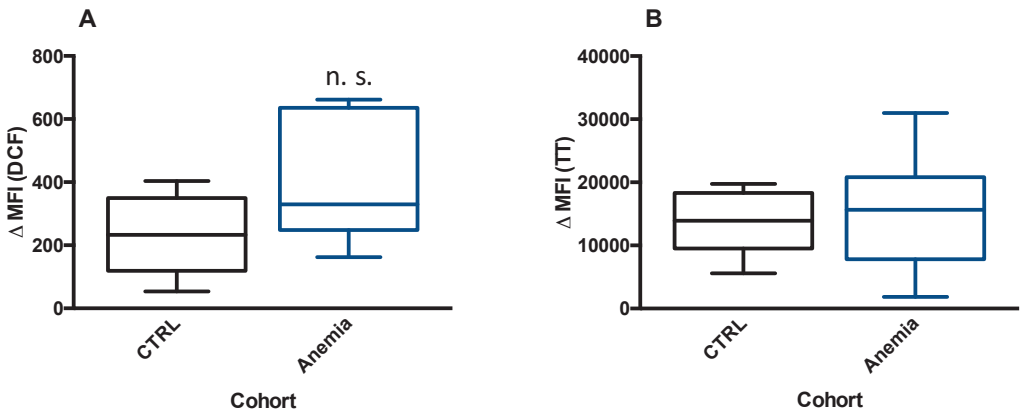

Figure 28 | Unchanged ROS and free thiol levels in RBCs with anemia in unstable CAD

(A) ROS levels do not change in occurrence of anemia in RBCs of patients with unstable CAD. Paired *t*-test, n. s. not significant $p = 0.11$. (B) Reduced thiol levels do not differ in RBCs of patients with unstable CAD by anemia compared to those with normal hemoglobin levels. Paired *t*-test, not significant $p = 0.72$. (A/B) Blood samples were incubated with 6.67 µM DCF-DA and 6.67 µM TT in PBS^+ for 30 minutes and analyzed via FACS. Data are presented by box & whiskers plot according to Tukey, n=9.

The Figures 28 A and B show no differences in ROS and free thiol levels between both study populations, RBCs of unstable CAD patients with and without anemia (Figure A/B).

Hence, it can be concluded that ROS and free thiol levels are independent of anemia in RBCs of patients with unstable CAD.

5 Discussion

The main hypothesis of this study was that human RBCs contain an active sGC/cGMP pathway and own non-canonical functions, which may be influenced by CAD or affect its outcome.

Hence, primary objective of this study was to find out whether cGMP levels are influenced by (1) NO, (2) eNOS activity and associated mechanisms (3) as well as sGC activity in mature human RBCs. The second part of this work aimed at finding out (4) whether sGC activity and the NO/sGC pathway are influenced by CAD, such as stable and unstable CAD compared to age-matched healthy controls. In this context, (5) NO levels and redox state in RBCs of healthy humans have been compared with RBCs from patients with stable and unstable CAD and (6) anemia (Figure 29).

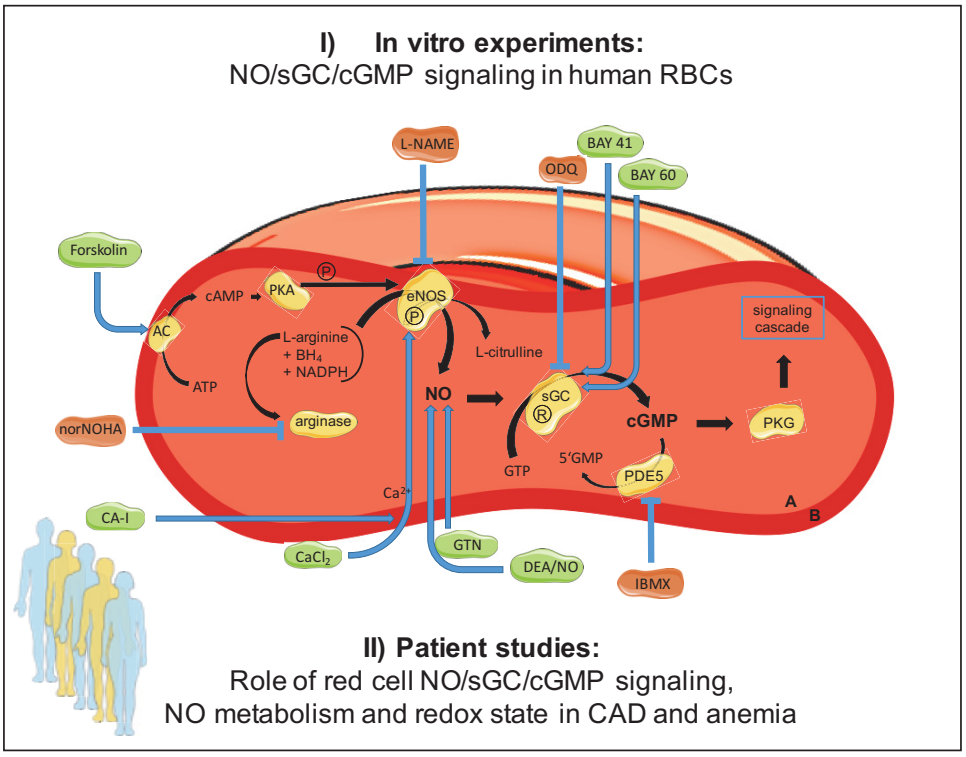

Figure 29 | Main aims of present study

I) NO/sGC/cGMP signaling in mature human RBCs. Used enzymes/chemical compounds: NO donor DEA/NO and GTN, PDE inhibitor IBMX, eNOS inhibitor L-NAME, arginase inhibitor norNOHA, AC stimulator Forskolin, $CaCl_2$, Ca-I, sGC stimulator BAY 41-2272, sGC activator BAY 60-2770 and sGC inhibitor ODQ. II) Role of NO/sGC/cGMP pathway, NO metabolism and redox regulation in RBCs from patients with (stable or unstable) CAD and anemia.

Key findings of this work are the following (cf. Figure 30):

(1) The first aim of the study was to find out whether NO influences cGMP levels and whether this effect is dependent on PDE activity in human RBCs. The present study shows that cGMP levels increase by NO application in a PDE-dependent manner in healthy human RBCs.
(2) Furthermore, this work tried to assess whether changes of red cell eNOS activity and associated mechanisms influence cGMP levels in human RBCs. Present data demonstrate that neither inhibition of arginase or red cell eNOS nor Ca^{2+} influx nor AC stimulation influences cGMP levels in human RBCs.
(3) To identify sGC activity and the NO/sGC pathway in human RBCs were further aims of the study. Present findings confirm that cGMP levels increase via sGC stimulation in healthy human RBCs. This increase is induced by NO and boosted by sGC stimulator BAY 41-2272. So human RBCs contain an active sGC and an associated NO/sGC pathway.
(4) The CAD study was performed to investigate whether sGC activity and NO/sGC signaling in RBCs are effected by CVD (such as stable and unstable CAD) compared to age-matched controls. Present findings show that sGC activity, sGC responsiveness to NO and its' stimulators are preserved in human RBCs with stable or unstable CAD.
(5) Furthermore, non-canonical RBC functions like redox state and NO levels were observed in stable and unstable CAD compared to age-matched controls. This work shows that redox state and NO metabolism are preserved in both, stable and unstable, CAD. Thus, human RBCs compensate the lack of NO bioavailability. An additional follow-up study with RBCs with unstable CAD further showed that levels of free thiols increase and levels of ROS decrease after a recovery time of 90 days after PCI. These results indicate clinical relevance of PCI, not only for vasculature, but also for functional features of RBCs.
(6) The second study aimed at analyzing possible changes in NO levels and redox state in RBCs in unstable CAD with anemia. Results demonstrate that these non-canonical functions are unchanged in such RBCs.

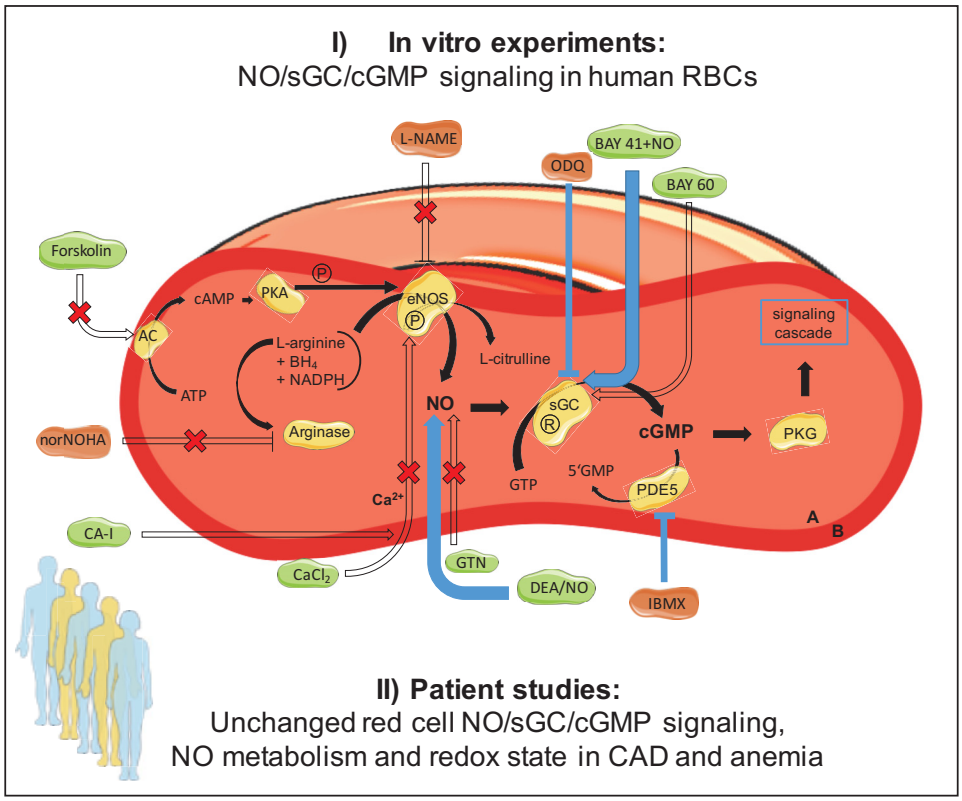

Figure 30 | Main findings of present study

I) Mature RBCs contain an active NO/sGC/cGMP signaling. cGMP is dependent on NO application and PDE activity as well as sGC activity in presence of NO. It is not dependent on eNOS activity, arginase activity, Ca^2 influx and AC stimulation. II) The sGC activity, sGC responsiveness to NO and to mentioned chemical compounds are preserved in human RBCs with stable or unstable CAD. Furthermore, NO metabolism and redox state are preserved in RBCs of patients with CAD and anemia as compared to age-matched controls.

5.1 Analysis of NO/sGC/cGMP signaling in human RBCs

5.1.1 NO increases cGMP levels in a PDE-dependent manner

The present study confirms that cGMP levels increase time-dependent with NO application with NO-donor DEA/NO in a PDE-dependent manner. PDE inhibition without presence of NO does not change cGMP levels in healthy human RBCs.

Previously, Turgut et al. demonstrated that DEA/NO elevate cGMP levels in smooth muscle cells of rats [157]. In agreement with these findings, present data show cGMP increase in mature human RBCs using DEA/NO. In accordance with presented results, cGMP level increase was previously proven in erythroid progenitor cells [140].

Current results further show that the effect of NO on cGMP levels is only heightened by PDE inhibition. Absence of NO does not cause any significant increase in cGMP levels by PDE inhibition although previous findings suggested a NO-independent activation of cGMP levels by PDE inhibition [158].

To the best of my knowledge, NO-donors DEA/NO and GTN were compared directly based on their effect on cGMP levels in human RBCs ex vivo for the first time in this work. Present data show that in contrast to DEA/NO, cGMP levels are unchanged after use of GTN regardless of PDE-inhibition although Feelisch et al. proved increased cGMP levels by GTN in human endothelial cells [159]. However, corresponding to the present findings, Clarkson et al. revealed that flow-mediated dilation, which was considered to be dependent on NO [160], was unchanged after sublingual use of GTN in humans [161]. Finally, based on the results of this study one can assume that the beneficial effect of NO donor DEA/NO on cGMP levels in healthy RBCs is greater than using organic nitrite GTN.

To sum up, present data confirm, that cGMP levels are dependent on NO, not only in endothelial cells [69], but also in RBCs. Moreover, cGMP level elevation by NO application is boosted by PDE inhibition, and thus correlated with PDE activity in human RBCs.

5.1.2 Influence of eNOS and regulating mechanisms on cGMP levels

Present study also included investigations on effects of the red cell eNOS and associated mechanisms on cGMP levels. Analysis of eNOS inhibition, arginase inhibition, Ca^{2+} influx and AC stimulation based on cGMP levels was performed.

5.1.2.1 Inhibition of arginase and eNOS do not effect cGMP levels

Data of the present study show that inhibition of both, arginase and eNOS does not have an influence on cGMP levels in human RBCs. NorNOHA, a powerful arginase inhibitor without an effect on eNOS activity [162], and L-NAME, a NOS inhibitor, were used.

In 1995, it was questioned, whether increase of L-arginine concentration, which is the substrate of eNOS and arginase, can cause elevated physiological NO levels [118, 64]. Earlier studies associated "up-regulated" arginase activity with cardiovascular dysfunction [118, 163, 164, 165, 166]. With respect to these studies, Jung et al. supposed that inhibition of arginase may hold back from myocardial infarction by supplying more L-arginine to eNOS [167]. Based on these assumptions, present work supposed that cGMP levels might increase by inhibition of arginase. Current findings disagree with mentioned hypothesis and show that cGMP levels are not affected by arginase activity.

Yang et al. presumed that the cardio-protective effect of arginase inhibition is dependent on eNOS activity [168]. Findings of Webb et al. were concordant with Yang

et al. and showed loss of increase in nitrite levels after incubation with L-arginine via eNOS inhibition [169]. However, the present results underline that cGMP levels were not influenced by eNOS inhibition.

To sum up, present data indicate that cGMP levels are neither dependent on arginase inhibition nor on eNOS inhibition in human RBCs.

5.1.2.2 Ca^{2+} does not influence cGMP levels in RBCs

The cGMP level increase is dependent on eNOS [67] and sGC activity [201]. This study does not show an effect of Ca^{2+} influx via $CaCl_2$ and Ca-I on cGMP levels in human RBCs. In consequence, present results do not agree with previous findings, which confirmed an influence of intracellular Ca^{2+} influx on eNOS activity [21, 45, 72, 109, 111, 171]. Results of this study also contradict findings of Zabel et al. that sGC got sensitized to NO in a Ca^{2+}-dependent manner [202] and thus it impacts cGMP levels.

Kazerounian et al. demonstrated sGC inhibition by Ca^{2+} via different mechanisms [172], which could be the possible reason for unchanged cGMP levels despite Ca^{2+} application in human RBCs. Another reason could be a Ca^{2}/calmodulin-dependent PDE, which decreases cGMP levels in human RBCs [203].

To sum up, present study shows that Ca^{2+} does not influence cGMP levels, although eNOS and sGC are described to be dependent on Ca^{2+} in human RBCs.

In contrast to these findings, cGMP levels increase, even if not significantly, in $HBSS^{+}$, a buffer containing Ca^{2+} when stimulating AC with Forskolin. This might indicate a Ca^{2+}-dependent change of cGMP levels in RBCs. As $HBSS^{+}$ contains other components besides Ca^{2+}, such as glucose or magnesium, the effect might not only caused by Ca^{2+}. This needs to be analyzed further in future.

5.1.2.3 AC stimulation by Forskolin do not effect cGMP levels in RBCs

Present data further demonstrate that cGMP levels are not affected by AC stimulation with Forskolin in human RBCs. Earlier studies reported elevation in intracellular cAMP levels by activating the PKA through AC stimulation via Forskolin in human T-cells [153]. Present study supposed an increase in cGMP levels via eNOS activation by AC stimulation and PKA signaling [113] in human RBCs. Two different mechanisms about PKA signaling were considered to be responsible for an increase in cGMP levels and vascular relaxation [113]. The first one is a Ca^{2+}-dependent pathway indirectly activated by PKA [171, 173]. The second one is an alternative way with direct eNOS activation by PKA without Ca^{2+} [174]. However, Forskolin does not cause any significant change in cGMP levels compared to the control sample.

Additionally, eNOS inhibition by L-NAME does not change the cGMP levels either, suggesting that cGMP levels are not dependent on eNOS activity as mentioned in chapter 5.1.2.1.

Two different buffers, PBS^- and $HBSS^+$, were used in this experiment. The effect of Forskolin is lower in PBS^- compared to $HBSS^+$. Main difference between the buffers is the presence of Ca^{2+} in HBSS+, but apart from Ca^{2+} it also contains other components such as glucose and magnesium. Therefore, the effect of Forskolin in $HBSS^+$ cannot be explained only as an effect of Ca^2.

In conclusion, the presented data show that cGMP levels are neither dependent on arginase activity nor on red cell eNOS activity nor on AC stimulation.

5.1.3 The cGMP levels are dependent on sGC activity in RBCs

Petrov et al. already assumed the existence of an active sGC in human RBCs in 1996. The present study confirms that healthy human RBCs contain a functional sGC, which was recently demonstrated by Cortese-Krott et al. [175]. Results of this work further emphasize that cGMP levels are dependent on sGC activity in presence of NO in human RBCs.

Zhao et al. and others previously described that ODQ inhibits activation of sGC by NO via oxidation [149, ,150, 152]. This is followed by elimination of the heme group on the beta subunit of the sGC [65]. In accordance, present data confirm that inhibition of sGC by ODQ reduces the NO-dependent increase of cGMP levels in human RBCs. In consequence, this finding indicates that an increase of cGMP levels by NO depends on sGC activity in human RBCs.

Although sGC stimulator BAY 41-2272 [176] and sGC activator BAY 60-2770 [177] were considered as NO-independent in the past, present data suggest a NO-dependent cGMP level increase by both substances in human RBCs. Positive interaction between NO-donors and BAY 41-2272 was also observed in elder studies [178]. Concordant with the present study, reduced form of sGC and the presence of NO were considered as necessary for BAY 41-2272 function in rat platelets [178]. Mullershausen et al. demonstrated that cGMP elevation via BAY 41-2772 was potentiated by the use of NO-donors in human platelets [179]. These findings are comparable with presented data. Current results show that the effect of an NO-donor was potentiated by addition of both, BAY 41-2772 and BAY 60-2770 in human RBCs. BAY 41-2272 combined with DEA/NO increases cGMP levels up to 1000-fold. Without addition of DEA/NO, BAY 41-2272 and BAY 60-2770 elevate the cGMP levels only up to 4-fold above the control sample.

Maximal cGMP level formation by sGC is obtained by treatment with BAY 41-2272 in presence of NO. BAY 41-2272 is known to co-act with NO [178] due to stabilization of the "nitrosyl-heme complex" of sGC [65, 66, 180]. In contrast, BAY 60-2770 selectively addresses "inactive, oxidized heme-free" sGC, which accumulates in pathological conditions with higher range of oxidative stress [66, 150, 152]. By oxidizing the heme iron, ODQ enlarged the effect of BAY 60-2770 on sGC [152, 175]. In the present work, the increase in cGMP levels via BAY 60-2770 is much lower in comparison to BAY 41-2772 independent of the presence of NO. This effect indicates lower levels of oxidized or heme free sGC in RBCs of young (23-33 years) healthy humans assuming less oxidative stress.

Summed up, the data presented here show that not only progenitor cells [140], but also mature human RBCs carry a functional sGC, which is involved in the sGC/cGMP pathway. In addition, cGMP levels are influenced by sGC activity in a NO-dependent manner. Beyond that, present data indicate that NO-insensitive sGC activation via BAY 60-2770 could help to compensate low NO bioavailability caused by oxidative stress. Therefore, this should be further investigated in the future.

5.2 Patient studies: Role of CAD and anemia in human RBCs

Two independent studies were performed with the intent to evaluate whether red cell sGC/cGMP pathway and non-canonical features, such as NO metabolism and redox state are influenced by clinical conditions, such as stable and unstable CAD or anemia.

5.2.1 NO induced sGC/cGMP signaling is preserved in RBCs in CAD

The Department of Cardiology, Pneumology and Angiology of the University Hospital of Düsseldorf performed the CAD study. The cGMP levels were determined in cooperation with the laboratory of the Ruhr-University of Bochum.

The present results show that sGC activity, response to NO and sGC-activity-dependent increase in cGMP levels are unchanged in RBCs of stable and unstable CAD patients compared to age-matched controls. cGMP levels increase to a greater extent in RBCs of both CAD patient groups compared to healthy age-matched subjects by BAY 41-2272 in presence of DEA/NO. Moreover, BAY 60-2770 elevates cGMP levels approximately to the same level in both CAD groups and the control group independently from the presence of NO.

Previously, it was shown that eNOS activity is reduced in RBCs of stable CAD patients, which corresponded to their stage of endothelial dysfunction [44, 131]. Present data

show that compared to the baseline cGMP level in the control group, cGMP levels in both CAD groups do not differ significantly. These findings indicate that sGC activity is preserved in CVD although eNOS activity and NO availability are reduced [44].

NO induced sGC-dependent cGMP level increase in human RBCs is revealed in healthy humans as well as in stable and unstable CAD patients. Use of ODQ decreases cGMP levels in RBCs in all cohorts to the same degree confirming preserved dependency of cGMP levels on sGC activity and responsiveness to sGC inhibitors in CAD.

Levels in cGMP by treatment with DEA/NO and BAY 41-2272 increase up to a greater extent in stable and unstable CAD cohorts compared to the age-matched controls. Cortese-Krott et al. recently showed that the expression and activity of sGC were unchanged despite decreased eNOS activity in RBCs from patients with stable CAD [175]. In addition, several studies in the past demonstrated that BAY 41-2272 modulates blood pressure [181] even when eNOS was inhibited in rats [128]. These results suggest that vascular disease is not dependent on diminished NO levels, but on sGC activity [128]. Furthermore, Masuyama et al. described that sGC agonists are able to reverse cardiac modeling and prevent heart failure [182, 183]. Presented data and mentioned literature indicate that BAY 41-2272 and sGC stimulation itself are preserved in RBCs of CAD patients. It can be assumed that RBCs are able to compensate lack of NO bioavailability, offering new possibilities in treatment of cardiovascular [66, 65, 184, 185] and other diseases with attenuated NO levels. The reason why NO responsiveness of sGC is elevated in both CAD groups needs to be further investigated in the future.

Oxidative stress is increased in clinical conditions associated with endothelial dysfunction, amongst others CVD [87, 88, 186], such as CAD [187]. The existence of NO-insensitive heme-free sGC was observed in pathological conditions with increased oxidative stress [150] in platelets [66]. BAY 60-2770 especially targets NO-insensitive sGC with oxidized heme group in RBCs [66]. Correlation between CVD and NO-insensitive heme-free sGC [150, 188] was supposed in previous studies. In contrast, presented data show that sGC activation by BAY 60-2770 does not change the cGMP levels in RBCs with (stable and unstable) CAD compared to healthy controls. Even the treatment of RBCs with BAY 60-2770 and DEA/NO scales lower cGMP levels in all study cohorts as compared with incubation with BAY 41-2272 and DEA/NO. This leads to the assumption that the levels of heme-free sGC are low in physiological and pathological conditions (like CAD). Hence, on the basis of the presented data one can assume that RBCs compensate not only low NO bioavailability [44], but also consequences of oxidative stress like oxidized heme of sGC in human RBCs. One

possible reason for this could be the abundant antioxidant system of RBCs with its own "enzymatic and non-enzymatic mechanisms" [91]. These probably maintain not only redox state of hemoglobin, but also the reduced form of sGC for appropriate function [175]. The clinical benefit of BAY 60-2770 remains to be investigated in case of increased oxidative stress [189] associated with CVD [181] with diminished NO levels.
In conclusion, the present study confirms that sGC activity, sGC responsiveness to NO and its stimulators as well as the NO/sGC pathway are preserved in human RBCs with stable or unstable CAD. Consequently, RBCs compensate reduced NO levels and oxidative stress in those pathological conditions. sGC stimulation with BAY 41-2272 and BAY 60-2770 as well as the NO/sGC pathway itself remain as targets for treatment of CVD with diminished NO levels or enhanced oxidative stress.

5.2.2 NO levels and redox state are unchanged in RBCs of patients with CAD

In addition, presented data of the CAD study further show that basal levels of NO in RBCs of stable and unstable CAD patients do not differ from those levels in age-matched healthy controls. NO levels in RBCs were analyzed by FACS with the fluorescent dye DAF-FM-DA based on its nitrosative chemistry [43]. In addition, data of the follow-up study demonstrate that basal levels of NO show no difference in RBCs of patients with unstable CAD before and after PCI.
Cortese-Krott et al. already showed that in RBCs of patients with CAD, eNOS bioavailability and expression are decreased [44]. In addition, reduced NO levels were described by Napoli et al. in RBCs of patients with vascular disease [20]. Hence, decreased NO levels were expected in RBCs of CAD patients. Unlike previous publications, present data show that NO levels are unchanged in RBCs of patients with stable and unstable CAD. This indicates that NO metabolism is preserved in RBCs in pathological conditions.
In addition, eNOS inhibition by NOS inhibitor L-NAME results in decrease of NO levels in all three study groups. This reveals that basal NO levels in human RBCs are dependent on eNOS regardless of stable or unstable CAD. These results are in line with findings of Cortese-Krott et al., which showed that an eNOS isoform produces continuously NO in human RBCs [43]. Furthermore, NO levels increase in all groups by the use of radical H_2O_2. This indicates that NO signal measured by DAF-FM-DA is dependent on radicals. DAF-FM-DA only reacts indirectly with NO [43] by forming a highly fluorescent triazole (DAF-FM-T) in presence of nitrosating species [190, 191] or oxidants like ROS [192]. This is in line with current results presented here. In conclusion, results show that NO metabolism is obtained in RBCs of patients with CAD

although eNOS activity is decreased. Hence, it can be assumed that RBCs are able to offset NO bioavailability changes.

The data further point out that measured levels of ROS and free thiols by using fluorescent dyes DCF and TT are unchanged in RBCs of stable and unstable CAD patients. Thus, present results reflect that both, stable and unstable CAD, do not have an influence on redox state in RBCs.

In reduced form, glutathione draws a large amount of intracellular free thiols, so that TT, which stains intracellular thiols, was used as an indirect marker for reduced glutathione [95]. Previous findings about correlation between CAD and antioxidant enzymes are discordant. In contrast to the present work, Blankenberg et al. demonstrated correlation between diminished glutathione peroxidase 1 activity and cardiovascular events [102]. Data of submitted work show that glutathione levels do not differ in RBCs of CAD patients as compared to age-matched controls. In accordance to the presented data, Pytel et al. confirmed no difference in glutathione peroxidase-1 activity in CAD patients in comparison to heathy subjects [103].

An "inverse association" between activity-levels of enzymes like superoxide dismutase, glutathione peroxidase as well as catalase and coronary heart disease was assumed by Flores-Mateo et al. as a consequence of higher oxidative stress [193, 103]. As mentioned in chapter 5.2.1, oxidative stress was described as increased in patients with CVD [65, 87, 88]. In addition, Ahrens et al. showed higher levels of oxidative stress particularly in platelets of patients with CAD [189]. Therefore, it was suspected that ROS levels are increased also in RBCs from patients with stable and unstable CAD. However, findings of this work contradict earlier studies and show that ROS levels are unchanged in RBCs of patients with stable and unstable CAD. This suggests that RBCs contain a functional antioxidant system as in conditions associated with CVD.

Results of the follow-up study with RBCs of unstable CAD patients emphasize that NO levels are unchanged after PCI, as well. In contrast, the levels of free thiols are increased and levels of ROS tended to decrease 90 days after PCI. This indicates a tendency towards an anti-oxidative change in redox state after PCI in human RBCs, although redox state in RBCs was unchanged by stable and unstable CAD compared to age-matched controls as described above. These results indicate clinical relevance of PCI, not only for vasculature, but also for functional features of RBCs. This needs to be further investigated in the future.

To sum up, present findings show that RBCs are able to obtain NO metabolism and redox state despite endothelial dysfunction like stable or unstable CAD.

5.2.3 Unchanged non-canonical features in anemic RBCs with unstable CAD

The Department of Cardiology, Pneumology and Angiology of the University Hospital of Düsseldorf performed the anemia study. Presented data of the anemia study demonstrate that NO levels are unchanged in RBCs of patients with unstable CAD with anemia compared to regular hemoglobin levels. Furthermore, NO levels are decreased using eNOS-inhibtior L-NAME correlating to above-mentioned results in RBCs of patients with CAD only. Dejam et al. described an eNOS-dependent NO metabolism in RBCs in hypoxic conditions [41]. Other studies have also reported that NO is produced by nitrite reduction in hypoxic conditions [42, 194, 195]. In contrast, present results prove a red cell eNOS dependency of basal NO levels in RBCs of unstable CAD patients independent of hemoglobin levels.

Although there seems to be a correlation between anemia and myocardial events [55, 196, 197, 198], present data show that this correlation seems not to be influenced by NO levels or redox state in RBCs, as anemia does not change these parameters in CAD patients.

As mentioned before, reduced glutathione draws a large amount of intracellular free thiols, which was measured by TT and used as an indirect marker for reduced glutathione [95]. Morris et al. showed that glutathione levels were decreased in anemic conditions like in SCD [90]. In contrast to Morris et al., present study shows that glutathione- and ROS levels are not changed in CAD with anemia.

In summary, the results of this work show that anemia does not change levels of NO, ROS and free thiols in RBCs of unstable CAD patients. Thus, NO metabolism and redox state are preserved in RBCs with CAD although hemoglobin level is diminished. In conclusion, it is assumable that RBCs compensate lack of NO bioavailability in hypoxic and normoxic conditions in an eNOS-dependent manner and contain a rich antioxidant system.

6 Summary and Conclusion

The presented study shows that in mature healthy human RBCs NO induces increase in cGMP levels by sGC stimulation. The sGC/cGMP pathway as well as the response of sGC to NO and to sGC activity influencing substances are preserved in RBCs in pathological conditions with NO deficiency and increased oxidative stress like CAD. Furthermore, NO metabolism and redox state in RBCs are unchanged by CAD independent of the hemoglobin level. Hence, it can be suggested that RBCs are compensating lack of NO bioavailability and oxidative stress in CVD such as CAD.

Several studies in the past were able to proof the existence of sGC in progenitor cells of RBCs [140]. Furthermore, Petrov et al. assumed an active sGC in mature RBCs in the year 1996 [199]. This assumption can be endorsed by the results of presented study. However, it must be noted that contamination with platelets might have an influence on the presented results, as these kind of blood cells are known to contain sGC, as well [200].

Having said that, as the sGC/cGMP pathway is preserved in human RBCs, it offers a potential therapeutic approach in endothelial disease with lack of NO bioavailability [65, 184] and oxidative stress, such as CAD. As others have reported before, there were contradictory findings concerning sGC activity in blood cells in CVD [189], further studies are needed to verify its relevance in clinical conditions in future.

References

1. Roger, V.L., et al., *Heart disease and stroke statistics--2012 update: a report from the American Heart Association.* Circulation, 2012. **125**(1): p. e2-e220.
2. Ross, R., *Atherosclerosis--an inflammatory disease.* N Engl J Med, 1999. **340**(2): p. 115-26.
3. World Health Organization. *Cardiovascular diseases (cvds)*. [Fact sheet] 2017, May 2017, November 27]; Available from: http://www.who.int/mediacentre/factsheets/fs317/en/.
4. World Health Organization. *Noncommunicable diseases*. [fact sheet] 2017, June 2017, November 27, 12.00 pm]; Available from: http://www.who.int/mediacentre/factsheets/fs355/en/.
5. Shanthi Mendis. Tim Armstrong, D.B., Francesco Branca, Jeremy Lauer, Cecile Mace, Shanthi Mendis, Vladimir Poznyak, Leanne Riley, Vera Da Costa E Silva, Gretchen Stevens,, *Global status report on noncommunicable diseases 2014*. 2014, World Health Organization. p. 298.
6. Kannel, W.B., et al., *Factors of risk in the development of coronary heart disease--six year follow-up experience. The Framingham Study.* Ann Intern Med, 1961. **55**: p. 33-50.
7. Napoli, C., et al., *Fatty streak formation occurs in human fetal aortas and is greatly enhanced by maternal hypercholesterolemia. Intimal accumulation of low density lipoprotein and its oxidation precede monocyte recruitment into early atherosclerotic lesions.* J Clin Invest, 1997. **100**(11): p. 2680-90.
8. Mitra, S., T. Goyal, and J.L. Mehta, *Oxidized LDL, LOX-1 and atherosclerosis.* Cardiovasc Drugs Ther, 2011. **25**(5): p. 419-29.
9. Michael Pittilo, R., *Cigarette smoking, endothelial injury and cardiovascular disease.* Int J Exp Pathol, 2000. **81**(4): p. 219-30.
10. Sowers, J.R., M. Epstein, and E.D. Frohlich, *Diabetes, hypertension, and cardiovascular disease: an update.* Hypertension, 2001. **37**(4): p. 1053-9.
11. Grundy, S.M., et al., *Primary prevention of coronary heart disease: guidance from Framingham: a statement for healthcare professionals from the AHA Task Force on Risk Reduction. American Heart Association.* Circulation, 1998. **97**(18): p. 1876-87.
12. Prado, C.M., et al., *Turbulent blood flow plays an essential localizing role in the development of atherosclerotic lesions in experimentally induced hypercholesterolaemia in rats.* Int J Exp Pathol, 2008. **89**(1): p. 72-80.
13. Kostner, K., et al., *Is oxidative stress causally linked to unstable angina pectoris? A study in 100 CAD patients and matched controls.* Cardiovasc Res, 1997. **36**(3): p. 330-6.
14. Inoue, T., et al., *Relationship of cigarette smoking to the severity of coronary and thoracic aortic atherosclerosis.* Cardiology, 1995. **86**(5): p. 374-9.
15. Wierzbicki, A.S., *Homocysteine and cardiovascular disease: a review of the evidence.* Diab Vasc Dis Res, 2007. **4**(2): p. 143-50.
16. Fuster, V., et al., *The pathogenesis of coronary artery disease and the acute coronary syndromes (1).* N Engl J Med, 1992. **326**(4): p. 242-50.

17. Fuster, V., et al., *The pathogenesis of coronary artery disease and the acute coronary syndromes (2).* N Engl J Med, 1992. **326**(5): p. 310-8.
18. Cai, H. and D.G. Harrison, *Endothelial dysfunction in cardiovascular diseases: the role of oxidant stress.* Circ Res, 2000. **87**(10): p. 840-4.
19. Charakida, M., et al., *Assessment of atherosclerosis: the role of flow-mediated dilatation.* Eur Heart J, 2010. **31**(23): p. 2854-61.
20. Napoli, C. and L.J. Ignarro, *Nitric oxide and pathogenic mechanisms involved in the development of vascular diseases.* Arch Pharm Res, 2009. **32**(8): p. 1103-8.
21. Horn, P., et al., *Circulating microparticles carry a functional endothelial nitric oxide synthase that is decreased in patients with endothelial dysfunction.* J Am Heart Assoc, 2013. **2**(1): p. e003764.
22. Heiss, C., et al., *Endothelial function, nitric oxide, and cocoa flavanols.* J Cardiovasc Pharmacol, 2006. **47 Suppl 2**: p. S128-35; discussion S172-6.
23. Lundberg, J.O., E. Weitzberg, and M.T. Gladwin, *The nitrate-nitrite-nitric oxide pathway in physiology and therapeutics.* Nat Rev Drug Discov, 2008. **7**(2): p. 156-67.
24. Lundberg, J.O., et al., *Nitrate and nitrite in biology, nutrition and therapeutics.* Nat Chem Biol, 2009. **5**(12): p. 865-9.
25. Moncada, S. and E.A. Higgs, *The discovery of nitric oxide and its role in vascular biology.* Br J Pharmacol, 2006. **147 Suppl 1**: p. S193-201.
26. Perticone, F., et al., *Prognostic significance of endothelial dysfunction in hypertensive patients.* Circulation, 2001. **104**(2): p. 191-6.
27. Arteel, G.E., P. Schroeder, and H. Sies, *Reactions of peroxynitrite with cocoa procyanidin oligomers.* J Nutr, 2000. **130**(8S Suppl): p. 2100S-4S.
28. Cannon, R.O., 3rd, *Role of nitric oxide in cardiovascular disease: focus on the endothelium.* Clin Chem, 1998. **44**(8 Pt 2): p. 1809-19.
29. Bornfeldt, K.E., et al., *Insulin-like growth factor-I and platelet-derived growth factor-BB induce directed migration of human arterial smooth muscle cells via signaling pathways that are distinct from those of proliferation.* J Clin Invest, 1994. **93**(3): p. 1266-74.
30. Sorensen, K.E., I.B. Kristensen, and D.S. Celermajer, *Atherosclerosis in the human brachial artery.* J Am Coll Cardiol, 1997. **29**(2): p. 318-22.
31. Shanthi Mendis. Tim Armstrong, D.B., Francesco Branca, Jeremy Lauer, Cecile Mace, Shanthi Mendis, Vladimir Poznyak, Leanne Riley, Vera Da Costa E Silva, Gretchen Stevens,, *Global status report on*

noncommunicable diseases 2014. World Health Organization. p. 298.
32. Rainer Klinke, H.-C.P., Armin Kurtz und Stefan Silbernagel,, *Physiologie*. 6 ed. 2009, November 18 Stuttgart, New York: Thieme.
33. Georg Löffler und Petro E. Petrides, *Biochemie und Pathobiochemie*. 7 ed. 2002, October, Heidelberg, Berlin: Springer.
34. Shiga, T., N. Maeda, and K. Kon, *Erythrocyte rheology.* Crit Rev Oncol Hematol, 1990. **10**(1): p. 9-48.
35. Parthasarathi, K. and H.H. Lipowsky, *Capillary recruitment in response to tissue hypoxia and its dependence on red blood cell deformability.* Am J Physiol, 1999. **277**(6 Pt 2): p. H2145-57.
36. Rybicki, A.C., et al., *Human erythrocyte protein 4.1 is a phosphatidylserine binding protein.* J Clin Invest, 1988. **81**(1): p. 255-60.

37. Rybicki, A.C., et al., *Deficiency of protein 4.2 in erythrocytes from a patient with a Coombs negative hemolytic anemia. Evidence for a role of protein 4.2 in stabilizing ankyrin on the membrane.* J Clin Invest, 1988. **81**(3): p. 893-901.
38. Tyler, J.M., B.N. Reinhardt, and D. Branton, *Associations of erythrocyte membrane proteins. Binding of purified bands 2.1 and 4.1 to spectrin.* J Biol Chem, 1980. **255**(14): p. 7034-9.
39. Patel, R.P., N. Hogg, and D.B. Kim-Shapiro, *The potential role of the red blood cell in nitrite-dependent regulation of blood flow.* Cardiovasc Res, 2011. **89**(3): p. 507-15.
40. Gothoskar, A.V., *Resealed Erythrocytes: A Review.* Pharmaceutical Technology, 2004. **28(3)**: p. p. 140-155.
41. Dejam, A., et al., *Erythrocytes are the major intravascular storage sites of nitrite in human blood.* Blood, 2005. **106**(2): p. 734-9.
42. Cosby, K., et al., *Nitrite reduction to nitric oxide by deoxyhemoglobin vasodilates the human circulation.* Nat Med, 2003. **9**(12): p. 1498-505.
43. Cortese-Krott, M.M., et al., *A multilevel analytical approach for detection and visualization of intracellular NO production and nitrosation events using diaminofluoresceins.* Free Radic Biol Med, 2012. **53**(11): p. 2146-58.
44. Cortese-Krott, M.M., et al., *Human red blood cells at work: identification and visualization of erythrocytic eNOS activity in health and disease.* Blood, 2012. **120**(20): p. 4229-37.
45. Kleinbongard, P., et al., *Red blood cells express a functional endothelial nitric oxide synthase.* Blood, 2006. **107**(7): p. 2943-51.
46. Cortese-Krott, M.M. and M. Kelm, *Endothelial nitric oxide synthase in red blood cells: key to a new erythrocrine function?* Redox Biol, 2014. **2**: p. 251-8.
47. Buehler, P.W. and A.I. Alayash, *Oxygen sensing in the circulation: "cross talk" between red blood cells and the vasculature.* Antioxid Redox Signal, 2004. **6**(6): p. 1000-10.
48. Minetti, M. and W. Malorni, *Redox control of red blood cell biology: the red blood cell as a target and source of prooxidant species.* Antioxid Redox Signal, 2006. **8**(7-8): p. 1165-9.
49. Rodriguez, J., et al., *Performance of diamino fluorophores for the localization of sources and targets of nitric oxide.* Free Radic Biol Med, 2005. **38**(3): p. 356-68.
50. Tsuda, K., et al., *Nitric oxide improves membrane fluidity of erythrocytes in essential hypertension: An electron paramagnetic resonance investigation.* Biochem Biophys Res Commun, 2000. **275**(3): p. 946-54.
51. Lipowsky, H.H., et al., *Effect of erythrocyte deformability on in vivo red cell transit time and hematocrit and their correlation with in vitro filterability.* Microvasc Res, 1993. **46**(1): p. 43-64.
52. Gerd Herold, *Innere Medizin*. 2013, Cologne: Gerd Herold.
53. Anand, I.S., et al., *Anemia and change in hemoglobin over time related to mortality and morbidity in patients with chronic heart failure: results from Val-HeFT.* Circulation, 2005. **112**(8): p. 1121-7.
54. Kulier, A., et al., *Impact of preoperative anemia on outcome in patients undergoing coronary artery bypass graft surgery.* Circulation, 2007. **116**(5): p. 471-9.
55. Sabatine, M.S., et al., *Association of hemoglobin levels with clinical outcomes in acute coronary syndromes.* Circulation, 2005. **111**(16): p. 2042-9.

56. Furchgott, R.F. and P.M. Vanhoutte, *Endothelium-derived relaxing and contracting factors.* FASEB J, 1989. **3**(9): p. 2007-18.
57. Furchgott, R.F., *Endothelium-derived relaxing factor: discovery, early studies, and identification as nitric oxide.* Biosci Rep, 1999. **19**(4): p. 235-51.
58. Furchgott, R.F. and J.V. Zawadzki, *The obligatory role of endothelial cells in the relaxation of arterial smooth muscle by acetylcholine.* Nature, 1980. **288**(5789): p. 373-6.
59. Balligand, J.L., O. Feron, and C. Dessy, *eNOS activation by physical forces: from short-term regulation of contraction to chronic remodeling of cardiovascular tissues.* Physiol Rev, 2009. **89**(2): p. 481-534.
60. Heiss, C., et al., *Plasma nitroso compounds are decreased in patients with endothelial dysfunction.* J Am Coll Cardiol, 2006. **47**(3): p. 573-9.
61. Griffith, O.W. and D.J. Stuehr, *Nitric oxide synthases: properties and catalytic mechanism.* Annu Rev Physiol, 1995. **57**: p. 707-36.
62. Chirkov, Y.Y. and J.D. Horowitz, *Impaired tissue responsiveness to organic nitrates and nitric oxide: a new therapeutic frontier?* Pharmacol Ther, 2007. **116**(2): p. 287-305.
63. De Caterina, R., et al., *Nitric oxide decreases cytokine-induced endothelial activation. Nitric oxide selectively reduces endothelial expression of adhesion molecules and proinflammatory cytokines.* J Clin Invest, 1995. **96**(1): p. 60-8.
64. Moncada, S. and E.A. Higgs, *Molecular mechanisms and therapeutic strategies related to nitric oxide.* FASEB J, 1995. **9**(13): p. 1319-30.
65. Stasch, J.P., P. Pacher, and O.V. Evgenov, *Soluble guanylate cyclase as an emerging therapeutic target in cardiopulmonary disease.* Circulation, 2011. **123**(20): p. 2263-73.
66. Evgenov, O.V., et al., *NO-independent stimulators and activators of soluble guanylate cyclase: discovery and therapeutic potential.* Nat Rev Drug Discov, 2006. **5**(9): p. 755-68.
67. Denninger, J.W. and M.A. Marletta, *Guanylate cyclase and the .NO/cGMP signaling pathway.* Biochim Biophys Acta, 1999. **1411**(2-3): p. 334-50.
68. Raj, U. and L. Shimoda, *Oxygen-dependent signaling in pulmonary vascular smooth muscle.* Am J Physiol Lung Cell Mol Physiol, 2002. **283**(4): p. L671-7.
69. Moncada, S., *Nitric oxide in the vasculature: physiology and pathophysiology.* Ann N Y Acad Sci, 1997. **811**: p. 60-7; discussion 67-9.
70. Palmer, R.M., D.S. Ashton, and S. Moncada, *Vascular endothelial cells synthesize nitric oxide from L-arginine.* Nature, 1988. **333**(6174): p. 664-6.
71. Schmidt, H.H., et al., *Arginine is a physiological precursor of endothelium-derived nitric oxide.* Eur J Pharmacol, 1988. **154**(2): p. 213-6.
72. Knowles, R.G., et al., *Formation of nitric oxide from L-arginine in the central nervous system: a transduction mechanism for stimulation of the soluble guanylate cyclase.* Proc Natl Acad Sci U S A, 1989. **86**(13): p. 5159-62.
73. Kelm, M. and J. Schrader, *Control of coronary vascular tone by nitric oxide.* Circ Res, 1990. **66**(6): p. 1561-75.
74. Lauer, T., et al., *Plasma nitrite rather than nitrate reflects regional endothelial nitric oxide synthase activity but lacks intrinsic vasodilator action.* Proc Natl Acad Sci U S A, 2001. **98**(22): p. 12814-9.

75. Ignarro, L.J., et al., *Oxidation of nitric oxide in aqueous solution to nitrite but not nitrate: comparison with enzymatically formed nitric oxide from L-arginine.* Proc Natl Acad Sci U S A, 1993. **90**(17): p. 8103-7.
76. Rassaf, T., et al., *Evidence for in vivo transport of bioactive nitric oxide in human plasma.* J Clin Invest, 2002. **109**(9): p. 1241-8.
77. Helms, C. and D.B. Kim-Shapiro, *Hemoglobin-mediated nitric oxide signaling.* Free Radic Biol Med, 2013. **61**: p. 464-72.
78. May, J.M., et al., *Nitrite uptake and metabolism and oxidant stress in human erythrocytes.* Am J Physiol Cell Physiol, 2000. **279**(6): p. C1946-54.
79. Crawford, J.H., et al., *Hypoxia, red blood cells, and nitrite regulate NO-dependent hypoxic vasodilation.* Blood, 2006. **107**(2): p. 566-74.
80. Betteridge, D.J., *What is oxidative stress?* Metabolism, 2000. **49**(2 Suppl 1): p. 3-8.
81. Suvorava, T. and G. Kojda, *Reactive oxygen species as cardiovascular mediators: lessons from endothelial-specific protein overexpression mouse models.* Biochim Biophys Acta, 2009. **1787**(7): p. 802-10.
82. Balcerczyk, A., M. Soszynski, and G. Bartosz, *On the specificity of 4-amino-5-methylamino-2',7'-difluorofluorescein as a probe for nitric oxide.* Free Radic Biol Med, 2005. **39**(3): p. 327-35.
83. Suzuki, H., et al., *In vivo evidence for microvascular oxidative stress in spontaneously hypertensive rats. Hydroethidine microfluorography.* Hypertension, 1995. **25**(5): p. 1083-9.
84. Harrison, D.G., *Cellular and molecular mechanisms of endothelial cell dysfunction.* J Clin Invest, 1997. **100**(9): p. 2153-7.
85. Ohara, Y., T.E. Peterson, and D.G. Harrison, *Hypercholesterolemia increases endothelial superoxide anion production.* J Clin Invest, 1993. **91**(6): p. 2546-51.
86. Alexander, R.W., *Atherosclerosis as disease of redox-sensitive genes.* Trans Am Clin Climatol Assoc, 1998. **109**: p. 129-45; discussion 145-6.
87. Harrison, D.G. and M.C. Gongora, *Oxidative stress and hypertension.* Med Clin North Am, 2009. **93**(3): p. 621-35.
88. Hare, J.M., *Nitroso-redox balance in the cardiovascular system.* N Engl J Med, 2004. **351**(20): p. 2112-4.
89. Kojda, G. and D. Harrison, *Interactions between NO and reactive oxygen species: pathophysiological importance in atherosclerosis, hypertension, diabetes and heart failure.* Cardiovasc Res, 1999. **43**(3): p. 562-71.
90. Morris, C.R., et al., *Erythrocyte glutamine depletion, altered redox environment, and pulmonary hypertension in sickle cell disease.* Blood, 2008. **111**(1): p. 402-10.
91. Kuhn, V., et al., *Red Blood Cell Function and Dysfunction: Redox Regulation, Nitric Oxide Metabolism, Anemia.* Antioxid Redox Signal, 2017. **26**(13): p. 718-742.
92. Kennett, E.C. and P.W. Kuchel, *Plasma membrane oxidoreductases: effects on erythrocyte metabolism and redox homeostasis.* Antioxid Redox Signal, 2006. **8**(7-8): p. 1241-7.
93. Nickel, C., et al., *Thioredoxin networks in the malarial parasite Plasmodium falciparum.* Antioxid Redox Signal, 2006. **8**(7-8): p. 1227-39.

94. Griffith, O.W., *Glutathione turnover in human erythrocytes. Inhibition by buthionine sulfoximine and incorporation of glycine by exchange.* J Biol Chem, 1981. **256**(10): p. 4900-4.
95. Mandavilli, B.S. and M.S. Janes, *Detection of intracellular glutathione using ThiolTracker violet stain and fluorescence microscopy.* Curr Protoc Cytom, 2010. **Chapter 9**: p. Unit 9 35.
96. Rassaf, T., et al., *Plasma nitrosothiols contribute to the systemic vasodilator effects of intravenously applied NO: experimental and clinical Study on the fate of NO in human blood.* Circ Res, 2002. **91**(6): p. 470-7.
97. Forgione, M.A., et al., *Heterozygous cellular glutathione peroxidase deficiency in the mouse: abnormalities in vascular and cardiac function and structure.* Circulation, 2002. **106**(9): p. 1154-8.
98. Lubos, E., D.E. Handy, and J. Loscalzo, *Role of oxidative stress and nitric oxide in atherothrombosis.* Front Biosci, 2008. **13**: p. 5323-44.
99. Wolin, M.S., *Interactions of oxidants with vascular signaling systems.* Arterioscler Thromb Vasc Biol, 2000. **20**(6): p. 1430-42.
100. Jourd'heuil, D., *Increased nitric oxide-dependent nitrosylation of 4,5-diaminofluorescein by oxidants: implications for the measurement of intracellular nitric oxide.* Free Radic Biol Med, 2002. **33**(5): p. 676-84.
101. Forsberg, L., U. de Faire, and R. Morgenstern, *Oxidative stress, human genetic variation, and disease.* Arch Biochem Biophys, 2001. **389**(1): p. 84-93.
102. Blankenberg, S., et al., *Glutathione peroxidase 1 activity and cardiovascular events in patients with coronary artery disease.* N Engl J Med, 2003. **349**(17): p. 1605-13.
103. Pytel, E., et al., *Increased oxidative stress and decreased membrane fluidity in erythrocytes of CAD patients.* Biochem Cell Biol, 2013. **91**(5): p. 315-8.
104. Jubelin, B.C. and J.L. Gierman, *Erythrocytes may synthesize their own nitric oxide.* Am J Hypertens, 1996. **9**(12 Pt 1): p. 1214-9.
105. Lafuente-Sanchis, A., D. Triguero, and A. Garcia-Pascual, *Changes in nerve- and endothelium-mediated contractile tone of the corpus cavernosum in a mouse model of pre-mature ageing.* Andrology, 2014. **2**(4): p. 537-49.
106. Siedlar, M., et al., *Demonstration of iNOS-mRNA and iNOS in human monocytes stimulated with cancer cells in vitro.* J Leukoc Biol, 1999. **65**(5): p. 597-604.
107. Rothe, F., K. Langnaese, and G. Wolf, *New aspects of the location of neuronal nitric oxide synthase in the skeletal muscle: a light and electron microscopic study.* Nitric Oxide, 2005. **13**(1): p. 21-35.
108. Chen, L.Y. and J.L. Mehta, *Evidence for the presence of L-arginine-nitric oxide pathway in human red blood cells: relevance in the effects of red blood cells on platelet function.* J Cardiovasc Pharmacol, 1998. **32**(1): p. 57-61.
109. Dimmeler, S., et al., *Activation of nitric oxide synthase in endothelial cells by Akt-dependent phosphorylation.* Nature, 1999. **399**(6736): p. 601-5.
110. Fulton, D., J.P. Gratton, and W.C. Sessa, *Post-translational control of endothelial nitric oxide synthase: why isn't calcium/calmodulin enough?* J Pharmacol Exp Ther, 2001. **299**(3): p. 818-24.
111. Marletta, M.A., *Nitric oxide synthase: aspects concerning structure and catalysis.* Cell, 1994. **78**(6): p. 927-30.

112. Corson, M.A., et al., *Phosphorylation of endothelial nitric oxide synthase in response to fluid shear stress.* Circ Res, 1996. **79**(5): p. 984-91.
113. Neto, M.d.A., et al., *Vasodilatation induced by forskolin involves cyclic GMP production.* Journal of Biophysical Chemistry, 2011. **02**(04): p. 373-379.
114. Moncada, S., R.M. Palmer, and E.A. Higgs, *Nitric oxide: physiology, pathophysiology, and pharmacology.* Pharmacol Rev, 1991. **43**(2): p. 109-42.
115. Heinzel, B., et al., *Ca2+/calmodulin-dependent formation of hydrogen peroxide by brain nitric oxide synthase.* Biochem J, 1992. **281 (Pt 3)**: p. 627-30.
116. Pou, S., et al., *Generation of superoxide by purified brain nitric oxide synthase.* J Biol Chem, 1992. **267**(34): p. 24173-6.
117. Ignarro, L.J., *Biological actions and properties of endothelium-derived nitric oxide formed and released from artery and vein.* Circ Res, 1989. **65**(1): p. 1-21.
118. Jung, C., et al., *Arginase inhibition mediates cardioprotection during ischaemia-reperfusion.* Cardiovasc Res, 2010. **85**(1): p. 147-54.
119. Conran, N., et al., *Increased soluble guanylate cyclase activity in the red blood cells of sickle cell patients.* Br J Haematol, 2004. **124**(4): p. 547-54.
120. Arnold, W.P., et al., *Nitric oxide activates guanylate cyclase and increases guanosine 3':5'-cyclic monophosphate levels in various tissue preparations.* Proc Natl Acad Sci U S A, 1977. **74**(8): p. 3203-7.
121. Lohmann, S.M., et al., *Distinct and specific functions of cGMP-dependent protein kinases.* Trends Biochem Sci, 1997. **22**(8): p. 307-12.
122. Degerman, E., P. Belfrage, and V.C. Manganiello, *Structure, localization, and regulation of cGMP-inhibited phosphodiesterase (PDE3).* J Biol Chem, 1997. **272**(11): p. 6823-6.
123. Mollinedo, F., et al., *Arginase as a new concern in blood transfusion.* Blood Transfus, 2014. **12 Suppl 1**: p. s165-6.
124. Shemyakin, A., et al., *Arginase inhibition improves endothelial function in patients with coronary artery disease and type 2 diabetes mellitus.* Circulation, 2012. **126**(25): p. 2943-50.
125. Ikuta, T., S. Ausenda, and M.D. Cappellini, *Mechanism for fetal globin gene expression: role of the soluble guanylate cyclase-cGMP-dependent protein kinase pathway.* Proc Natl Acad Sci U S A, 2001. **98**(4): p. 1847-52.
126. Wood, K.C., et al., *Circulating blood endothelial nitric oxide synthase contributes to the regulation of systemic blood pressure and nitrite homeostasis.* Arterioscler Thromb Vasc Biol, 2013. **33**(8): p. 1861-71.
127. Horn, P., et al., *Nitric oxide influences red blood cell velocity independently of changes in the vascular tone.* Free Radic Res, 2011. **45**(6): p. 653-61.
128. Zanfolin, M., et al., *Protective effects of BAY 41-2272 (sGC stimulator) on hypertension, heart, and cardiomyocyte hypertrophy induced by chronic L-NAME treatment in rats.* J Cardiovasc Pharmacol, 2006. **47**(3): p. 391-5.
129. Bor-Kucukatay, M., et al., *Effects of nitric oxide on red blood cell deformability.* Am J Physiol Heart Circ Physiol, 2003. **284**(5): p. H1577-84.
130. Lluch, P., G. Segarra, and P. Medina, *Asymmetric dimethylarginine as a mediator of vascular dysfunction in cirrhosis.* World J Gastroenterol, 2015. **21**(32): p. 9466-75.
131. Heiss, C., et al., *Nitric oxide synthase expression and functional response to nitric oxide are both important modulators of circulating angiogenic cell*

response to angiogenic stimuli. Arterioscler Thromb Vasc Biol, 2010. **30**(11): p. 2212-8.
132. Zabel, U., et al., *Human soluble guanylate cyclase: functional expression and revised isoenzyme family.* Biochem J, 1998. **335 (Pt 1)**: p. 51-7.
133. Brune, B., K.U. Schmidt, and V. Ullrich, *Activation of soluble guanylate cyclase by carbon monoxide and inhibition by superoxide anion.* Eur J Biochem, 1990. **192**(3): p. 683-8.
134. Yamashita, T., et al., *Mechanisms of reduced nitric oxide/cGMP-mediated vasorelaxation in transgenic mice overexpressing endothelial nitric oxide synthase.* Hypertension, 2000. **36**(1): p. 97-102.
135. Lincoln, T.M. and T.L. Cornwell, *Intracellular cyclic GMP receptor proteins.* FASEB J, 1993. **7**(2): p. 328-38.
136. Pacher, P., et al., *Nitrosative stress and pharmacological modulation of heart failure.* Trends Pharmacol Sci, 2005. **26**(6): p. 302-10.
137. Bor-Kucukatay, M., et al., *Effects of nitric oxide on red blood cell deformability.* Am J Physiol Heart Circ Physiol, 2003. **284**: p. H1577-H1584.
138. Zhang, G., et al., *Biphasic roles for soluble guanylyl cyclase (sGC) in platelet activation.* Blood, 2011. **118**(13): p. 3670-9.
139. Ikuta, T., S. Ausenda, and M.D. Cappellini, *Mechanism for fetal globin gene expression: Role of the soluble guanylate cyclase–cGMP-dependent protein kinase pathway.* Proceedings of the National Academy of Sciences, 2001. **98**(4): p. 1847-1852.
140. Cokic, V.P., et al., *Hydroxyurea nitrosylates and activates soluble guanylyl cyclase in human erythroid cells.* Blood, 2008. **111**(3): p. 1117-23.
141. Ignarro, L.J., K.S. Wood, and M.S. Wolin, *Activation of purified soluble guanylate cyclase by protoporphyrin IX.* Proc Natl Acad Sci U S A, 1982. **79**(9): p. 2870-3.
142. Adderley, S.P., et al., *Identification of cytosolic phosphodiesterases in the erythrocyte: a possible role for PDE5.* Med Sci Monit, 2011. **17**(5): p. CR241-7.
143. Allerston, C.K., F. von Delft, and O. Gileadi, *Crystal structures of the catalytic domain of human soluble guanylate cyclase.* PLoS One, 2013. **8**(3): p. e57644.
144. Winger, J.A. and M.A. Marletta, *Expression and characterization of the catalytic domains of soluble guanylate cyclase: interaction with the heme domain.* Biochemistry, 2005. **44**(10): p. 4083-90.
145. Ignarro, L.J., et al., *Activation of purified guanylate cyclase by nitric oxide requires heme. Comparison of heme-deficient, heme-reconstituted and heme-containing forms of soluble enzyme from bovine lung.* Biochim Biophys Acta, 1982. **718**(1): p. 49-59.
146. Craven, P.A. and F.R. DeRubertis, *Restoration of the responsiveness of purified guanylate cyclase to nitrosoguanidine, nitric oxide, and related activators by heme and hemeproteins. Evidence for involvement of the paramagnetic nitrosyl-heme complex in enzyme activation.* J Biol Chem, 1978. **253**(23): p. 8433-43.
147. Roy, B., E.J. Halvey, and J. Garthwaite, *An enzyme-linked receptor mechanism for nitric oxide-activated guanylyl cyclase.* J Biol Chem, 2008. **283**(27): p. 18841-51.

148. Ignarro, L.J., et al., *Activation of soluble guanylate cyclase by NO-hemoproteins involves NO-heme exchange. Comparison of heme-containing and heme-deficient enzyme forms.* J Biol Chem, 1986. **261**(11): p. 4997-5002.
149. Zhao, Y., et al., *Inhibition of soluble guanylate cyclase by ODQ.* Biochemistry, 2000. **39**(35): p. 10848-54.
150. Stasch, J.P., et al., *Targeting the heme-oxidized nitric oxide receptor for selective vasodilatation of diseased blood vessels.* J Clin Invest, 2006. **116**(9): p. 2552-61.
151. Bauersachs, J., et al., *Vasodilator dysfunction in aged spontaneously hypertensive rats: changes in NO synthase III and soluble guanylyl cyclase expression, and in superoxide anion production.* Cardiovasc Res, 1998. **37**(3): p. 772-9.
152. Lasker, G.F., et al., *The sGC activator BAY 60-2770 has potent erectile activity in the rat.* Am J Physiol Heart Circ Physiol, 2013. **304**(12): p. H1670-9.
153. Rodriguez, G., et al., *Forskolin-inducible cAMP pathway negatively regulates T-cell proliferation by uncoupling the interleukin-2 receptor complex.* J Biol Chem, 2013. **288**(10): p. 7137-46.
154. Life technologies. *ELISA plate*. 2015 2015, November 7, 11:39 pm]; Available from: http://abcommunity.lifetechnologies.com/servlet/JiveServlet/showImage/38-1270-1291/96%2Bwell%2Bplate.PNG.png.
155. Steiner, A.L., et al., *Radioimmunoassay for the measurement of cyclic nucleotides.* Adv Cyclic Nucleotide Res, 1972. **2**: p. 51-61.
156. Alice Longobardi Givan, *Flow Cytometry*. 2 ed. 2001, Weinheim: Wiley-Liss. 2 ff.
157. Turgut, N.H., et al., *Investigation of the role of the NO-cGMP pathway on YC-1 and DEA/NO effects on thoracic aorta smooth muscle responses in a rat preeclampsia model.* Can J Physiol Pharmacol, 2013. **91**(10): p. 797-803.
158. Kellawan, J.M., et al., *Phosphodiesterase-5 inhibition preserves exercise onset vasodilator kinetics when NOS activity is reduced.* J Appl Physiol (1985), 2017: p. jap 00483 2017.
159. Feelisch, M. and M. Kelm, *Biotransformation of organic nitrates to nitric oxide by vascular smooth muscle and endothelial cells.* Biochem Biophys Res Commun, 1991. **180**(1): p. 286-93.
160. Joannides, R., et al., *Nitric oxide is responsible for flow-dependent dilatation of human peripheral conduit arteries in vivo.* Circulation, 1995. **91**(5): p. 1314-9.
161. Clarkson, P., et al., *Exercise training enhances endothelial function in young men.* J Am Coll Cardiol, 1999. **33**(5): p. 1379-85.
162. Moali, C., et al., *Substrate-specific modulation of a multisubstrate proteinase. C-terminal processing of fibrillar procollagens is the only BMP-1-dependent activity to be enhanced by PCPE-1.* J Biol Chem, 2005. **280**(25): p. 24188-94.
163. Durante, W., F.K. Johnson, and R.A. Johnson, *Arginase: a critical regulator of nitric oxide synthesis and vascular function.* Clin Exp Pharmacol Physiol, 2007. **34**(9): p. 906-11.
164. Kashyap, S.R., et al., *Insulin reduces plasma arginase activity in type 2 diabetic patients.* Diabetes Care, 2008. **31**(1): p. 134-9.
165. Ryoo, S., et al., *Endothelial arginase II: a novel target for the treatment of atherosclerosis.* Circ Res, 2008. **102**(8): p. 923-32.

166. Hein, T.W., et al., *Ischemia-reperfusion selectively impairs nitric oxide-mediated dilation in coronary arterioles: counteracting role of arginase.* FASEB J, 2003. **17**(15): p. 2328-30.
167. Vanhoutte, P.M., *Arginine and arginase: endothelial NO synthase double crossed?* Circ Res, 2008. **102**(8): p. 866-8.
168. Yang, J., et al., *Arginase regulates red blood cell nitric oxide synthase and export of cardioprotective nitric oxide bioactivity.* Proc Natl Acad Sci U S A, 2013. **110**(37): p. 15049-54.
169. Webb, A.J., et al., *Mechanisms underlying erythrocyte and endothelial nitrite reduction to nitric oxide in hypoxia: role for xanthine oxidoreductase and endothelial nitric oxide synthase.* Circ Res, 2008. **103**(9): p. 957-64.
170. Radomski, M.W., R.M. Palmer, and S. Moncada, *An L-arginine/nitric oxide pathway present in human platelets regulates aggregation.* Proc Natl Acad Sci U S A, 1990. **87**(13): p. 5193-7.
171. Bredt, D.S. and S.H. Snyder, *Isolation of nitric oxide synthetase, a calmodulin-requiring enzyme.* Proc Natl Acad Sci U S A, 1990. **87**(2): p. 682-5.
172. Kazerounian, S., et al., *Nitric oxide activation of soluble guanylyl cyclase reveals high and low affinity sites that mediate allosteric inhibition by calcium.* Biochemistry, 2002. **41**(10): p. 3396-404.
173. Govers, R. and T.J. Rabelink, *Cellular regulation of endothelial nitric oxide synthase.* Am J Physiol Renal Physiol, 2001. **280**(2): p. F193-206.
174. Boo, Y.C., et al., *Endothelial NO synthase phosphorylated at SER635 produces NO without requiring intracellular calcium increase.* Free Radic Biol Med, 2003. **35**(7): p. 729-41.
175. Cortese-Krott, M.M., et al., *Identification of a soluble guanylate cyclase in RBCs: preserved activity in patients with coronary artery disease.* Redox Biol, 2017. **14**: p. 328-337.
176. Stasch, J.P., et al., *NO-independent regulatory site on soluble guanylate cyclase.* Nature, 2001. **410**(6825): p. 212-5.
177. Pankey, E.A., et al., *Pulmonary and systemic vasodilator responses to the soluble guanylyl cyclase activator, BAY 60-2770, are not dependent on endogenous nitric oxide or reduced heme.* Am J Physiol Heart Circ Physiol, 2011. **300**(3): p. H792-802.
178. Roger, S., et al., *The anti-aggregating effect of BAY 41-2272, a stimulator of soluble guanylyl cyclase, requires the presence of nitric oxide.* Br J Pharmacol, 2010. **161**(5): p. 1044-58.
179. Mullershausen, F., et al., *Inhibition of phosphodiesterase type 5 by the activator of nitric oxide-sensitive guanylyl cyclase BAY 41-2272.* Circulation, 2004. **109**(14): p. 1711-3.
180. Schmidt, P., et al., *Mechanisms of nitric oxide independent activation of soluble guanylyl cyclase.* Eur J Pharmacol, 2003. **468**(3): p. 167-74.
181. Stasch, J.P., et al., *Cardiovascular actions of a novel NO-independent guanylyl cyclase stimulator, BAY 41-8543: in vivo studies.* Br J Pharmacol, 2002. **135**(2): p. 344-55.
182. Masuyama, H., et al., *Soluble guanylate cyclase stimulation on cardiovascular remodeling in angiotensin II-induced hypertensive rats.* Hypertension, 2006. **48**(5): p. 972-8.

183. Masuyama, H., et al., *Pressure-independent effects of pharmacological stimulation of soluble guanylate cyclase on fibrosis in pressure-overloaded rat heart.* Hypertens Res, 2009. **32**(7): p. 597-603.
184. Follmann, M., et al., *The chemistry and biology of soluble guanylate cyclase stimulators and activators.* Angew Chem Int Ed Engl, 2013. **52**(36): p. 9442-62.
185. Boerrigter, G., et al., *Cardiorenal and humoral properties of a novel direct soluble guanylate cyclase stimulator BAY 41-2272 in experimental congestive heart failure.* Circulation, 2003. **107**(5): p. 686-9.
186. Heistad, D.D., *Oxidative stress and vascular disease: 2005 Duff lecture.* Arterioscler Thromb Vasc Biol, 2006. **26**(4): p. 689-95.
187. Miller, F.J., Jr., et al., *Superoxide production in vascular smooth muscle contributes to oxidative stress and impaired relaxation in atherosclerosis.* Circ Res, 1998. **82**(12): p. 1298-305.
188. Schrammel, A., et al., *Characterization of 1H-[1,2,4]oxadiazolo[4,3-a]quinoxalin-1-one as a heme-site inhibitor of nitric oxide-sensitive guanylyl cyclase.* Mol Pharmacol, 1996. **50**(1): p. 1-5.
189. Ahrens, I., et al., *Measuring oxidative burden and predicting pharmacological response in coronary artery disease patients with a novel direct activator of haem-free/oxidised sGC.* Atherosclerosis, 2011. **218**(2): p. 431-4.
190. Nakatsubo, N., et al., *Direct evidence of nitric oxide production from bovine aortic endothelial cells using new fluorescence indicators: diaminofluoresceins.* FEBS Lett, 1998. **427**(2): p. 263-6.
191. Nagano, T. and T. Yoshimura, *Bioimaging of nitric oxide.* Chem Rev, 2002. **102**(4): p. 1235-70.
192. Wardman, P., *Fluorescent and luminescent probes for measurement of oxidative and nitrosative species in cells and tissues: progress, pitfalls, and prospects.* Free Radic Biol Med, 2007. **43**(7): p. 995-1022.
193. Flores-Mateo, G., et al., *Antioxidant enzyme activity and coronary heart disease: meta-analyses of observational studies.* Am J Epidemiol, 2009. **170**(2): p. 135-47.
194. Aamand, R., et al., *Generation of nitric oxide from nitrite by carbonic anhydrase: a possible link between metabolic activity and vasodilation.* Am J Physiol Heart Circ Physiol, 2009. **297**(6): p. H2068-74.
195. Nagababu, E., et al., *Active nitric oxide produced in the red cell under hypoxic conditions by deoxyhemoglobin-mediated nitrite reduction.* J Biol Chem, 2003. **278**(47): p. 46349-56.
196. Jolicoeur, E.M., et al., *Transfusion and mortality in patients with ST-segment elevation myocardial infarction treated with primary percutaneous coronary intervention.* Eur Heart J, 2009. **30**(21): p. 2575-83.
197. Gonzalez-Ferrer, J.J., et al., *Influence of hemoglobin level on in-hospital prognosis in patients with acute coronary syndrome.* Rev Esp Cardiol, 2008. **61**(9): p. 945-52.
198. Bassand, J.P., et al., *Relationship between baseline haemoglobin and major bleeding complications in acute coronary syndromes.* Eur Heart J, 2010. **31**(1): p. 50-8.
199. Petrov, V. and P. Lijnen, *Regulation of human erythrocyte Na+/H+ exchange by soluble and particulate guanylate cyclase.* Am J Physiol, 1996. **271**(5 Pt 1): p. C1556-64.

200. Bohme, E., R. Jung, and I. Mechler, *Guanylate cyclase in human platelets.* Methods Enzymol, 1974. **38**: p. 199-202.

201. Di Pietro, N., A. Giardinelli, V. Sirolli, C. Riganti, P. Di Tomo, E. Gazzano, S. Di Silvestre, C. Panknin, M. M. Cortese-Krott, C. Csonka, M. Kelm, P. Ferdinandy, M. Bonomini and A. Pandolfi (2016). "Nitric oxide synthetic pathway and cGMP levels are altered in red blood cells from end-stage renal disease patients." Mol Cell Biochem **417**(1-2): 155-167.

202. Zabel, U., C. Kleinschnitz, P. Oh, P. Nedvetsky, A. Smolenski, H. Muller, P. Kronich, P. Kugler, U. Walter, J. E. Schnitzer and H. H. Schmidt (2002). "Calcium-dependent membrane association sensitizes soluble guanylyl cyclase to nitric oxide." Nat Cell Biol **4**(4): 307-311.

203. Petrov, V., R. Fagard and P. Lijnen (1998). "Human erythrocytes contain Ca2+, calmodulin-dependent cyclic nucleotide phosphodiesterase which is involved in the hydrolysis of cGMP." Methods Find Exp Clin Pharmacol **20**(5): 387-393.

Acknowledgement

This dissertation is a result of hard work and scientific research, which would not be possible without the help and support of other persons.

Special thanks to Prof. Dr. rer. nat. Dr. Miriam M. Cortese-Krott, for giving me this opportunity to start my PhD thesis, for being my doctoral supervisor, for her encouragement and the constant willingness to discuss.

I would also like to thank Prof. Dr. med. Malte Kelm, chief of the department of Cardiology, Pneumology and Angiology, Düsseldorf for letting me explore science and gain new experiences in the cardiology laboratory.

Moreover, I thank Dr. rer. nat. Christina Panknin, my laboratory colleague and a good friend, for always taking care of me and helping me with a part of the FACS measurements of the CAD-study. Heartily thanks to Sivatharsini Thasian-Sivarajah for valuable input on numerous issues and problems in the laboratory. Additionally, I thank the team members of the cardiovascular research laboratory and the research team from the department of Cardiology, Pneumology and Angiology, University Hospital of Düsseldorf for their guidance in the laboratory. Especially, I thank Dr. med. Georg Wolff and Dr. med. Ralf Erkens, who collected the subjects and their characteristics for both studies of this work. Besides, I thank Jonathan Schmidt, who helped me with a part of the GTN kinetic. Furthermore, I thank David Vujnovac for showing me the method for cGMP extraction for ELISA.

My special thanks to Dr. rer. nat. Evanthia Mergia, who did the main RIA measurement of this work, and the laboratory of the Ruhr-University of Bochum for fruitful cooperation. Apart from that, I thank the biological and medical research centre (BMFZ) of Düsseldorf for their willingness to help by letting me use their vacuum concentrator. Furthermore, I ask those persons, who were not mentioned here, but deserve an acknowledgement, kindly for excuse.

I owe also great thanks to my friends, who always kept encouraging and motivating me through this work for the past 5 years.

Finally, saying thanks to some people is not enough, but even though I would like to thank my parents and my brother, Sayjohn Manokaran. They have always been the biggest support in my life and especially in this work. Thank you so much for your presence and kind encouragement.